Technical Report Documentation Page

1. Report No.	2. Government Accession No.	3. Recipient's Catalog No.
FHWA/TX-0-1855-1		

4. Title and Subtitle	5. Report Date
Anchorage Behavior of Headed Reinforcement: Literature Review	May 2002
	6. Performing Organization Code

7. Author(s)	8. Performing Organization Report No.
M. K. Thompson, J. O. Jirsa, J. E. Breen, and R. E. Klingner	Research Report 1855-1

9. Performing Organization Name and Address	10. Work Unit No. (TRAIS)
Center for Transportation Research The University of Texas at Austin 3208 Red River, Suite 200 Austin, TX 78705-2650	11. Contract or Grant No. Research Project 0-1855

12. Sponsoring Agency Name and Address	13. Type of Report and Period Covered
Texas Department of Transportation Research and Technology Implementation Office P.O. Box 5080 Austin, TX 78763-5080	Research Report (9/99-8/01)
	14. Sponsoring Agency Code

15. Supplementary Notes

Project conducted in cooperation with the U.S. Department of Transportation, Federal Highway Administration, and the Texas Department of Transportation

16. Abstract

The findings of a literature review of topics related to the anchorage of headed reinforcement are presented. The topics are grouped in three broad categories: conventional anchorage of reinforcement, anchorage of headed reinforcement, and a review of strut-and-tie modeling.

The review of conventional anchorage focuses on the mechanics of bond and code provisions for development length. A review of hooked bar anchorage is also included. The review of headed reinforcement includes historical background, a survey of commercially available products, a summary of the published research on headed reinforcement and related topics such as deeply embedded anchor bolts and the bearing capacity of rigid plates, and a review of pertinent code provisions. The review of strut-and-tie modeling (STM) includes an historical background, an overview of the STM design process, a review of code provisions, and a summary of selected research.

17. Key Words	18. Distribution Statement
concrete reinforcement, headed reinforcement, strut-and-tie modeling, anchorage	No restrictions. This document is available to the public through the National Technical Information Service, Springfield, Virginia 22161.

19. Security Classif. (of report)	20. Security Classif. (of this page)	21. No. of pages	22. Price
Unclassified	Unclassified	116	

Form DOT F 1700.7 (8-72) Reproduction of completed page authorized

ANCHORAGE BEHAVIOR OF HEADED REINFORCEMENT: LITERATURE REVIEW

by

M. K. Thompson, J. O. Jirsa, J. E. Breen, and R. E. Klingner

Research Report 1855-1

Research Project 0-1855

EXPLORE NEW USES FOR T-HEADED BARS IN STRUCTURAL CONCRETE REINFORCEMENT APPLICATIONS

conducted for the

Texas Department of Transportation

in cooperation with the

U.S. Department of Transportation
Federal Highway Administration

by the

CENTER FOR TRANSPORTATION RESEARCH
BUREAU OF ENGINEERING RESEARCH
THE UNIVERSITY OF TEXAS AT AUSTIN

May 2002

Research performed in cooperation with the Texas Department of Transportation and the U.S. Department of Transportation, Federal Highway Administration.

ACKNOWLEDGEMENTS

We greatly appreciate the financial support from the Texas Department of Transportation that made this project possible. The support and guidance of the Project Director, Dean VanLanduyt, (BRG) and Project Coordinator, Richard Wilkison, (BRG) is also very much appreciated.

DISCLAIMER

NOT INTENDED FOR CONSTRUCTION,

PERMIT, OR BIDDING PURPOSES

J. O. Jirsa, P.E., Texas #31360

J. E. Breen, P.E., Texas #18479

R. E. Klingner, P.E., Texas #42483

Research Supervisors

TABLE OF CONTENTS

LIST OF FIGURES

LIST OF TABLES

SUMMARY

The findings of a literature review of topics related to the anchorage of headed reinforcement are presented. The topics are grouped in three broad categories: conventional anchorage of reinforcement, anchorage of headed reinforcement, and a review of strut-and-tie modeling.

The review of conventional anchorage focuses on the mechanics of bond and code provisions for development length. A review of hooked bar anchorage is also included. The review of headed reinforcement includes historical background, a survey of commercially available products, a summary of the published research on headed reinforcement and related topics such as deeply embedded anchor bolts and the bearing capacity of rigid plates, and a review of pertinent code provisions. The review of strut-and-tie modeling (STM) includes an historical background, an overview of the STM design process, a review of code provisions, and a summary of selected research.

CHAPTER 1: INTRODUCTION

1.1 OVERVIEW

In structural concrete, the provisions for anchorage of straight bars and hooks sometimes present detailing problems due to the long development lengths and large bend diameters that are required, particularly when large-diameter reinforcing bars are used. Occasionally, the requirements for straight bar anchorage and lap splices cannot be provided within the available dimensions of elements. Hooked bars can be used to shorten anchorage length, but in many cases, the bend of the hook will not fit within the dimensions of a member or the hooks create congestion and make an element difficult to construct. Similarly, mechanical anchorage devices can be used to shorten lap splice lengths, but they frequently require special construction operations and careful attention to tolerances.

To address the problems that arise from the use of conventional anchorages (straight bar development length and hooks), headed bars were developed for use in the construction of concrete platforms for the offshore oil industry. Headed bars (Figure 1-1) are formed by the attachment of a plate or the forging of an upset bearing surface at the end of a straight reinforcing bar. Such bars are anchored by a combination of bond along the straight bar length and direct bearing at the head. Like a hooked bar, they can develop within a short distance, but they do not create as much congestion. Headed reinforcement has been used in the construction of platforms for the offshore oil industry. However, headed bars have not been widely used in other structures such as bridges, buildings, or other traditional concrete structures. There is little guidance currently available for the design of headed bar anchorage either in the form of code provisions or published research.

Figure 1.1: Various headed bars compared to a standard hook (#8 size)

Headed bars can potentially simplify the design and construction of complex bridge details such as closure strips, in which reduced splice lengths can be used to reduce the width of the closure gap (Figure 1-2), knee joints, in which unwieldy hooks can be replaced by compact headed bars (Figure 1-3), and deviation saddle blocks for external post-tensioning of segmental box-girder superstructures, in which complex bend details can be replaced by double headed ties (Figure 1-4).

Project 1855 was funded by the Texas Department of Transportation (TxDOT) to examine the behavior of headed bars in bridge details and to evaluate the feasibility of using headed bars for Texas transportation

structures. Additionally, the findings of an extensive literature review and experimental program are to be reported and design guidelines for the use of headed bars are to be developed.

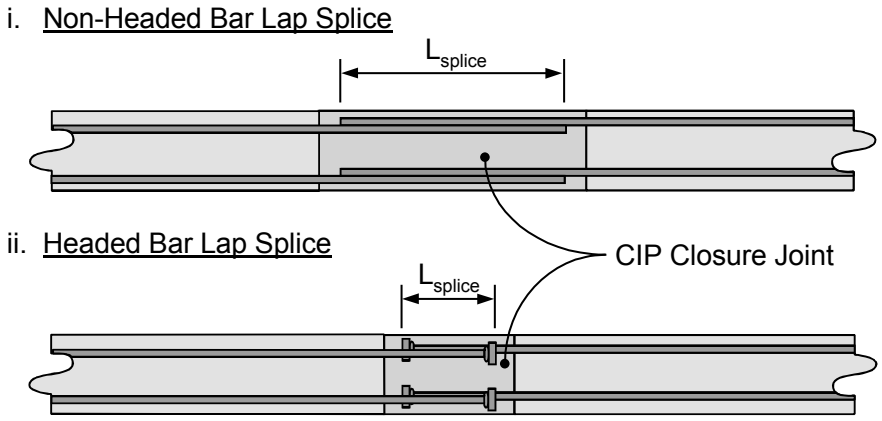

Figure 1.2: Reduction of closure strip width using headed bars

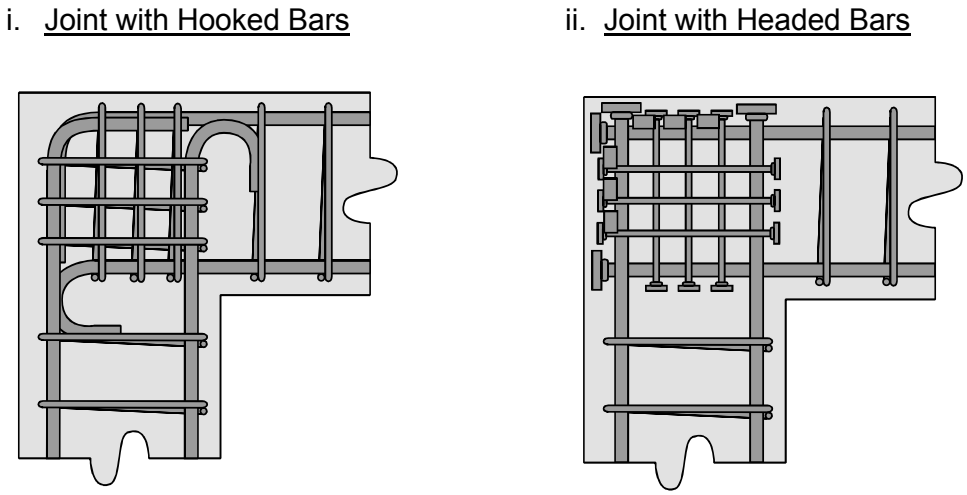

Figure 1.3: Reduction of congestion in a knee joint using headed bars

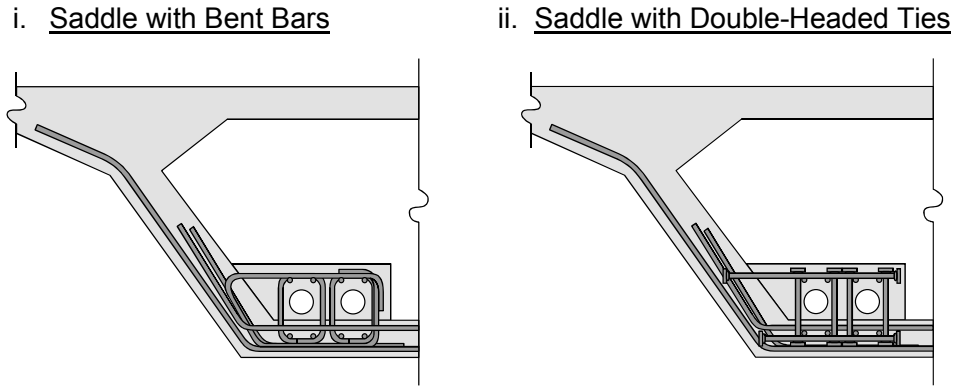

Figure 1.4: Simplification of bar details in a deviation saddle using headed bars

1.2 PROJECT DIRECTION AND SCOPE

After several meetings between the research team and TxDOT bridge design engineers to identify bridge details for which headed bars showed the most promise, two experimental directions were decided upon. TxDOT representatives expressed the most interest in the use of headed bars to reduce lap lengths and to replace hooked bars in congested discontinuity regions. Two specimen types were selected: lap splices and compression-compression-tension (CCT) nodes. These specimens were designed to be as general as possible so that the behavior of the headed bars in these details could be extrapolated to a variety of specific applications in which lap splices and CCT nodes occur.

A CCT node specimen was developed to test the anchorage of a single headed bar in a CCT node. Companion specimens with non-headed bars and hooked bars were also tested. Other variables of the test program included the angle of the compression strut, head size and shape, bar size, and the presence of confinement in the nodal zone. A total of 64 CCT node specimens were tested. In addition to studying the anchorage performance of headed bars, these specimens were used to determine the behavior of CCT nodes and the current provisions related to strut-and-tie modeling (STM) were evaluated against the results.

A lap splice specimen was developed to test the anchorage of multiple headed bars anchored within a single layer lap splice. Companion specimens with non-headed bars were also tested. Other variables of the lap splice test program included the lap length, the head size and shape, the bar spacing, contact versus non-contact laps, and the presence of confinement in the lap zone. A total of 27 lap splices were tested.

This report, CTR 1855-1, contains the summary of a comprehensive literature review. Topics within the literature review are divided into three categories: conventional anchorage focusing on bond of straight reinforcing bars and hooks (Chapter 2), headed reinforcement and related topics (Chapter 3), and strut-and-tie modeling (Chapter 4). Additional reports will describe the test program and results:

CTR 1855-2 *"Anchorage of Headed Reinforcement in CCT Nodes"* [103]

CTR 1855-3 *"Anchorage of Headed Reinforcement in Lap Splices"* [104]

CHAPTER 2: BOND AND DEVELOPMENT LENGTH OF DEFORMED BARS

2.1 INTRODUCTION

Before discussing the state-of-the-art of headed reinforcement, a brief overview of conventional anchorage of reinforcing bars will be presented emphasizing bond of straight reinforcement and standard hook details. In this chapter, the nature of bond stress and how it is utilized to achieve development of reinforcement will be discussed. The behavior of hooked bar anchorages is also discussed. Review of design provisions focuses on the two American codes that are pertinent to the project sponsors: ACI 318 [2] and the AASHTO LRFD Specifications [1]. ASTM Standards will also be referenced for some topics.

2.2 THE MECHANICS OF BOND

2.2.1 What Is Bond?

Bond refers to the interaction between reinforcing steel and the surrounding concrete that allows for transfer of tensile stress from the steel into the concrete. Bond is the mechanism that allows for anchorage of straight reinforcing bars and influences many other important features of structural concrete such as crack control and section stiffness. Figure 2-1 shows a straight bar embedded into a block of concrete. When the bond stress is sufficient to resist design tensile loads in the bar, then the bar is "developed" and the embedment length necessary for anchorage of the fully stressed reinforcing bar is referred to as its development length.

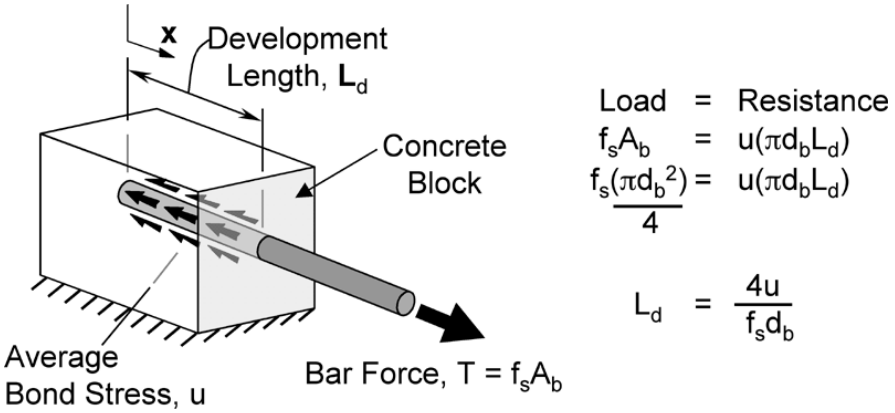

Figure 2-1: Simple concept of bond stresses

Deformed reinforcing bars develop bond stresses by means of transverse ribs that bear directly on the concrete. As tensile forces develop in a reinforcing bar, transverse cracks propagate from the edges of the ribs. This was experimentally shown by Goto [50] and is reproduced in Figure 2-2. The bond stress produced by the bearing of the ribs is not uniform. Mains [67] showed experimentally that local bond stress can be more than twice the average bond stress. Figure 2-2 also shows the distribution of tensile and bond stresses for a bar embedded in a concrete prism and loaded in tension. Bond stress peaks near cracks and tapers off as the concrete carries more of the tensile load. The bond stress then reverses sign when another primary crack is formed. The process by which concrete around reinforcing bars shares tensile loads is called "tension stiffening." It is important to note that a bar does not uniformly yield in cracked concrete when it is properly bonded. Yielding occurs only locally near cracks.

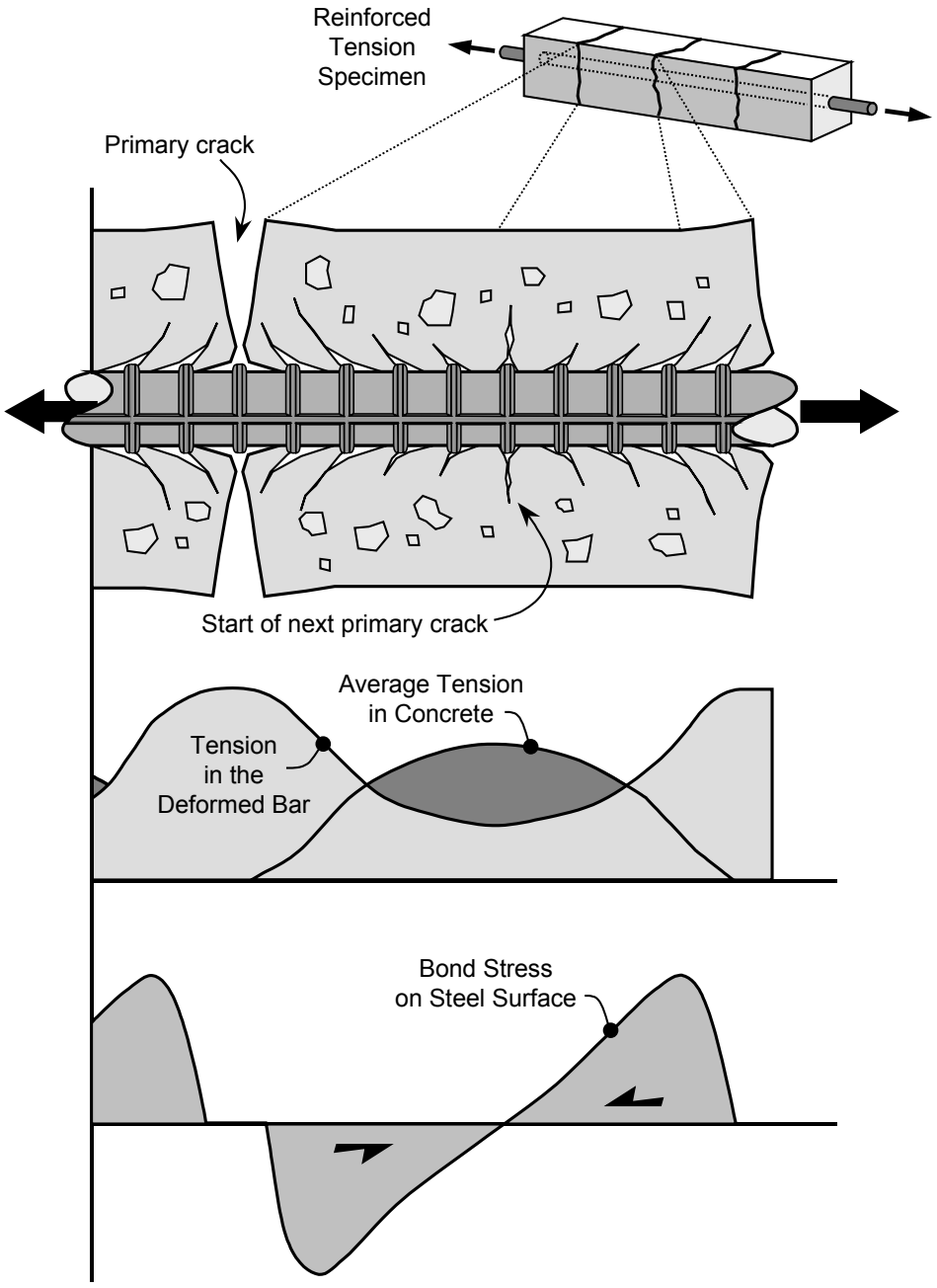

Figure 2-2: Transverse cracking at deformations

Bearing stresses on the ribs act in a direction roughly normal to the face of the rib. Figure 2-3, part i shows bearing stresses acting at an angle, θ_{bond}, relative to the bar axis. These bearing forces can be split into parallel and perpendicular components (Figure 2-3, part ii). The components parallel to the bar constitute the bond responsible for resisting the tensile force in the reinforcement. The components perpendicular to the bar act outward from the bar surface as splitting stresses on the concrete. These radial splitting stresses must be counteracted by ring tension stresses in the concrete surrounding the reinforcing bar, section A-A of Figure 2-3, part iii. Ultimately, the radial splitting stresses exceed the tensile capacity of the surrounding concrete and splitting cracks begin to propagate from the bar surface.

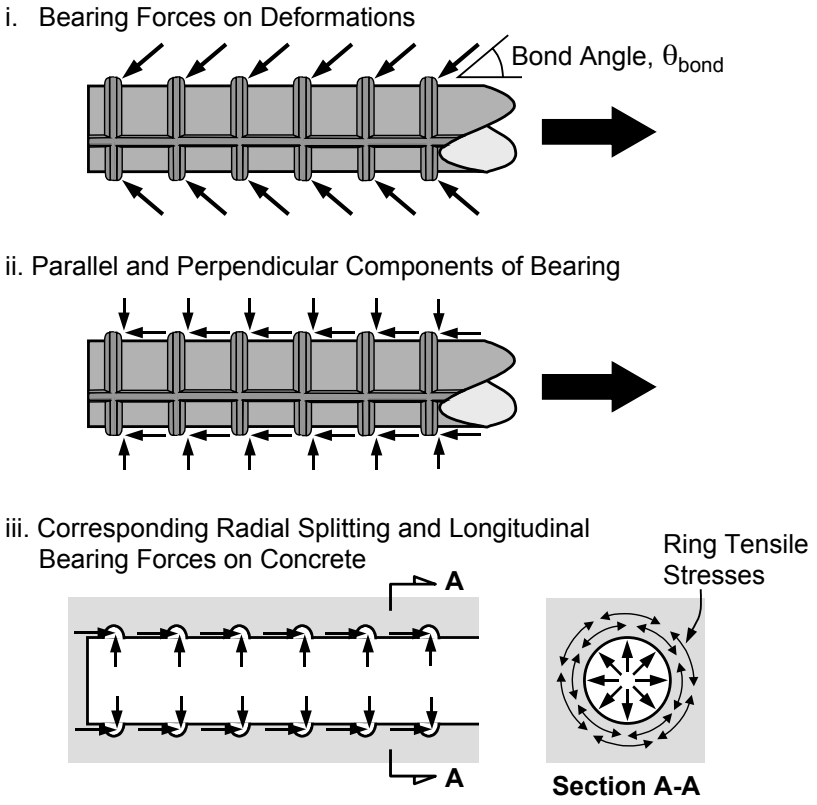

Figure 2-3: Bond and splitting components of rib bearing stresses

Bond can fail in multiple ways. The longitudinal bond stresses can exceed the shear strength of the concrete keys between ribs and the bar can pull free. This is referred to as a "pullout" failure (It is also sometimes termed a "shear-out" failure, but this report will use the more common term of pullout.). More commonly though, splitting cracks will propagate from the bar to the surface of the concrete and the cover will spall off. Figure 2-4 shows some of the many splitting cracks that can occur. The type of splitting failure that occurs in unconfined concrete is governed by bar spacing and cover dimensions. Limitless cover does not provide limitless bond. Beyond a certain level of splitting resistance, pullout failure will govern. Typically though, splitting resistance governs the level of bond stress that concrete can sustain. The rest of the discussion in this section will deal with bond and splitting.

As a rib begins to bear on the concrete a wedge of crushed paste is formed in front of the rib. This wedge acts to change the effective face angle of the rib (Figure 2-5). Thus, the bond angle, θ_{bond}, tends to change as a reinforcing bar acquires load. The effect of this is that radial splitting stresses tend to increase at a rate greater than the longitudinal bond stresses as tensile load in the reinforcing bar rises. Furthermore, efforts to reduce splitting stresses in reinforcing bar by fabricating a steep rib angle into the bars tend to be unsuccessful because the formation of the concrete wedges neutralizes the effect of the different rib angles. Lutz [66] performed experimental studies of single rib specimens. He observed that at failure the angle of the concrete wedge was between 30^o and 45^o and that ribs with face angles less than 30^o showed poor bond-slip performance in tests.

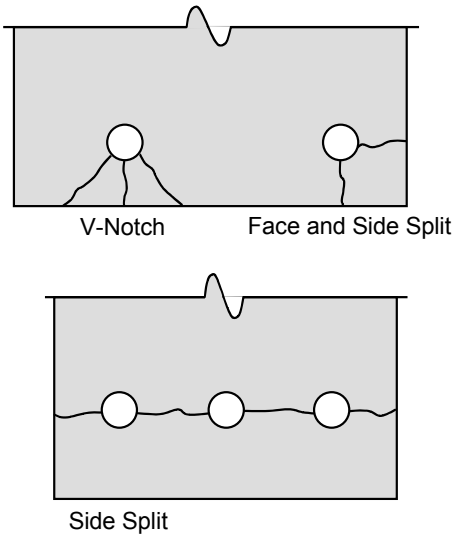

Figure 2-4: Possible splitting crack failures

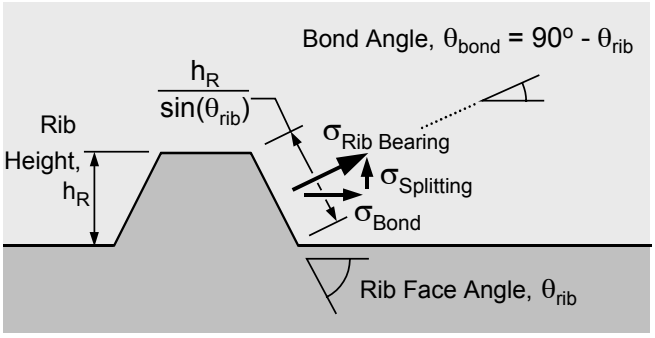

i. Initial Bearing of Rib on Concrete

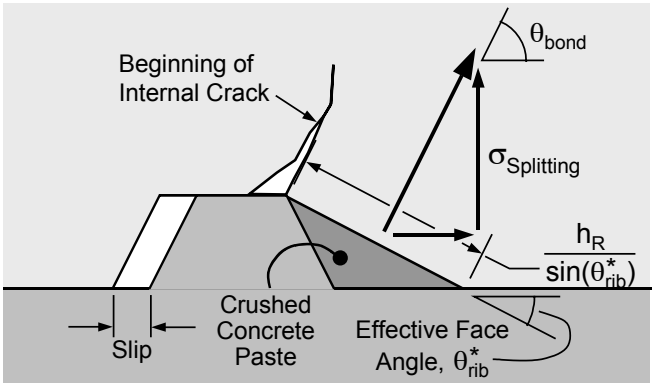

ii. Final Bearing of Rib on Concrete

Figure 2-5: Mechanics of rib bearing on concrete

While rib face angle does not significantly affect bond strength within certain limits, rib bearing area has been shown to be important. Rib bearing area can be increased by manipulating one or both of two geometric parameters: the height of the ribs or the spacing of the ribs. Rib bearing area is generally

referred to by the ratio of rib bearing area to shearing area of the concrete keys between successive ribs. This ratio is referred to as the relative rib area, R_r. The effect of the relative rib area has been studied since the earliest research on bond. Abrams [14] was the first to recognize that bond was enhanced by increases in relative rib area. Later studies by Clark [32, 33] supported Abrams' conclusions. Clark's studies were used to establish the modern ASTM standards for deformation requirements on reinforcing bars [3]. Both Abrams and Clark recommended deformation criteria that translate to relative rib areas around 0.2 for optimum bond performance. However, the current ASTM requirements only provide for relative rib areas less than 0.1 for reinforcing bars. Most recently, studies by Darwin et al. [36, 37] and Hamad [51] have led to a reconsideration of the issue of rib geometry and bond performance. Darwin and Hamad have also recommended a relative rib area of 0.2 for optimal bond performance of reinforcing bars with the limitation that ribs not be spaced too closely. The primary reason for the lower relative rib areas is the cost and difficulty of producing bars with more pronounced rib patterns. To date bar producers have not been willing or convinced that the advantages of higher relative rib areas are warranted from a cost/benefit point of view.

Based on the experimental evidence on the mechanics of rib bearing, several models have been developed to calculate bond as a function of ring-tension stresses in the surrounding concrete. All of the models are based on various stress-strain relationships for concrete tensile strength. Figure 2-6 illustrates the basic models. The elastic-uncracked model assumes that once the tensile strength of the concrete is reached and splitting cracks begin, bond failure is imminent. In this case, the bond capacity is limited by purely elastic material behavior. The elastic-cracked model achieves a slightly greater bond capacity by allowing a cracked zone around the reinforcing bar with elastic behavior outside of that zone. No tensile stress is allowed within the cracked zone. The elastic-cracked model has a higher capacity than the purely elastic model by allowing the region of maximum tensile stress to move away from the bar surface to a distance where the stresses act over a larger circumference. The elastic-cohesive model allows for tensile stresses within the cracked zone based on cohesive material theory that derives from concrete fracture mechanics. The plastic model allows for a perfectly plastic distribution of tensile stress and gives the highest capacity. The first, second and fourth models were first analyzed by Tepfers [102]. The third model was developed by Rosati and Schumm [49, 96].

The elastic-cohesive model of concrete tensile behavior was derived to adapt principles of fracture mechanics to analysis of concrete materials [9]. Ordinary linear elastic fracture mechanics does not properly describe concrete cracking. In order to apply fracture mechanics theory, a zone of material softening is included in the crack model. This zone is called the "fracture process zone" (Figure 2-7). Within the fracture process zone, micro-cracked concrete carries some tensile resistance. At the tail of this zone, the "true crack" grows by spreading from micro-crack to micro-crack. At the head of the zone, micro-cracks begin to form as strains in the concrete exceed a certain tensile limit. The truly cracked concrete does not carry any tensile resistance. The elastic-cohesive model of bond stress thus assumes that the cracked-cohesive zone around the reinforcing bar is still within the process of crack development and has exceeded the threshold of elastic behavior where optimal tensile resistance occurs.

Tepfers compared his models of bond resistance to experimental results from pullout tests and beam tests of lapped specimens [102]. Rosati and Schumm later added their model to Tepfer's analysis [49]. Figure 2-8 shows the predictions of the four different models on a plot of bond capacity versus cover dimension (the parameters are normalized with respect to bar diameter and concrete tensile strength, f_{ct}). Tepfer's experimental data are included in the plot. There is much scatter in the experimental data, but it is obvious that the elastic-cracked model forms a good lower bound and the plastic model a good upper bound for ultimate bond capacity governed by splitting. Only, the elastic-cohesive model cuts through the data. As a description of behavior it is probably the best, but there is too much scatter in the actual data for any model to accurately predict capacity.

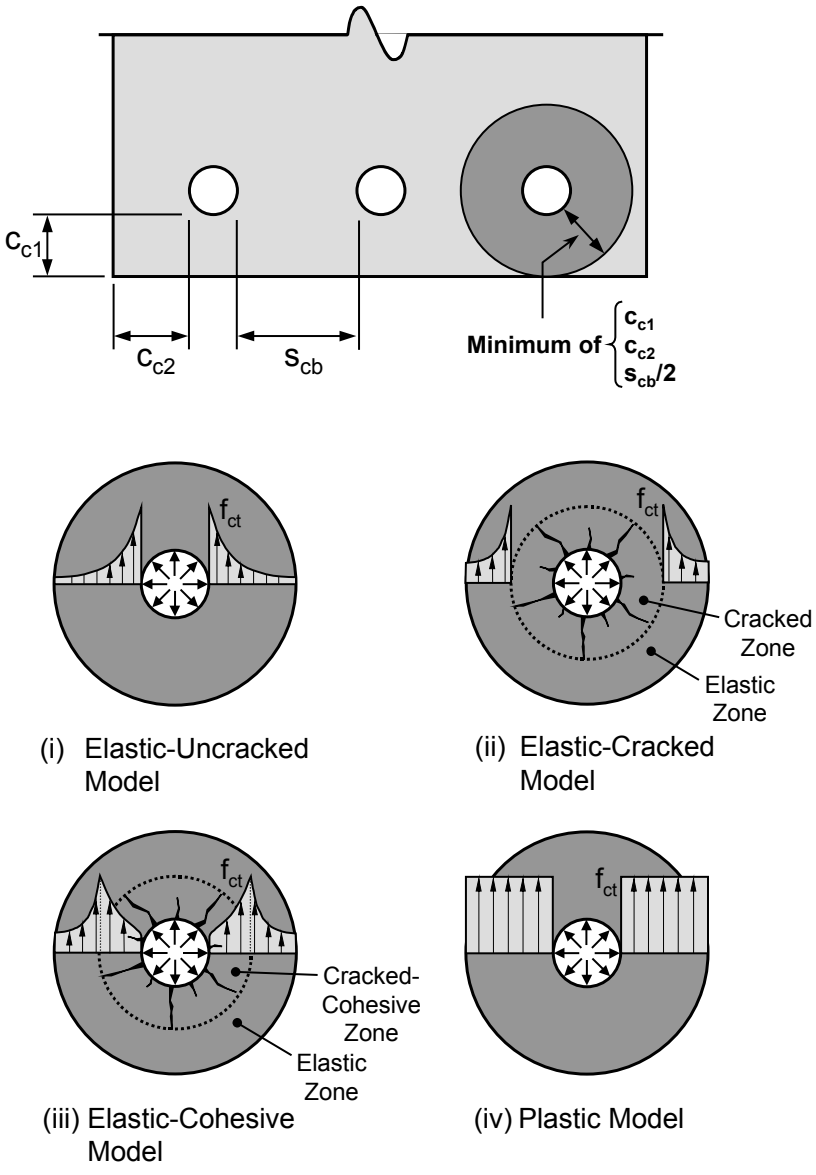

Figure 2-6: Models for ring-tension behavior

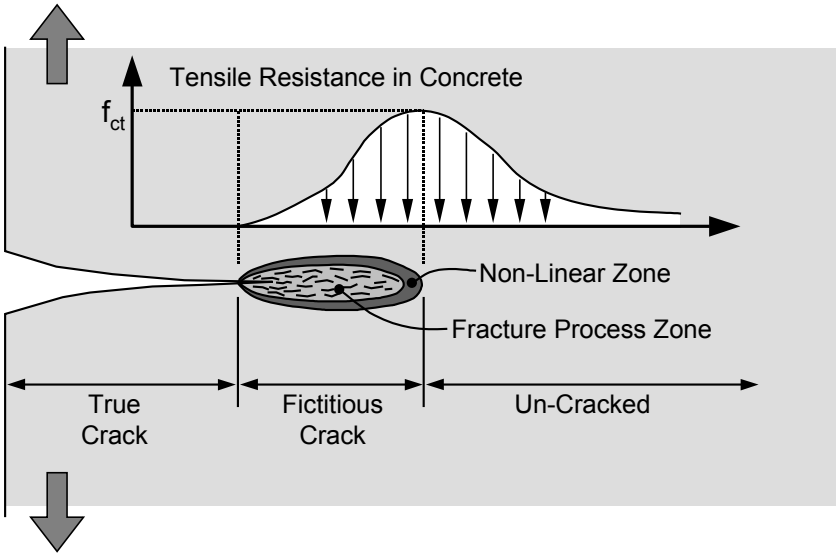

Figure 2-7: Cohesive crack growth (after Bažant [9])

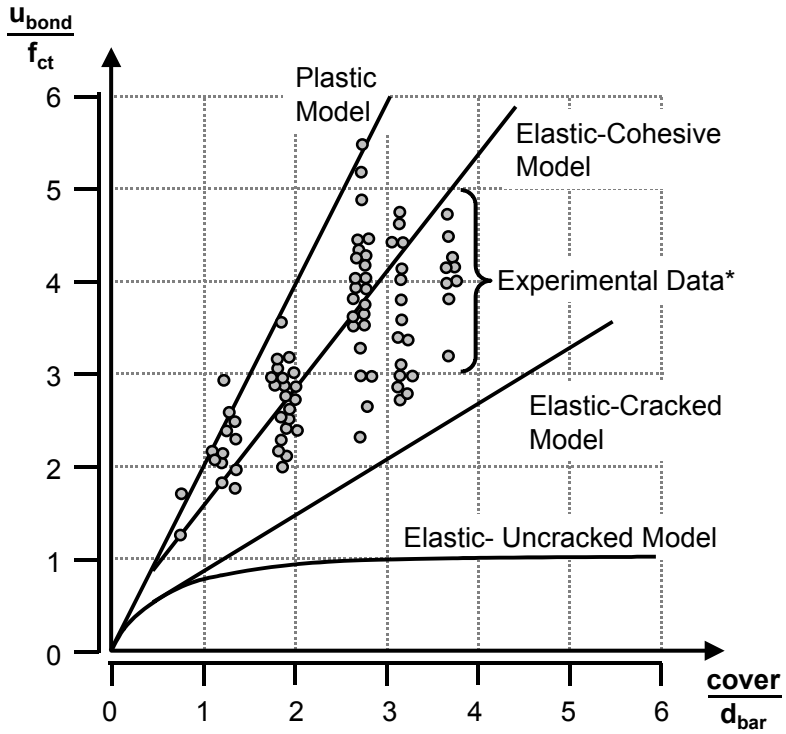

Figure 2-8: Comparison of various bond model predictions with experimental data (after Tepfers [102] and Gambarova [49])

***Data credited to Tepfers**

2.2.2 Lap Splices

When bars are lap spliced, they are typically laid adjacent to one another. The interaction of ring-tension stresses around the bars creates an oval shaped tensile zone, but otherwise, the bond developed by the bars is comparable to that of single bars in tension. Figure 2-9 shows the zone of ring tension stresses and the common splitting crack patterns.

Older research by Chamberlin [29] and Chinn, Ferguson, and Thompson [31] demonstrated that there is no significant change in bond strength for increasing clear space between spliced bars. Their studies showed that adjacent deformed bars which are tied together can achieve greater than normal bond strengths due to interlocking of the ribs on each bar. More recent research by Hamad and Mansour [52] showed an optimal lap spacing of $5d_b$ where a 7 - 10% increase in bond strength over contact splices was observed. Beyond $5d_b$ the bond strength dropped off below the contact splice bond strength. Their tests were for lap lengths of 17 to $20d_b$. Altogether, the research suggests that lapped bar data can be compared to non-lapped bar data for analysis of anchorage and bond.

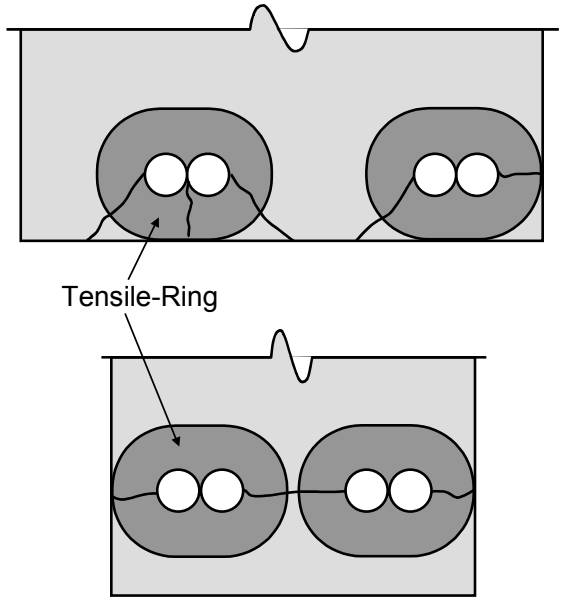

Figure 2-9: Splitting around lapped bars

2.2.3 Confinement of Splitting Stresses

The splitting strength of concrete can be enhanced if compressive stresses are superimposed onto the tensile-ring stresses around the reinforcing bar. The concrete is said to be "confined" when compressive forces are used to counteract internal splitting forces. Confinement can be classified as two types: active and passive. Active confinement will refer to stress fields that are created by the actions of superimposed structural loads such as dead and live loads and prestress forces. Passive confinement will refer to stress fields that are created by forces in the mild reinforcement placed around anchorage zones such as stirrups or spiral rings.

Figure 2-10 shows the state of stress that occurs at a beam end where the longitudinal reinforcement terminates. This is an example of active confinement. Over the bearing pad a vertical compression field is created by the balance of the bearing reaction and the beam shear. This vertical compression field is superimposed onto the ring-tension field caused by bond of the reinforcing bars. The vertical components of the ring tension field are partially counteracted. As a result, the beam end has an enhanced resistance to horizontal splitting cracks and the anchorage of the longitudinal reinforcing bars is improved.

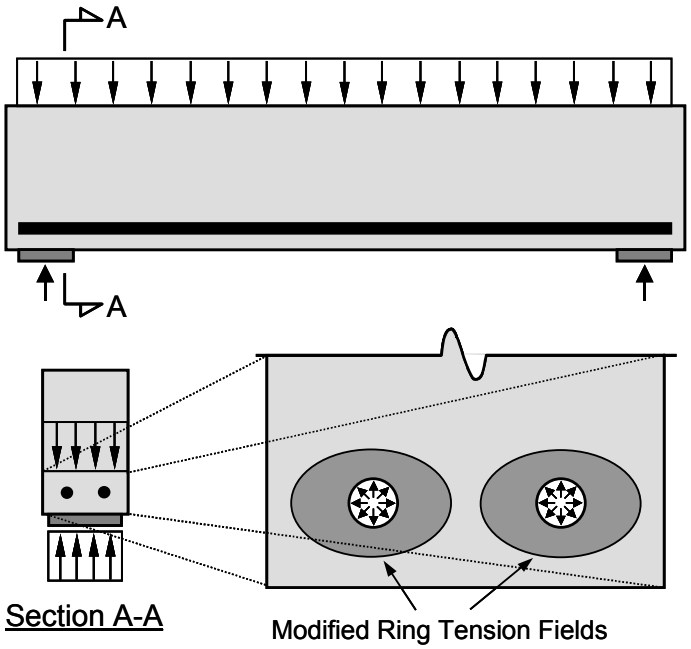

Figure 2-10: Active confinement in a beam end bearing

Spirals, transverse ties, and stirrups in anchorage zones are examples of passive confinement. These systems are distinguished from active confinement because they are dependent on crack propagation to become effective. Such confinement systems do not begin to counteract splitting forces until radial cracks emanating from the bar surface cross the axis of the confining steel (Figure 2-11). Because confining steel does not play any part in resisting tensile splitting stresses until the splitting cracks intersect the steel, they are termed a passive system. The splitting resisted by confining reinforcement is dependent on the width of splitting cracks, which taper along their length from the bar being developed (Figure 2-12). Thus, the confining reinforcement is more effective when it is placed close to the surface of a bar.

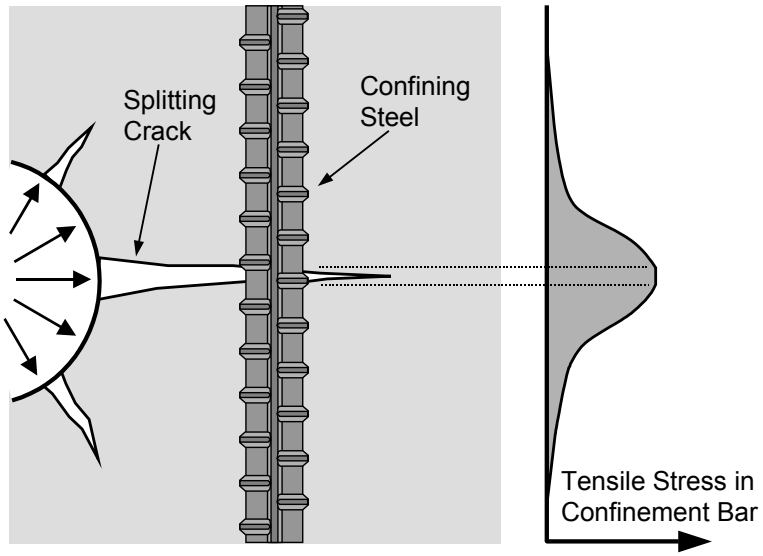

Figure 2-11: Confinement steel in the vicinity of a splitting crack

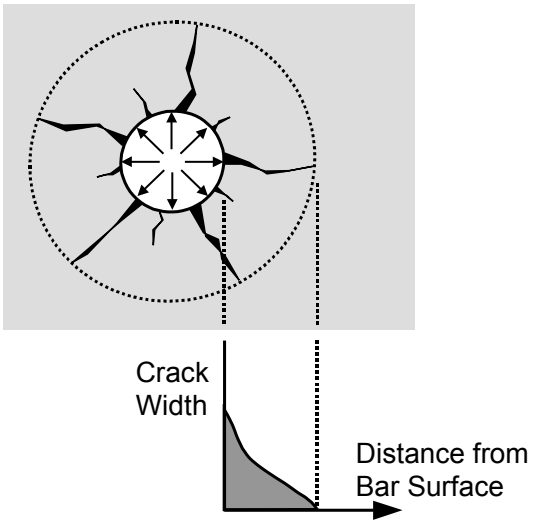

Figure 2-12: Crack widths of splitting cracks

Many experimental studies have been performed on passive confinement. The results of those studies have been incorporated into the development length modification factors found in the ACI 318 code [2], the AASHTO Bridge Design Specifications [1], and in many other structural concrete design codes found around the world. In general, mild reinforcement, placed so that it intersects splitting crack planes, helps to improve bond capacity if splitting failure modes control. Beyond a certain level, pullout failure modes begin to determine the bond capacity and additional confining steel fails to improve bond capacity.

Three references have been found regarding the effects of active confinement on bond:

Untrauer and Henry [106] studied the effects of lateral pressure on 6" sided cube pullout specimens with #6 and #9 bar sizes. Their lateral pressures ranged from 0 % to 50 % of f_c', or 0 psi to around 2500 psi. They found that there was a slight increase in bond strength related to the square root of the lateral pressure. They also concluded that the effect of the lateral pressure was more pronounced for smaller embedment lengths.

Lormanometee [64] studied specimens modeled after the Untrauer and Henry tests but with the addition of studying the effect of the proximity of the lateral load application. Lormanometee found slightly higher bond capacities than Untrauer and Henry had with less dependence on the magnitude of the lateral pressure. This may have been due to the method of load application or differences in the deformation pattern of the reinforcing bars or the mix parameters of the concrete. Lormanometee determined that the lateral pressure was more effective when applied close to the surface of the reinforcing bar and diminished with increasing concrete cover between the bar and the applied lateral load.

Thrö [105] performed pullout tests with similar lateral pressures, but with bars anchored over much shorter development lengths (~ $3d_b$). Thrö maintained a constant ratio between the lateral pressure and the steel stress as the test was being performed. He found increases in bond stress for increasing lateral pressures. He recommended a reduction factor for development length that is linearly proportional to the active lateral pressure with a cutoff at 1,160 psi. The reduction factor reduces the development length by half at that value. Thrö's results showed a much greater impact on bond from lateral compression than the previous tests, but it should be noted that his specimens used a short bar embedment length which may not be translatable to longer development lengths.

The effect of lateral active confinement is an important issue for the anchorage performance of deformed bars in nodal zones which is discussed in Chapter 4. So far, the research has been limited and the results

inconsistent. Furthermore, the effects of platen restraint (additional restraint provided by load plates which provides biaxial lateral compression – see Figure 2-13) have not always been clearly separated from the effects of lateral compression in the available studies. Thus, the topic remains a gray area in the knowledge of bond and development of reinforcement. However, in practice, when lateral confinement forces are provided by design loads, no enhancement to bond should be taken into account due to the unpredictability of actual loading conditions.

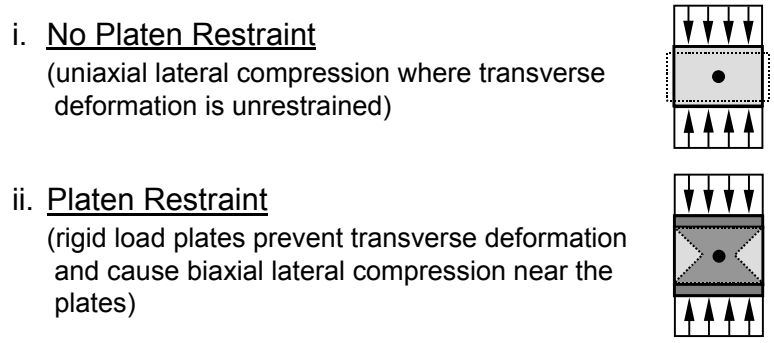

Figure 2-13: Platen restraint in lateral compression studies

2.2.4 Effect of Concrete Properties

The splitting failure mode of bond is dependent on the tensile strength of concrete. Thus, the mechanical properties of concrete are important for good deformed bar development. Two other concrete related parameters can also have significant affects on bond capacity: lightweight concrete and top cast bars.

Lightweight concretes are produced by using special porous lightweight aggregates or by aerating the cement paste. In both cases, the pore spaces introduced into the hardened mix make lightweight concretes weaker in tension and shear than normal weight concretes with equivalent compression strengths. Because of their weaker tensile properties, lightweight concretes generally give lower bond capacities than normal concretes. In some cases, the shear strengths are low enough that deformed bars will pullout rather than split the concrete in pullout tests. Because of their weaker bond capacities, lightweight concretes are penalized in design code development length equations. Generally a factor of 1.3 is applied to the development length when lightweight concrete is used (this equates to a 23% reduction in predicted bond capacity).

When concrete is placed and vibrated, lighter components of the mix will rise as heavier components settle to the bottom. When this occurs near reinforcing bars, air pockets and bleed water tend to collect on the undersides of the bars in place of coarse aggregates (Figure 2-14). When the concrete sets, the bond around the bar is weaker on its underside because of the inferior quality of the concrete there. This effect is more pronounced for bars that have greater quantities of concrete placed under them than bars that are positioned close to the bottom surface of forms. Design code equations for development length distinguish this effect by requiring a “top-cast bar” factor for reinforcement with more than 12" of concrete placed beneath them. No top-cast bars were included in this research project, but the understanding that bond on the underside of deformed bars is weaker than bond on the top of deformed bars helped to determine the placement of strain gages when reinforcing bars were instrumented in this project.

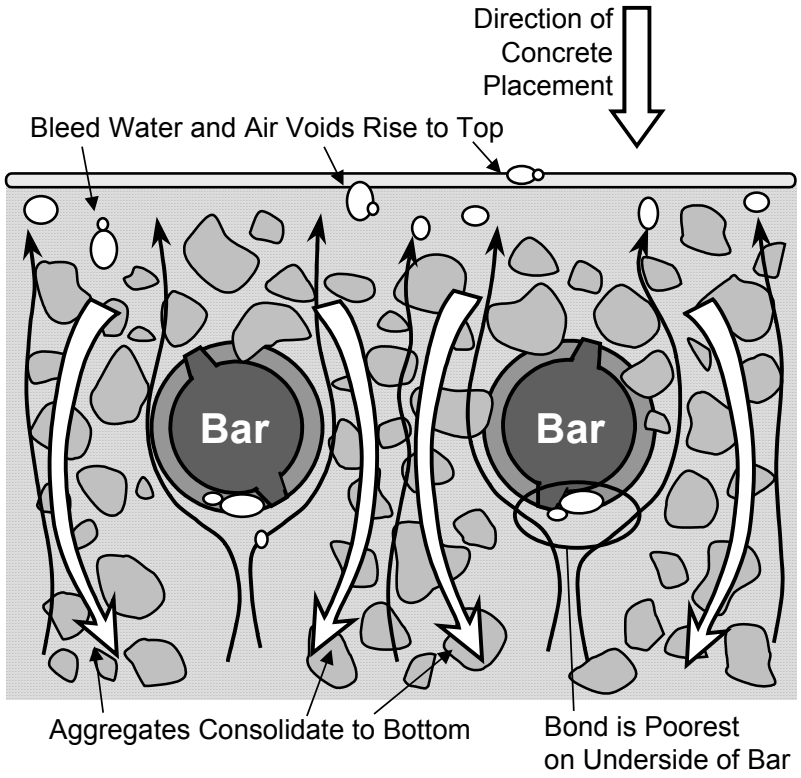

Figure 2-14: Top cast bar effect

2.2.5 Epoxy-Coated Reinforcement

Epoxy-coatings are placed on reinforcing bars to provide corrosion protection. However, the presence of the epoxy coating inhibits the ability of the reinforcing bar deformations to bear on the concrete by acting as a friction reducer and by partially concealing the height of the deformations. Epoxy-coated bars have substantially reduced bond from uncoated bars. Research on high relative rib area reinforcing bars (Darwin et al. [36] and Hamad [51]) has shown that the loss of bond from epoxy coating is less when rib deformations are large indicating that epoxy-coating has a lessened effect when anchorage relies more on direct bearing. However, in practice high relative rib area reinforcing bars are typically harder to coat than normal reinforcing bars.

2.2.6 Measurement of Bond Stress

Theoretical understanding of bond provides a framework for design methodologies, but data are needed to calibrate theoretical derivations into design equations. Such data can only be obtained through experimental studies. Because the experimental data for bond stress has been critical for the empirical calibration of design equations, it is important to understand the ways in which bond has been traditionally measured. Several different types of experimental tests have been reviewed in the literature on bond. Five categories of bond specimens have been categorized from the literature: single bar pullout specimens, beam specimens, beam-end specimens, lap splice tensile specimens and lap splice beam specimens. Though several experimental studies may be said to use the same category of specimen, the particular details of specimens used in different studies may vary. There is little standardization of the different types of bond specimens and the categories discussed herein are broad generalizations based on certain similarities of mechanics.

Figure 2-15 presents the classic pullout specimen. A single bar is cast into a block or cylinder of concrete. Confining reinforcement may or may not be placed around the embedded bar. Failure generally occurs by splitting to the closest cover surface unless confinement is very heavy in which case a pullout failure can be forced. These specimens were used extensively by Abrams for his acclaimed study of bond though he also used beam specimens [14]. Bar force can be measured directly as well as slip at the loaded and free ends of the bar. Pullout specimens have the disadvantage that the load ram bears directly on the concrete surface and provides platen restraint near the loaded end of the bar. Such compression is not always present when bars are developed in practice and the results of pullout tests can tend to over-estimate bond stresses.

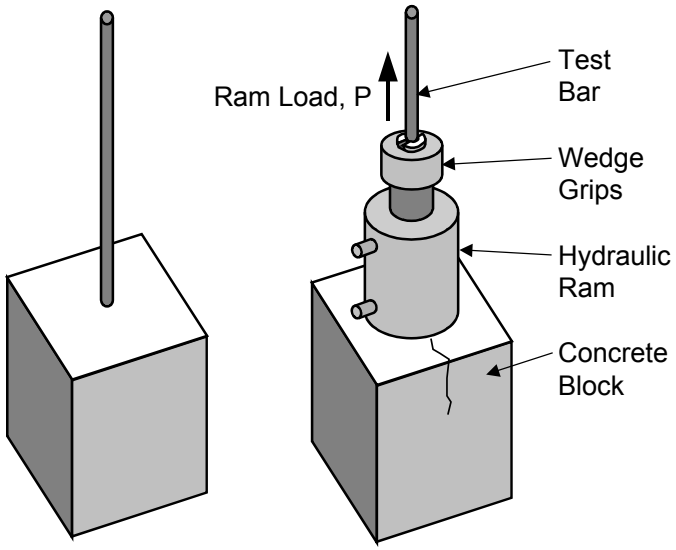

Figure 2-15: Typical pullout specimen

Beam specimens are more accurate representations of bar anchorage than pullout specimens. The test bars are cast into a concrete beam that is then loaded in flexure. The termination point of the bars is placed away from load points where local compression can enhance the bond and restrain splitting cracks. Figure 2-16 shows a typical specimen. The direction and placement of reaction loads in the beam specimen can be manipulated to create constant moment or moment with shear along the bar development length. Beam specimens are more realistic than pullout specimens, but are much more costly in material, space, and labor to fabricate and test. It is also harder to determine the bar forces in beam tests. Bar forces must be calculated from beam moments or from strain gage readings. Thus test data from beams are much less common than from other forms of bond tests.

A compromise specimen somewhat between a pullout test and a beam test is the stub-beam or beam-end specimen. Figure 2-17 shows a typical beam-end specimen. Only the end region of the beam is fabricated for such a test. Less material is necessary than for a full beam test and the exposure of the bar for loading makes determination of the bar force simple. Direct compression of the concrete near the loaded end of the bar is avoided by separating the load ram from the surface of the specimen. The free end of the bar is either terminated outside of the rear reaction point or debonded over its length in that zone so that active lateral pressure is avoided. Access to the bar's free and loaded ends is available for slip measurements. The test bar is placed in direct tension, which may or may not be representative of actual bond situations. The beam-end specimen was recently standardized in ASTM Specification A944-99 "*Standard Test Method for Comparing Bond Strength of Steel Reinforcing Bars to Concrete Using Beam-End Specimens*" [4] and is the only standardized bond specimen at this time. The main disadvantage of the beam-end test is the complex load arrangement required to test the specimen.

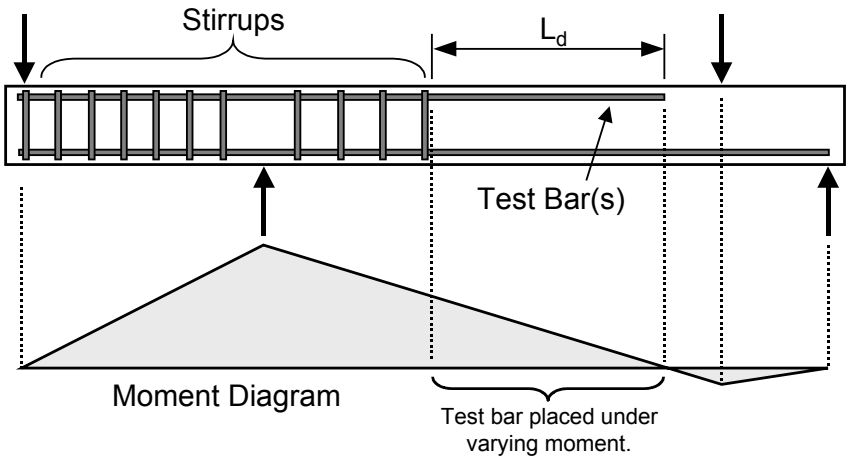

Figure 2-16: Typical beam specimen for bond tests

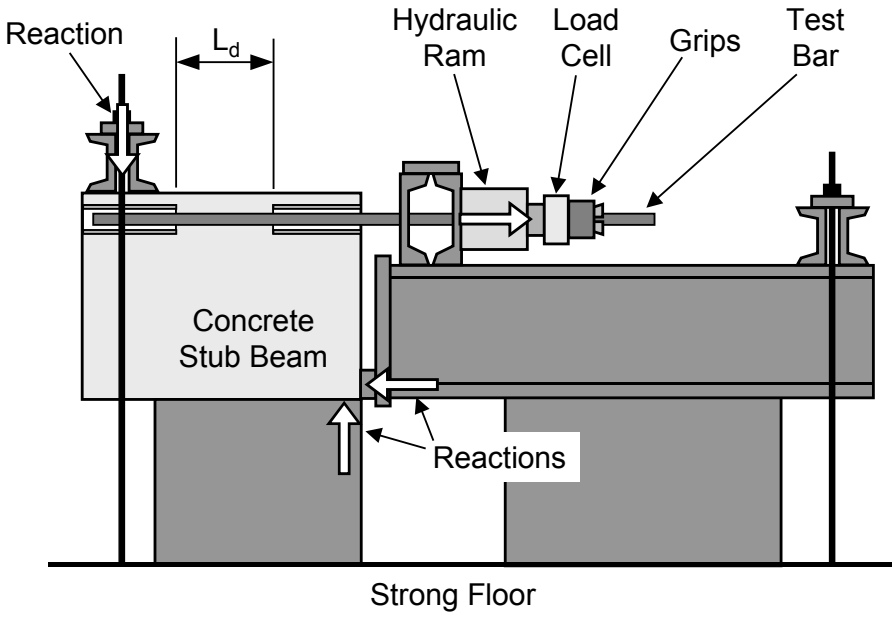

Figure 2-17: Typical beam-end test

The remaining two categories of bond tests utilize lap splices. Tensile lap splice specimens resemble the basic pullout test, but no direct compression of the concrete is caused by the loading of the specimen. Figure 2-18 shows some typical specimens. The test is essentially a modified form of the pullout specimen. The last type of bond test, the lap splice beam test is shown in Figure 2-19. The lap zone can be placed in constant moment or a varying moment zone with shear depending on the arrangement of external loads.

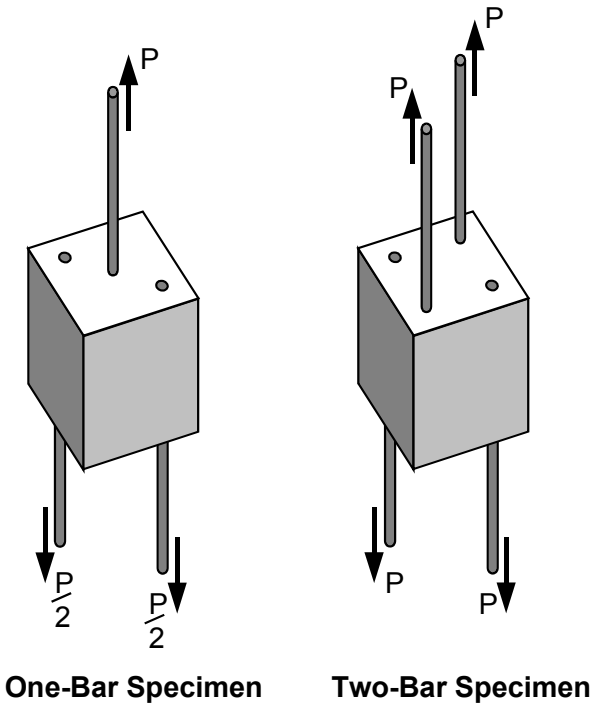

Figure 2-18: Typical tensile lap splice specimens

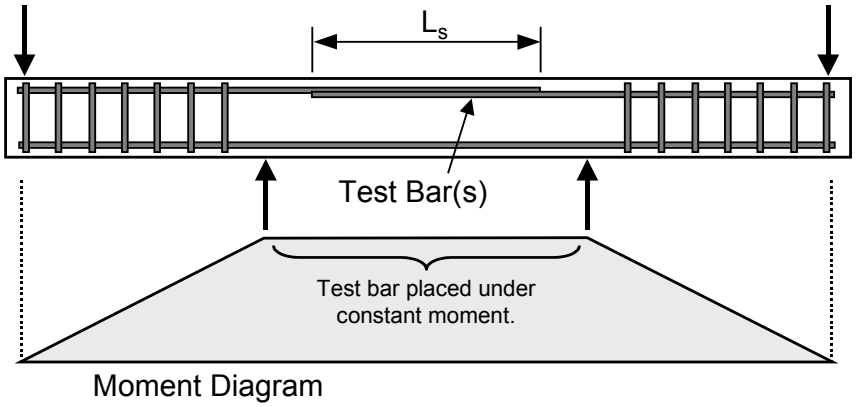

Figure 2-19: Typical beam specimen for lap tests

2.3 CODE PROVISIONS FOR DEFORMED BARS

2.3.1 Quality of Reinforcing Bars: ASTM A615

Quality of deformed reinforcing bars is controlled by ASTM A615 "*Standard Specification for Deformed and Plain Billet-Steel Bars for Concrete Reinforcement*" [3]. This document contains standards for chemical composition, deformation geometry, tensile strength, bending strength, and weight of deformed reinforcing bars. With respect to deformation geometry, four parameters are controlled: rib spacing, included rib angle (not to be confused with the rib face angle), rib height, and the gap caused in the transverse ribs by the main (longitudinal) rib of the bar. Figure 2-20 graphically presents these parameters.

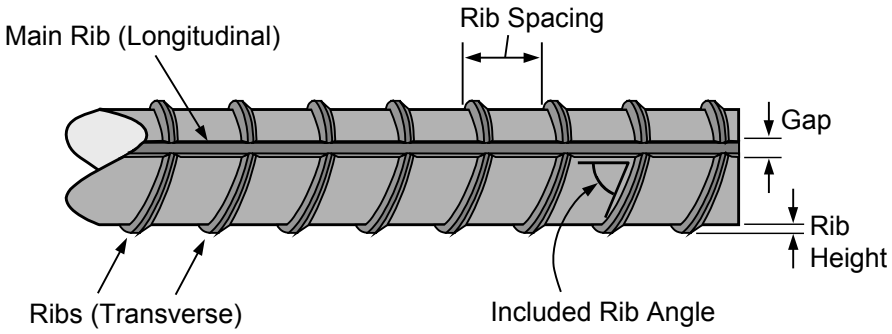

Figure 2-20: Important dimensions for reinforcing bar specifications

The spacing of ribs shall not exceed 0.7 bar diameters and shall be uniform along the bar length. The included rib angle relative to the axis of the bar shall not be less than 45°. No gap shall be more than 12.5% of the perimeter of the rib and the sum of all gaps within the path of a rib shall not total more than 25% of the perimeter of the rib. The average minimum height of the ribs is required to be between 0.04 - 0.05 bar diameters. Specific values for each bar size are tabulated in the ASTM specification. The ASTM requirements for deformations are listed in Table 2-1.

Table 2-1: ASTM A615 requirements for reinforcing bar deformations

Bar Size	Maximum Avg. Spacing (in)	Minimum Avg. Height (in)	Maximum Gap (in)
# 3	0.262	0.015	0.143
# 4	0.350	0.020	0.191
# 5	0.437	0.028	0.239
# 6	0.525	0.038	0.286
# 7	0.612	0.044	0.334
# 8	0.700	0.050	0.383
# 9	0.790	0.056	0.431
# 10	0.889	0.064	0.487
# 11	0.987	0.071	0.540
# 14	1.185	0.085	0.648
# 18	1.580	0.102	0.864

2.3.2 Code Equations for Development Length

Design equations for the anchorage of reinforcing bars do not present results in terms of predicted bond stresses, rather they provide a required development length necessary to achieve the full yield strength of a bar. Two code provisions are discussed in this section: the ACI 318 code and the AASHTO Bridge Design Specifications.

2.3.2.1 ACI 318-02

The ACI 318-02 *Building Code Requirements for Structural Concrete* [2] contains provisions for straight bar development in Section 12.2 "Development of deformed bars and deformed wire in tension." Two methods for calculating a development length are allowed. A table is provided in sub-section 12.2.2 that

contains simplified and conservative equations for development length given certain conditions of cover, spacing, etc. for the bars being anchored. Sub-section 12.2.3 contains a more accurate and involved equation for development length. This equation (12-1 in the ACI code) is shown below:

$$\frac{L_d}{d_b} = \frac{3}{40}\frac{f_y}{\sqrt{f_c'}}\frac{\alpha\beta\gamma\lambda}{\left(\frac{c + K_{tr}}{d_b}\right)} \qquad (2\text{-}1)$$

with

$$\frac{c + K_{tr}}{d_b} \le 2.5$$

and

$$K_{tr} = \frac{A_{tr} f_{yt}}{1500sn} \qquad (2\text{-}2)$$

L_d = development length of bar (same units as d_b , typically inches)

d_b = nominal bar diameter (inches)

f_y = yield stress of reinforcing steel being developed (psi)

f_c' = cylinder compressive stress of concrete (psi, limited to 10,000 psi maximum in section 12.1.2)

α = reinforcement location factor (1.3 if 12" of concrete cast below bar)

β = coating factor (1.5 for epoxy-coated bars with minimum clear dimension $\le 3d_b$, 1.2 for all other epoxy-coated bars)

γ = reinforcement size factor (0.8 for # 6 bars and smaller)

λ = lightweight aggregate factor (1.3 when lightweight aggregates are used)

c = minimum of half the center to center bar spacing or the cover dimension measured from the center line of the bar to the surface of the concrete

K_{tr} = transverse reinforcement index

s = maximum spacing of transverse reinforcement within L_d , center-to-center (in)

n = number of bars or wires being developed along the plane of splitting

A_{tr} = total area of transverse reinforcement within the spacing, s, that crosses the plane of splitting through the reinforcement being developed (in^2)

f_{yt} = yield stress of transverse reinforcement (psi)

Development length is limited to a minimum of 12".

The ACI development length equation is based on work performed by Orangun, Jirsa, and Breen [86, 87]. They evaluated the results of several well-documented studies on lap lengths and development lengths from the United States and Europe and used data from those studies to fit an equation via regression analysis. The choice of terms and positioning of variables within the equation was based on theoretical considerations, but the final selection of constants was based on regression analysis. The equation they developed is not quite the same as the ACI code equation, but is very close. They recommended the factors used in the ACI equation plus an additional factor for widely spaced bars that would shorten the necessary development length. They recommended a ϕ factor of 0.8 for their equation. The ACI equation has a ϕ of 0.9 built into it.

Though Orangun, Jirsa, and Breen reported that they found no difference in the development length required for single bars and lapped bars and many other researchers have noted the same results, the ACI

Code, Section 12.15 requires multipliers for lapped bars in most situations. Splices are categorized according to the ratio of steel provided to that required and the amount of steel being spliced at a given location. Table 2-2 summarizes the categories and the required splice lengths, L_s. The multipliers are used as a penalty (by increasing the lap length) to dissuade designers from needlessly or unwisely using lap splices in a structural design and particularly to prevent the Class B splice situation in which all tensile bearing bars in a section are spliced at a single location.

Table 2-2: ACI 318-02 multipliers for development length of lap splices

$\frac{A_s \text{ provided}}{A_s \text{ required}}$	Maximum % of A_s Spliced Within the Required Lap Length	
	50%	100%
≥ 2	Class A Splice $L_s = 1.0L_d$	Class B Splice $L_s = 1.3L_d$
< 2	Class B Splice $L_s = 1.3L_d$	Class B Splice $L_s = 1.3L_d$

2.3.2.2 AASHTO LRFD Bridge Design Specifications (2nd Ed., 1998)

The AASHTO LRFD *Bridge Design Specifications* [1] contain equations for reinforcing bar development length in Section 5.11.2 "Development of Reinforcement." Three equations for development length are provided in sub-section 5.11.2.1.1 and multipliers for these equations are provided in the subsequent sub-sections 5.11.2.1.2 and 5.11.2.1.3. One development length equation is for # 11 bars and smaller, one for # 14 bars, and one for # 18 bars. The first of these equations (for # 11's and smaller) is presented below:

$$L_d = \frac{1.25A_b f_y}{\sqrt{f_c'}} \geq 0.4 d_b f_y \qquad (2\text{-}3)$$

L_d = development length (inches)

A_b = area of bar or wire (in^2)

f_y = yield stress of bar being developed (ksi)

f_c' = compressive strength of concrete (ksi)

d_b = diameter of bar being developed (inches)

Note that the units of stress used in the equation are in ksi rather than psi as in the ACI equation. Modification factors are provided for many of the same conditions as the ACI equation. The factors are listed below:

- Top cast concrete (12" of concrete below bar): 1.4
- Clear dimension (cover or ½ spacing) ≤ d_b: 2.0
- Lightweight aggregates used: 1.3
- Sand lightweight concrete used: 1.2
- Epoxy-coated bars with clear dimension ≤ $3d_b$: 1.5
- All other epoxy-coated bars: 1.2
- Clear cover ≥ 3" and center-to-center bar spacing ≥ 6": 0.8

- Reinforcement confined within a # 2 or greater bar size spiral with pitch ≤ 4": 0.75

AASHTO limits development length to a minimum of 12".

The AASHTO equation is based on the ACI 318-71 development length equation. That equation was in turn based on ultimate bond stresses specified in ACI 318-63. The derivation of the equation is as follows:

Ultimate bond stress:
$$u_{bond} = \frac{9.5\sqrt{f_c'}}{d_b} \le 800 \text{ psi} \tag{2-4}$$

The value of f_c' used in equation (2-4) is in psi. Subsequent variables with units of stress will be in psi until a conversion is specified to ksi. The bar force at 125% of yield (a safety factor to insure ductile development of the bar) is equated to the resultant of bond resistance:

Resultant of Bond Stresses = Tensile Force in Bar

$$L_d \pi d_b u_{bond} = A_b (1.25 \cdot f_y) \tag{2-5}$$

Equation (2-5) is rearranged to solve for L_d and equation (2-4) for the ultimate bond stress is substituted for u_{bond}:

$$L_d = \frac{A_b (1.25 \cdot f_y)}{\pi d_b u_{bond}} \tag{2-6}$$

$$L_d = \frac{A_b (1.25 \cdot f_y)}{\pi d_b \left(\frac{9.5\sqrt{f_c'}}{d_b} \right)} \tag{2-7}$$

$$L_d \cong \frac{0.04 \cdot A_b f_y}{\sqrt{f_c'}} \tag{2-8}$$

Equation (2-8) is made to look like the AASHTO equation (2-3) with a unit conversion from psi to ksi:

$$\frac{0.04 \cdot A_b f_y[\text{psi}]}{\sqrt{f_c'[\text{psi}]}} \cdot \left(\frac{1000}{\sqrt{1000}} \right) \cong \frac{1.25 \cdot A_b f_y[\text{ksi}]}{\sqrt{f_c'[\text{ksi}]}} \tag{2-9}$$

The development of the original equation for bond stress (Equation 2-4) is undocumented. It is believed to have been developed by ACI Committee 408 based on the test data available in the early 1960's, but no published report has been identified that provides an explanation for its development. The majority of the test data available at that time would have been from pullout tests, which tend to over-estimate bond stress. No ϕ factor is included in the AASHTO equation because flexural equations used to determine the area of steel required already include a $\phi = 0.9$. Additionally, the equation is already based on a steel stress that is 125% of the specified steel yield stress. The 1.25 factor that first appears in equation (2-5) can be considered equivalent to a built-in ϕ of 0.8.

The AASHTO LRFD Specifications also require additional development length multipliers when bars are spliced. The multipliers are given in Section 5.11.5.3. Like ACI, AASHTO categorizes splices into classes based on the amount of reinforcement being spliced and the ratio of steel area provided to that required, however, they have more classes of splices and more stringent requirements for some splice categories. Table 2-3 summarizes the splice multipliers.

Table 2-3: AASHTO LRFD multipliers for development length of lap splices

$\frac{A_s \text{ provided}}{A_s \text{ required}}$	Maximum % of A_s Spliced Within the Required Lap Length		
	50%	75%	100%
≥ 2	Class A Splice $L_s = 1.0L_d$	Class A Splice $L_s = 1.0L_d$	Class B Splice $L_s = 1.3L_d$
< 2	Class B Splice $L_s = 1.3L_d$	Class C Splice $L_s = 1.7L_d$	Class C Splice $L_s = 1.7L_d$

Both the ACI and AASHTO code equations for development length are based on deformed bars conforming to ASTM A615. Darwin et al. [37] studied bars with deformations exceeding the minimal requirements of ASTM A615, and recommended development length equations for bars with high relative rib area.

2.4 STANDARD HOOKS

When anchorage by bond requires too long a straight bar development, a viable option is the use of a hooked bar. Hooked bars achieve their anchorage by a combination of bond and direct bearing of the hook on concrete.

Both ACI and AASHTO provide standard dimensions for hooks with 90^o and 180^o bends. These standard dimensions are the same for both codes. Thoughout this report a hook which fits the dimensions specified in those codes will simply be called a "standard hook." The ACI 318-95 code contains information for detailing and designing standard hooks in Section 12.5. The AASHTO LRFD Specifications deal with standard hooks in Section 5.11.2.4. Figure 2-21 shows the dimensions of the two standard hooks. The bend radius dimensions are based on safe flexural strains that can be imposed on reinforcement without fracture of the steel.

Both the ACI and AASHTO codes provide a development length equation applicable for the 90^o or 180^o hooks. The equation is the same in both codes but appears in different forms because the units used for stress are different in each code specification. The form of the equation presented below uses units of ksi for the concrete and steel stresses.

$$L_{hb} = \frac{38 \cdot d_b f_y}{60 \cdot \sqrt{f_c'}} \tag{2-10}$$

L_{hb} = basic development length of hooked bar (inches)

The development length of the hook, L_{dh}, is determined by the product of the basic hooked bar development length, L_{hb}, and any applicable multipliers listed below:

- Side cover ≥ 2.5" and cover over 90^o hook extension ≥ 2.0": 0.7
- Hook enclosed within stirrups or ties all along L_{dh} at spacing ≤ $3d_b$: 0.8
- Lightweight aggregate factor: 1.3
- Epoxy-coated bar factor: 1.2

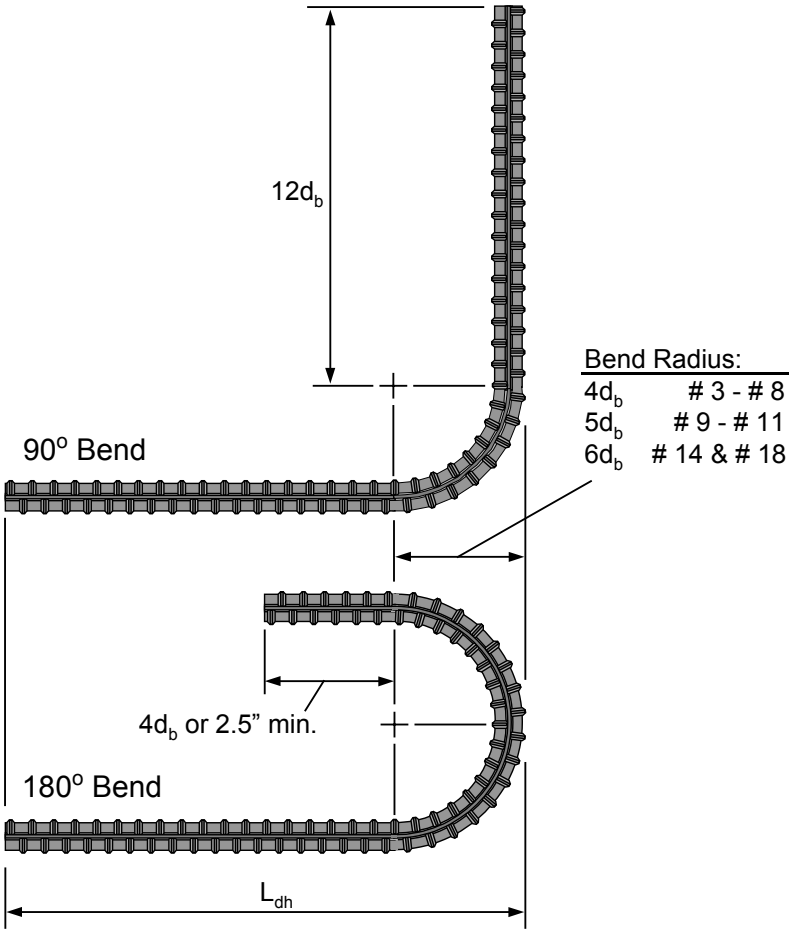

Figure 2-21: Standard hook dimensions

There is no factor for top-cast bars because hooks develop most of their anchorage by direct bearing, and not by bond along the surface area of the bar. Hooked bars can be developed over significantly shorter lengths than straight bars, particularly at low concrete strengths. Figure 2-22 demonstrates this by plotting the code development lengths for hooked and straight bars as a function of concrete compressive strength. Lap splice lengths are also included. The plots are for #8 bars with the maximum benefits from confinement and cover multipliers.

The mechanism of stress transfer in hooked bars is shown in Figure 2-23. The concrete in front of the hook, where it just begins to bend away from the straight portion of bar, is typically crushed at full development of the bar. 90^o hooks tend to be pulled straight around the bend of the bar as load is applied. Thus it is important that the hook extension be well confined on 90^o bends or the extension may cause spalling of concrete cover behind the hook. 180^o bends tend to pull forward as a unit without slipping around the bend of the hook. Hooked bars tend to fail by side spalling of concrete cover (Figure 2-24).

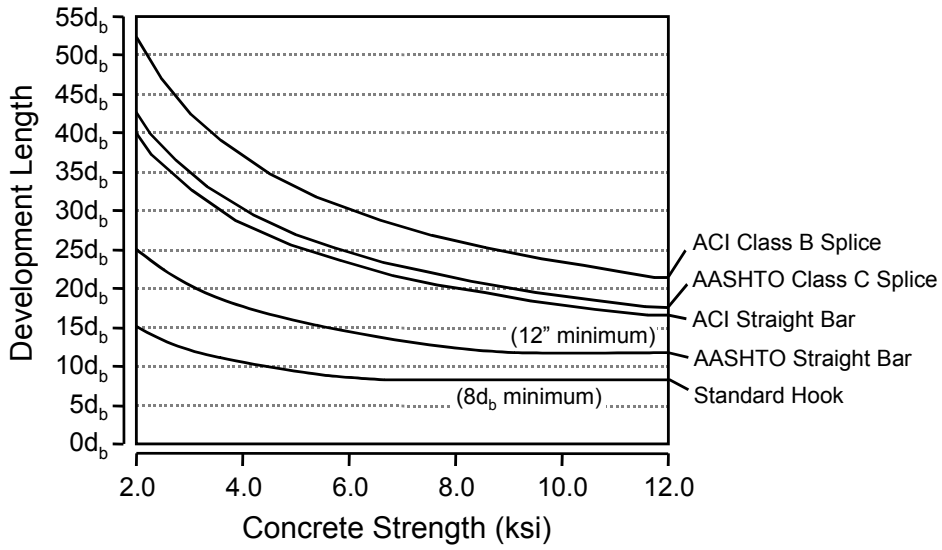

Figure 2-22: Development lengths of standard hooks and straight bars

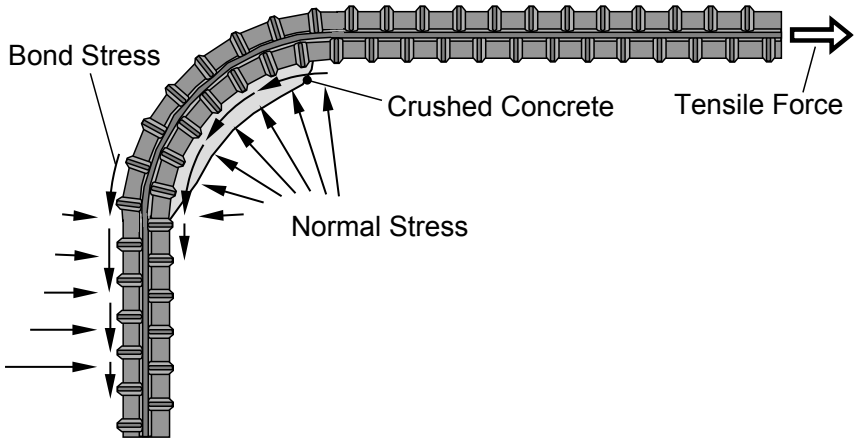

Figure 2-23: Stress transfer in a hooked bar

Studies by Minor [77] have shown that 180° hooks experience more slip than 90° hooks and both of these hooks exhibit more slip than straight bars as load is applied. Follow-up studies by Marques [68] have demonstrated that compressive pressure within the plane of the bend does not significantly enhance the anchorage capacity of the hook. Thrö [105] studied U-bent bars with lateral pressure applied perpendicularly to the plane of the bend. Thrö found increasing anchorage strength as lateral pressure was increased. He recommended a reduction factor for development length that cut the length by half at a pressure of 1160 psi, the same as his recommended reduction factor for straight bars (see Section 2.2.3). Mattock [73] also studied U-bent bars with applied lateral pressure. Mattock found increasing anchorage capacity with lateral pressure for bars with the minimum allowable bend diameter ($6d_b$). He recommended a capacity formula that was proportional to $(f_n/f_{ct})^{0.7}$ where f_n is the applied lateral pressure and f_{ct} is the tensile strength of the concrete.

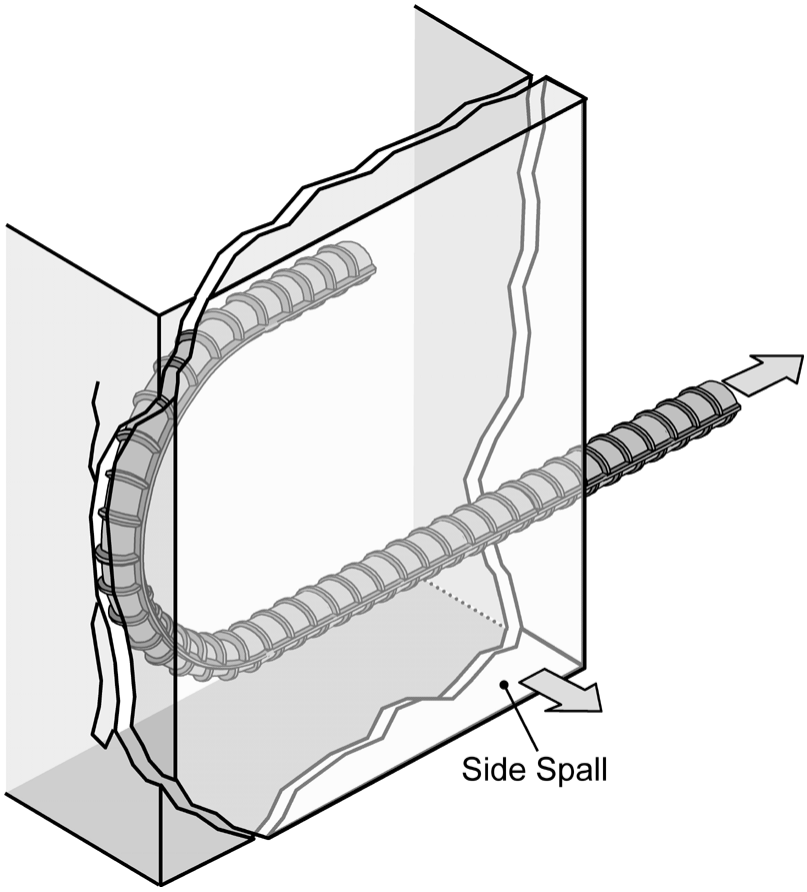

Figure 2-24: Side spall failure of a hooked bar

CHAPTER 3: BACKGROUND ON HEADED BARS

3.1 INTRODUCTION

Headed bars are created by the attachment of a plate or nut to the end of a reinforcing bar to provide a large bearing area that can help anchor the tensile force in the bar. Figure 3-1 shows an example of a headed bar. The tensile force in the bar can be anchored by a combination of bearing on the ribs and on the head. This chapter discusses the current state-of-the-art of headed bar technology. The current products available on the market are discussed; the available research is reviewed; and pertinent code provisions are discussed.

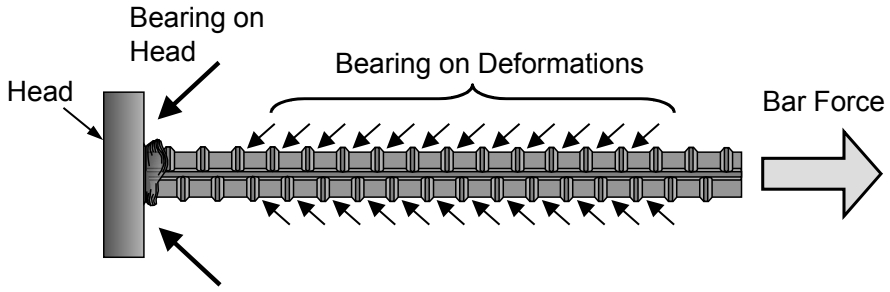

Figure 3-1: Anchorage of a headed bar

Throughout this chapter and through most of this report, the central parameter used for comparing different heads will be the area of the heads. In order to normalize results with respect to different bar sizes the ratio of head area to nominal bar area is repeatedly used. Specifically, this ratio, termed the relative head area, is defined as the net head area divided by the nominal bar area; the net head area being the gross head area (defined by the outer dimensions and shape of the head) minus the nominal bar area:

$$\text{Relative Head Area} = \frac{A_{nh}}{A_b} = \frac{A_{gh} - A_b}{A_b} \quad (3\text{-}1)$$

A_{nh} = the net head area (in^2)

A_{gh} = the gross head area (in^2)

A_b = the nominal bar area defined by ASTM A615 [3] (in^2)

3.2 HISTORICAL DEVELOPMENT OF HEADED BARS

Headed reinforcing bars have evolved from headed stud anchors. Extensive studies on stud anchors first began in the 1960's. Most of this work was conducted by the Nelson Stud Welding Company and researchers at Lehigh University [75]. Their research established the pullout cone design method for anchors under combined shear and tension. Headed studs are commonly used only as shallow anchorage devices or to provide composite action between steel girders and overlying concrete deck slabs. The behavioral understanding of headed studs was limited to these applications and there was little similarity to the anchorage problems associated with deformed reinforcing bars.

Subsequently shear studs were adapted for use as punching shear reinforcement in flat slabs. This work was conducted by Dilger and Ghali at the University of Calgary [40, 79] in the late 1970's. They found the current methods of slab shear reinforcement, which used small closed stirrups, to be structurally deficient and difficult to construct. They began to examine alternative methods of shear reinforcement

and looked to double-headed shear studs as a possible solution. Initially, these headed studs were created by cutting thin sections out of steel I-beams, by fusion welding existing shear stud connectors to flat plates creating a prototype studrail, or by welding square plates to both ends of short deformed bar lengths to create double-headed ties (Figure 3-2). The first method (I-sections) was found to be economically unfeasible and the second failed because the head sizes of the existing shear stud products were too small to properly anchor the heads into the top of the slab. The third method proved very effective. Eventually, the second and third methods were combined to create an improved studrail with larger head areas. This product was patented and is now produced commercially by Decon (founded in 1989). An important aspect of the Calgary research was the recommendation that a head size of 10 times the bar area was necessary for proper anchorage of the studs.

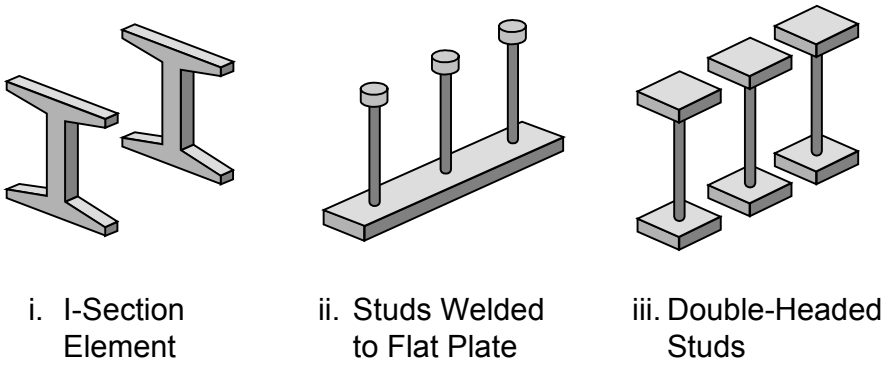

Figure 3-2: Shear reinforcement tested at University of Calgary

Caltrans also performed a small study of headed reinforcement in the 1970's [100]. Their interest was in determining a method of anchoring large diameter bars used in monolithic connections between bridge piers and box-girder superstructures. They wanted to shorten the development length of the bars without resorting to congestion prone hooks. They tested three methods of attaching the head to the end of the bar: allowing the bar to pass through a hole in the head plate and fillet welding on the back side of the head, a tapered-threaded connection, and a cylindrical metal sleeve with a filler metal material connecting the sleeve to the bar (also referred to as a "cad-weld"). These bars were supplied by ERICO who already had experience producing headed studs in the stud anchor industry. ERICO did not find much interest in these headed bars at the time and never developed the welded or cad-welded headed bars into a commercial product [115].

After the Dilger and Ghali studies demonstrated the potential benefits of double-headed ties for use as shear reinforcement, the Alaska Oil and Gas Association (AOGA) began to study the technology in the early 1980's. They were interested in the possible use of double-headed bars as shear reinforcement in heavily reinforced concrete offshore oil platforms. They were also interested in using headed bars to alleviate high congestion created by the use of hooked bars. Additionally, they believed the headed bars could supply superior anchorage to conventional hooks. Several series of tests were conducted by AOGA. Most of the results of these tests are proprietary, but some findings have been reported by Berner, Gerwick, and Hoff [25].

Following their research, AOGA recommended the use of headed bars to Norwegian Contractors, a firm specializing in the design and construction of offshore oil platforms [25]. Norwegian Contractors began a program to design a headed bar product that could be mass produced economically but with a consistent level of high-grade quality. They teamed up with Metalock, a British supplier of industrial services for structural contractors. These two companies contracted the services of the SINTEF Group, a private research organization linked to the Foundation for Scientific and Industrial Research at the Norwegian Institute of Technology [117]. Based on the work performed by Norwegian Contractors, Metalock and

SINTEF, a friction-welded headed bar was conceived. This bar design has since been used extensively in several offshore and coastal structures including: Oseburg Platform A, Gullfaks Platform C, the Ekofisk Barrier Wall, Sleipner Platform A (both the original and revised designs), the Snorre Foundation, Draugen Platform, Troll East Platform, and the Hibernia Platform (all of which are located in the North Sea) [26]. Metalock patented the friction-welding technology and eventually formed a North American subsidiary to produce and sell friction-welded headed bars. This subsidiary became the Headed Reinforcement Corporation (HRC), the primary supplier of headed bars in the United States and the sponsor of much of the research that has been conducted on the new technology.

At the same time that Metalock was developing the friction-welded headed bar in the 1980's, ERICO developed a threaded headed bar. They first marketed the bar in Europe on a limited basis during the 1980's [115]. In the 1990's, after the use of headed bars in the offshore industry created greater interest in headed bars, ERICO began to sell their product under the trademark Lenton Terminator in the U.S. Their headed bars utilize a smaller head than the products of HRC and Decon. The Lenton heads are only 4 times the bar area rather than 10. This head size was derived from accepted head sizes used in the stud anchor industry [115]. ERICO and HRC are currently the only suppliers of headed bars. HRC has been a main supporter of headed bar research though ERICO has recently helped to sponsor some studies. Although the early work aimed at applications within the offshore industry, recent headed bar research has become focused primarily on bridge and seismic related applications.

3.3 HEADED BAR FABRICATORS

This section discusses the products of the two main companies that provide headed bars in North America: Headed Reinforcement Corporation (HRC) and ERICO. Decon, the manufacturer of the Studrail is excluded because their product does not have the versatility of HRC's and ERICO's products and is solely intended for use in flat slabs.

3.3.1 Headed Reinforcement Corporation

The Headed Reinforcement Corporation (HRC) is currently centered in Fountain Valley, California. HRC manufactures only two products, both of which can qualify as headed bars: a friction welded head that comes in four varieties and a forged head product that is intended for a mechanical coupler system. The forged head is very small but it is easy to fabricate, particularly in field conditions and shows promise for some applications in which only a small enhancement to reinforcement anchorage is required.

3.3.1.1 Friction-Welded Heads

The friction-welded or T-headed bar is HRC's main consumer product. The friction-welded heads are manufactured by pressing the end of a deformed reinforcing bar onto a plate spinning at very high speed. The heat produced by the friction between the deformed bar and plate causes the bar material to melt and form a weld between the two. The machinery required for this process is quite large and the headed bars can only be created in factory conditions. The headed bars come in four shapes: square, rectangular, circular, and oval. The circular and oval shaped heads are fatigue rated. All of the headed bars manufactured by HRC provide relative head areas between 8.6-11.9. Table 3-1 lists the head dimensions, head areas, and relative head areas for HRC's square and rectangular T-headed bars. Figure 3-3 shows a typical HRC friction-welded head.

Table 3-1: HRC head sizes (friction-welded heads)

Bar Size	Square Head Size	Gross Area, A_{gh} (in^2)	$\frac{A_{nh}}{A_b}$	Rectangular Head Size	Gross Area, A_{gh} (in^2)	$\frac{A_{nh}}{A_b}$
# 5	2" x 2"	4.00	11.90	$1^1/_4$" x $2^1/_2$"	3.13	9.08
# 6	$2^1/_4$" x $2^1/_4$"	5.06	10.51	$1^1/_2$" x 3"	4.50	9.23
# 7	$2^1/_2$" x $2^1/_2$"	6.25	9.42	$1^1/_2$" x 4"	6.00	9.00
# 8	3" x 3"	9.00	10.39	2" x 4"	8.00	9.13
# 9	$3^1/_4$" x $3^1/_4$"	10.56	9.56	2" x 5"	10.00	9.00
# 10	$3^1/_2$" x $3^1/_2$"	12.25	8.65	$2^1/_2$" x 5"	12.50	8.84
# 11	4" x 4"	16.00	9.26	$2^1/_2$" x 6"	15.00	8.62
# 14	5" x 5"	25.00	10.11	3" x $7^1/_2$"	22.50	9.00

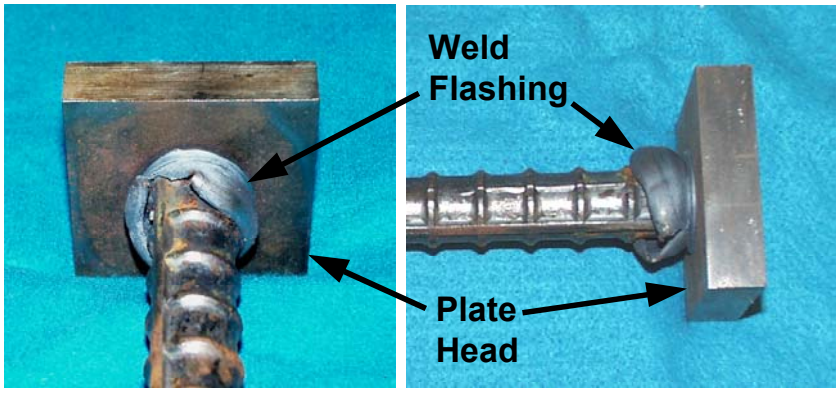

Figure 3-3: HRC friction-welded head

3.3.1.2 Forged Heads

The forged head system developed by HRC is part of a mechanical coupling system called the Xtender. The system is shown in Figure 3-4. Threaded mechanical sleeves are slipped over the ends of the bars, then upset ends are forged onto the bar ends. When the mechanical sleeves are coupled together, they bear on the forged heads and hold the separate bars together.

The Xtender forged heads can be created in the field. First the bar end is preheated with a blowtorch, then a special hydraulic vise is used to forge the head out of the material of the bar. An ICBO (**I**nternational **C**onference of **B**uilding Code **O**fficials) evaluation report [10] supplied by HRC lists minimum acceptance standards for Xtender head dimensions. The minimum head diameters specified by HRC are typically about 1.3 times the bar diameter providing a relative head area of about 0.7. In practice however, the final heads are slightly bigger. Measurements made of the Xtender headed bars supplied to this project by HRC showed that the forged head diameters were generally 1.5 times the bar diameter providing a relative head area of 1.3. These measurements are summarized in Chapter 6, Section 6.6.3.

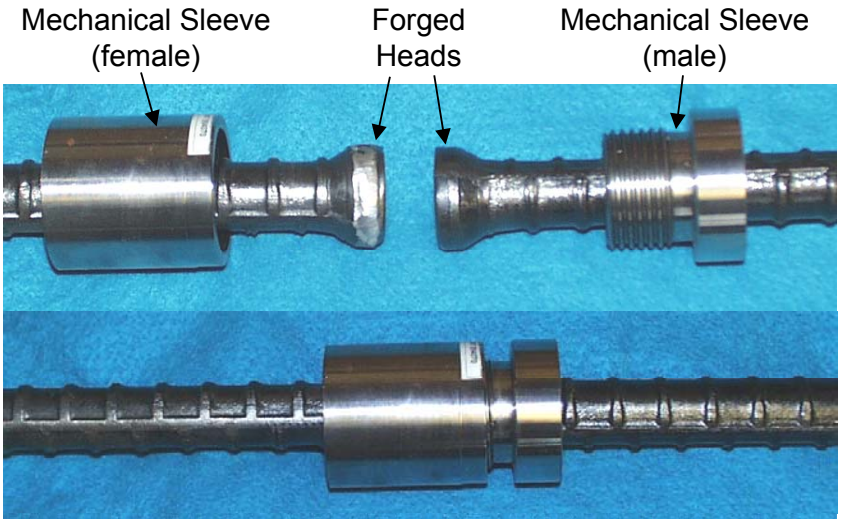

Figure 3-4: The Xtender coupler system

3.3.2 ERICO

ERICO (short for the **E**lectric **R**ailway **I**mprovement **CO**mpany) was founded in 1903 and manufactures products for a variety of marketplaces including construction, electrical, railway, utilities, and communications. Their Lenton subsidiary produces products for reinforcement applications mostly consisting of mechanical splicing devices. Their Lenton Terminator utilizes a tapered thread connection between the reinforcing bar and a special nut that is screwed onto the bar to provide a head. Currently, this is their only headed bar product. Figure 3-5 shows the Lenton Terminator.

Figure 3-5: ERICO's Lenton Terminator head

The tapered thread of the Terminator head allows a more efficient stress transfer than conventional straight thread connections. ERICO's product literature claims that the tapered thread connection can support 125% of yield for a grade 60 reinforcing bar. Terminator heads are circular and generally have a relative head area around 3 or 4. Table 3-2 lists the available Terminator head sizes. ERICO also provides information on the development lengths of the terminator bars and these values are supplied in Table 3-2 as well.

Table 3-2: Lenton Terminator head sizes and development lengths

Bar Size	Head Diameter (in)	Gross Area, A_{gh} (in^2)	$\frac{A_{nh}}{A_b}$	Terminator Development Length (in)
# 4	1 3/8	1.48	6.40	3.6
# 5	1 3/8	1.48	3.77	4.6
# 6	1 1/2	1.77	3.02	5.5
# 7	1 3/4	2.41	3.02	6.5
# 8	2 1/4	3.98	4.04	7.3
# 9	2 1/4	3.98	2.98	8.4
# 10	3	7.07	4.57	9.3
# 11	3	7.07	3.53	10.4
# 14	3 3/4	11.04	3.91	12.4
# 18	4 1/2	15.90	2.98	16.8

Terminator heads can be applied in the field provided the bar ends are pre-threaded. Threading may be accomplished in the field. Reinforcing bars may even be tied in place before the head is attached. To attach the head, all that is needed is the Terminator nut and a torque wrench. Table 3-3 lists the manufacturer's required torque values for installation of the Terminator heads.

Table 3-3: Setting torques for Lenton Terminator heads

Bar Sizes	Setting Torque
# 4	30 ft-lbs
#5	90 ft-lbs
#6	130 ft-lbs
#7	160 ft-lbs
# 8 - # 18	200 ft-lbs

3.4 PREVIOUS RESEARCH ON HEADED BARS

The available research on headed bars can be separated into two categories: application studies and general behavior studies. The distinction between the two categories derives from the scope of the research. The research grouped under application studies tends to focus on particular structural uses of headed bars and utilizes test specimens whose behavior cannot be extrapolated beyond the specific application that is being modeled in the study. General behavior studies are those research programs aimed at determining mode of behavior that can extrapolated to many different types of structural situations. For the most part these studies entail research on development length or anchorage capacity.

This research program is intended to fall under the latter category of general behavioral research. Only the research that was deemed to study general behavioral trends is reviewed in detail within this section. The remaining literature is described briefly at the end of this section.

3.4.1 Caltrans Study

Nineteen pullout tests of headed bars were conducted at the Transportation Laboratory of the California Department of Transportation (Caltrans) in the early 1970's [100]. Their test specimens used large diameter reinforcing bars with #11, #14, and #18 sizes. The purpose of the tests was to determine if headed bars could represent a viable alternative to hooks in monolithic bridge pier/superstructure connections. The scope of the study also involved testing of several different head-bar connections. The various connections are shown in Figure 3-6. With only two exceptions, the headed bars tested used very large head sizes: relative head areas of 15.0 for the #11 and #14 bars tested and 13.1 for the # 18 bars tested. The two exceptions included one non-headed #18 bar and one small headed #18 bar using only a cad-weld coupler sleeve as anchorage (the sleeve provided a relative head area of 1.8).

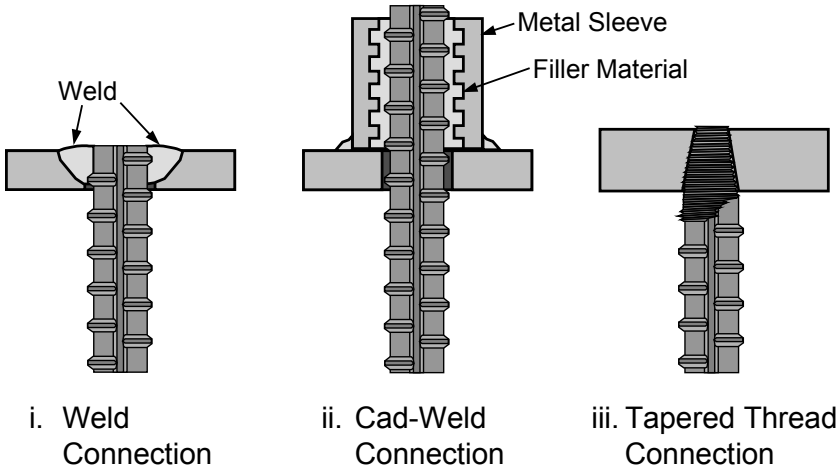

Figure 3-6: Head-bar connections tested by Caltrans

The test specimens consisted of tensile pullout specimens similar to those shown in Figure 2-17. Large embedment lengths were provided for the bars. Additionally, supplementary transverse reinforcement was used around the perimeter of the specimen blocks. The variables tested included: bar size (#11, #14, or #18), single versus group action (four bar groups of #11's), concrete cover ($7^1/_2$" or 19"), embedment depth (h_d/d_b = 8 to 32), method of head attachment (see Figure 3-6), and head size (A_{nh}/A_b = 0.0, 1.8, or 13.0). Most test specimens used fully bonded bars so that anchorage occurred by a combination of bond and bearing of the head.

The Caltrans researchers discovered that the bonded lengths of their bars were too long to allow much anchorage capacity of the bars to be carried by the heads. In most tests the test bar yielded in tension or the load to failure exceeded the capacity of the test frame. The research provided the following conclusions:

- The head sizes selected for testing were more than adequate for the development lengths tested in the research program.
- One test of a much smaller head size (A_{nh}/A_b = 1.8) provided comparable results to similar tests of larger head sizes (A_{nh}/A_b = 13) indicating that smaller head sizes could achieve yield. The

Caltrans researchers recommended that smaller heads should be investigated in any forthcoming research.

- More load was carried by the head as the bonded length of the bar was reduced. When compared to stress results measured from the non-headed test specimen in which anchorage was carried completely by bond, the measured load carried by the heads compared favorably to the forces that would be predicted assuming that the remainder of the load would be carried by normal bond stresses along a fully bonded bar. Figure 3-7 shows data from the Caltrans study. In the figure, the percent of load carried by the heads aligns well with the load distribution curves measured from the fully bonded test bar. The data indicate that the portion of the load carried by bond in a headed bar follows a similar load distribution as the case in which no head is present. One data point suggests that the head may carry a greater percentage of the load for smaller development lengths at greater stress levels and that bond resistance breaks down in favor of transferring the load to the head under such conditions.
- Load-slip measurements of the test bars indicated that more slip is experienced for bars acting in groups than single headed bars.

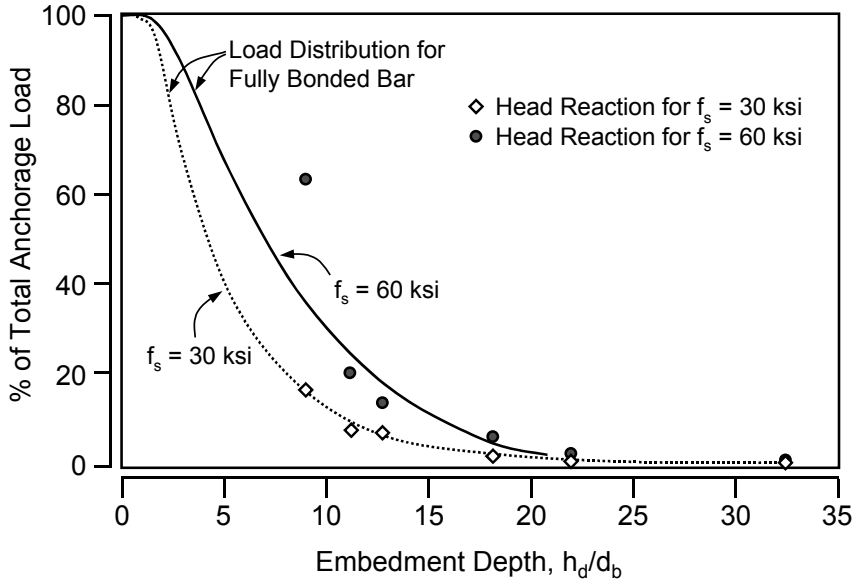

Figure 3-7: Head reaction versus embedment depth compared to fully bonded load profiles (after Caltrans data [100])

The Caltrans researchers made several recommendations for the use of headed bars including specifications for acceptable head-bar connections (any of the three connection types tested was found to be acceptable for the given embedment depths) and staggering arrangements for headed bars in groups (staggered termination points were recommended to avoid overlap of the heads). The recommendations were restricted to grade 60, #18 bars with at least four feet of embedment depth.

3.4.2 SINTEF Studies

Most of the literature regarding the SINTEF studies [41, 46, 47, 48, 88, 89] is proprietary and unavailable for review. The information presented here comes from a summary paper written by two engineers from Norwegian Contractors: Dyken and Kepp [42].

SINTEF performed a number of studies primarily intended to demonstrate the strength and ductility of the friction-welded head-bar connection. These studies included static tension, static bending, and fatigue tension tests on the headed bars in air. Three groups of tests studied the performance of the headed bars embedded in concrete: static pullout bond tests, fatigue pullout bond tests, and beam shear tests.

Figure 3-6 shows a typical static pullout specimen. The Dyken and Kepp report suggests that only headed bars with the head size shown in Figure 3-8 were studied ($A_{nh}/A_b = 6.0$) and that studies of the effects of head area were not a parameter of the study. Specimens were tested with normal weight concrete with 8,700 psi compressive strength and light-weight aggregate concrete of compressive strength 10,400 psi. Bond between the concrete and the deformed portion of the bar was prevented by use of a plastic sleeve. All specimens tested failed by yielding of the bars ($f_y = 80$ ksi). Minimal slip of the heads was observed in all tests. Comparison tests with hooked bars were also studied. All that is reported in the available literature is that the headed bars had a better load-slip response than the hooked bars.

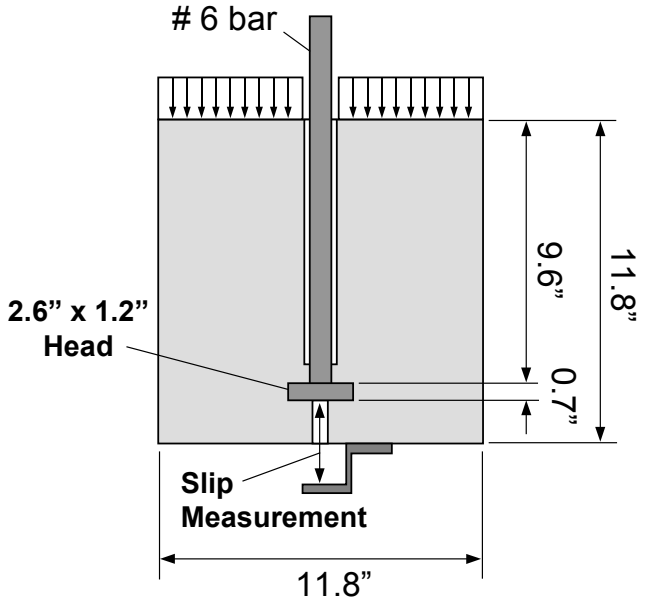

Figure 3-8: Static pullout test performed by SINTEF

The fatigue pullout test used identical specimens as the static tests, but specimens were tested with #6 and #8 size bars. The tests were intended only for a fatigue test of the head-bar connection. The bars were embedded in concrete only to provide a realistic support condition for the head. In order to prevent premature failure of the concrete, deliberately high compressive strengths of 12,000 psi were used. All specimens failed by fatigue fracture of the friction-welded head-bar connection.

Three shear beam specimens were tested. Two specimens used headed bars for the shear reinforcement and the third used a standard stirrup detail. All three beams failed at nearly identical loads thus demonstrating that the headed bars were an adequate substitute for standard stirrups.

It is known that the SINTEF research was related to the development of HRC's headed bars. They developed tests to show the quality of the friction-welded head-bar connection and influenced the choice of the head sizes adopted. However, the HRC head sizes may also derive from the recommendations for studrail heads that were derived at the University of Calgary [40, 79]. The SINTEF study serves as the basis for many of the standards required in ASTM A970 *"Standard Specification for Welded Headed Bars for Concrete Reinforcement*" [5] which is discussed later in this chapter.

3.4.3 University of Kansas Study

Beam-end bond tests of headed bars were conducted at the University of Kansas [113]. The research was sponsored by HRC and all headed test bars were supplied by them. The test specimens were modeled after specifications contained in ASTM A944 "*Standard Test Method for Comparing Bond Strength of Steel Reinforcing Bars to Concrete Using Beam-End Specimens*" [4] (see Figure 2-17 for an example of this specimen type). Seventy specimens were tested. Test bars were non-headed, hooked with 180° bends, or friction-welded headed bars. The goal of these tests was to determine a development length formula for headed bars. Parameters studied in the research were:

- **Concrete cover** – cover was 2 or $3d_b$ measured to the surface of the bar (not the head).
- **Bar exposure** – in some specimens, plastic sheathing was placed over the deformed bar in order to test the strength of the head by itself.
- **Transverse reinforcement** – four arrangements of stirrup bars were tested as confining reinforcement for the pullout tests and compared against unconfined test results. Figure 3-9 shows the four stirrup arrangements.

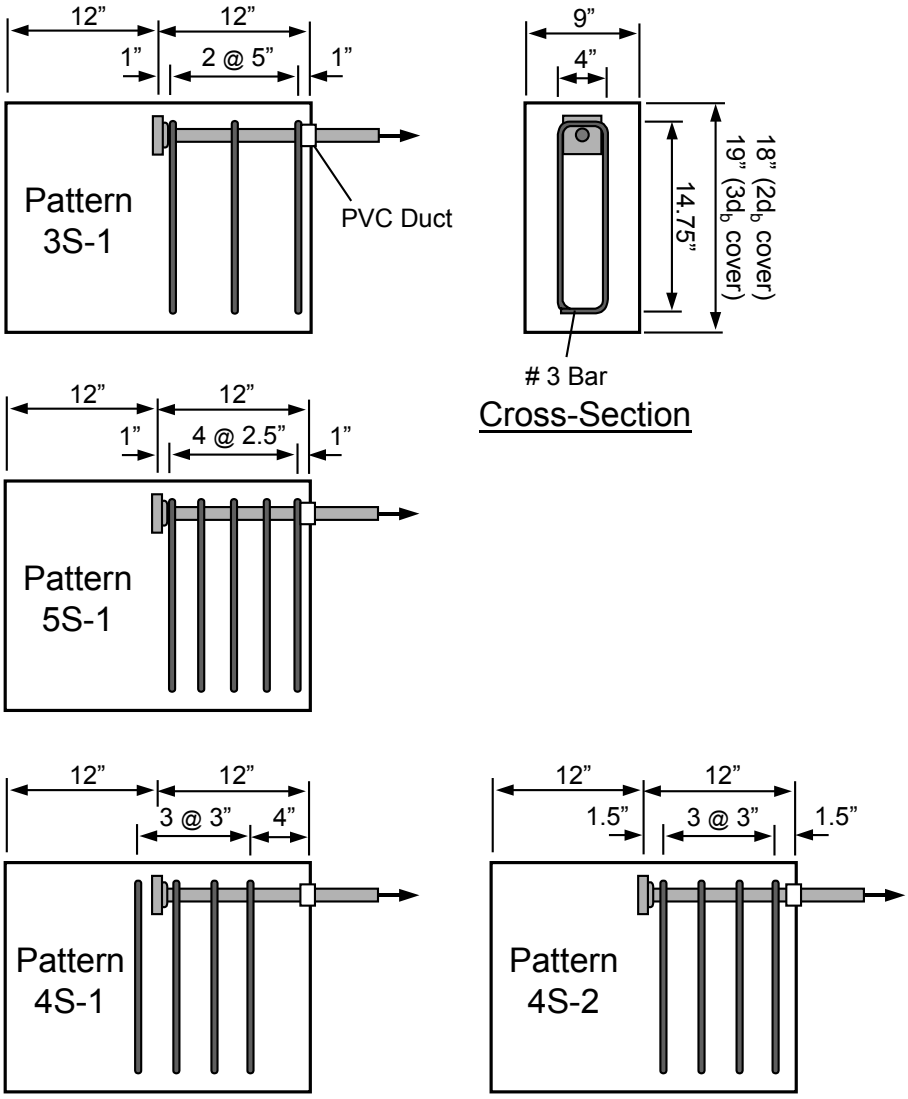

Figure 3-9: Transverse reinforcement patterns studied at Kansas [113]

Parameters that were kept constant throughout the study were bar size (#8), embedment length (12"), concrete strength (4,500 – 5,000 psi), and the size and shape of the friction-welded heads (HRC's standard #8 square head size: 3" x 3"). Additionally, all bars were bottom-cast and only single bar groups were tested.

Results of the Kansas study indicated the following:

- Headed bars failed at equal or higher loads than hooked bars. Both types of bar anchorages exhibited similar load-slip and failure behavior. In addition, the response of hooked and headed bars to transverse reinforcement and increases in cover were similar.
- The benefit from increases in cover was diminished when increasing amounts of transverse confinement were provided.
- Capacity was increased by 50% by the addition of transverse reinforcement. Thereafter, additional transverse reinforcement provided diminishing returns in capacity.
- PVC sheathing over the straight bar length of the headed bars increased the capacity of the headed bar. Additionally, PVC sheathing also lessened the degree of surface cracking exhibited before failure of the anchorage. This occurred because splitting forces and cracking associated with bond of the deformed bar were eliminated and the ability of the concrete to carry forces from the head was increased.
- The optimal anchorage performance from the headed bar was achieved by sheathing the straight bar deformations over the embedment length and providing $3d_b$ clear cover over the bar if no transverse reinforcement was used or providing transverse reinforcement if only $2d_b$ clear cover was provided. There was minimal advantage to providing both large amounts of cover and transverse reinforcement.

Following the experimental testing, a regression analysis was performed to provide a best-fit equation for development length of the headed bars tested. Many forms of design equations were used, most of them based on straight bar development length. However, none of the straight bar based equations was found to be adequate as a design expression. Eventually, an equation based on the ACI 318 [2] expression for hooked bars was used. The following were recommended in a proposal [113] for an addition to ACI 318 Building Code:

1. The headed bar development length, L_{dt}, shall be calculated as the following:

$$L_{dt} = \frac{22 d_b f_y}{60\sqrt{f_c'}} \left(\frac{3 d_b}{c + K_{tr}} \right) (\alpha\beta\lambda\psi) \qquad (3\text{-}2)$$

2. The basic development length, L_{dt}, shall not be less than $6d_b$ or 6".
3. Concrete cover shall not be less than $3d_b$.
4. A minimum of three transverse stirrups shall be positioned within the development length, L_{dt}.
5. The amount of transverse reinforcement within the development length, L_{dt}, required is $A_{tr}f_{ytr}/s \geq$ 2000 lb/in or no less than $5d_b$ of clear cover must be provided.

d_b = bar diameter (in)

f_y = bar yield strength (ksi)

f_c' = concrete compressive strength (ksi)

c = minimum cover dimension to the surface of the bar (in)

K_{tr} = transverse reinforcement index (as defined in Equation 2-2)

α = casting position factor *(to be determined by future research)*

λ = lightweight aggregate factor *(to be determined by future research)*

β = epoxy-coated reinforcement factor *(to be determined by future research)*

ψ = excess reinforcement factor *(to be determined by future research)*

The Kansas recommendation for headed bars is essentially 7/12 of the existing ACI Building Code formula for hooked bars. However, the formula limited to the type of headed bar tested in the Kansas program, the standard HRC friction-welded head ($A_{nh}/A_b \cong 9$ for most bar sizes). Ideally, the nature of the connection of the head to the bar should not have any impact on development length provided that the connection is strong enough, so it should not matter that the bars tested were friction-welded. However, the size and geometry of the head is important. By testing only one head size and basing proposed code text on that head size, the Kansas study presents the danger of standardizing that head size. Since all head geometry parameters were kept constant throughout the test series and the development length proposals are based only on those parameters, the proposed anchorage requirements depend on the head size used. As a result, this "standard" head then becomes the only choice for designers and contractors, and all other products or head geometries cannot be considered. This problem is discussed later in regard to certain headed bar provisions that have already been included in standards.

3.4.4 University of Texas Study

An extensive study sponsored by the Headed Reinforcement Corporation was conducted at the Phil M. Ferguson Engineering Research Laboratory of the University of Texas at Austin. This research was conducted by two PhD students, Richard DeVries and Tarek Bashandy, and is documented in their dissertations [38, 22]. In the first phase of the study, over 160 pullout tests were conducted studying a variety of variables. Tests in that phase of the study can be further subdivided into shallow and deep embedment tests. In the second phase of the study, 32 large-scale specimens simulating exterior beam-column joints were tested, then one full exterior beam-column sub-assemblage was constructed and tested under cyclic loading. Once again, design equations were fit to the data and recommendations proposed for code implementation.

Figure 3-10 shows some geometric parameters that must be defined to discuss the Texas study. The embedment depth, h_d, is the length measured from the critical section where the full load of the bar must be carried to the inside face of the head. This is distinguished from bond length, L_{bond}, which is the length over which bond of the bar can occur and might not be the full length of the embedment depth. In test specimens, the bonded length (L_{bond}) of the straight deformed bar was controlled by PVC sheathing placed over the bar surface. Perpendicular to the bar axis are the two axes of clear cover, 1 and 2. Axis 1 is oriented in the direction parallel to the minimum clear cover to the bar axis; axis 2 is perpendicular to axis 1. Consequently, clear distances contain subscripts related to the axis along which they are measured: c_1, the minimum cover distance to the center line of the bar; c_{c1}, the clear cover distance measured to the bar surface along axis 1; and c_{h1}, the minimum clear cover distance measured to the head surface along axis 1. The variables c_2, c_{c2}, and c_{h2} are the analogous cover distances measured along axis 2. The variables h_1 and h_2 are the edge lengths of rectangular heads measured along axes 1 and 2.

Most pullout tests were of single bars in tension. Bars were generally cast in the vertical position unless otherwise noted. Bar sizes were #6, #8 and #11.

3.4.4.1 Shallow Embedment Pullout Tests

Twenty-one shallow embedment pullout tests were conducted by DeVries [38]. Shallow embedment tests were somewhat arbitrarily distinguished from deep embedment tests by having a ratio of embedment depth, h_d, to bar clear cover, c_{c1}, less than 5. Among these tests, the primary variables were concrete

strength (4 to 11 ksi), embedment depth and edge distances. Also studied were the effects of transverse reinforcement, development length, and head size. Figure 3-11 shows the basic shallow embedment test specimen.

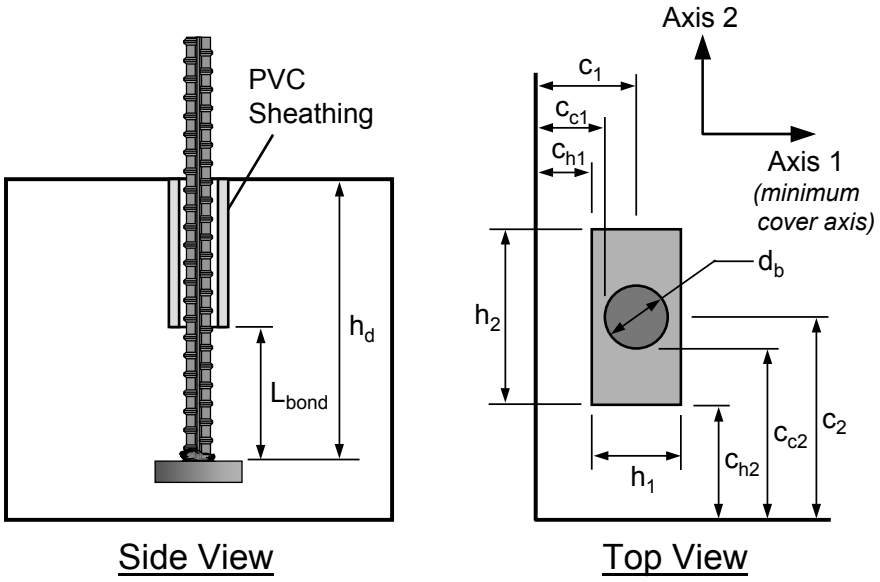

Figure 3-10: Definition of geometric parameters for University of Texas study

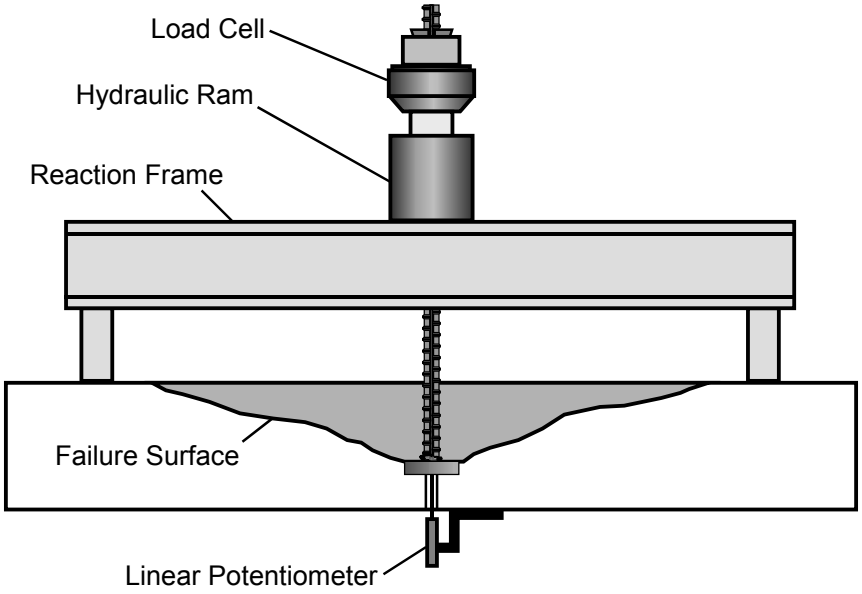

Figure 3-11: Shallow embedment pullout specimen used by DeVries

DeVries determined that transverse reinforcement did not significantly affect the ultimate pullout strength of the headed bar but did add post-peak residual strength to the anchorage. Bonded development length added some contribution to ultimate capacity primarily when transverse reinforcement was used and helped to reduce head slip. Tests studying head size were limited (only one pair of comparable tests both

with rather large heads: A_{nh}/A_b = 5.7 and 7.4) but showed no effect due to head size. This conclusion may not be true for smaller head sizes.

All but three tests failed by pullout of a large concrete cone initiating at the head (see Figure 3-11). The three exceptions failed by fracturing of the bar steel. DeVries compared his pullout capacities to several models of anchorage and found that the Concrete Capacity Design (CCD) method for breakout of anchor bolts best fit his data. In the CCD method, a cone failure surface is projected from the head of the anchor bolt or headed bar and the area of this surface is used in capacity calculations [44]. DeVries modified the coefficient of the equation slightly to account for lower head bearing stresses in headed bars than are typical of anchor bolts. He also proposed basing the projected failure surface on the head perimeter rather than the center of the bar, as is typical of anchor bolts (Figure 3-12). The following equations for concrete breakout capacity were proposed:

Concrete Breakout Capacity,
$$N_n = \frac{A_N}{A_{No}} \Psi_1 N_b \tag{3-3}$$

$$N_b = 22.5(h_d)^{1.5}\sqrt{f_c'} \tag{3-4}$$

$$\Psi_1 = 0.7 + 0.3\frac{c_{min}}{1.5h_d} \leq 1 \tag{3-5}$$

N_b = the basic concrete breakout capacity (lbs)

Ψ_1 = modification factor for stress disturbance caused by proximity to an edge

A_{No} = basic projected area of a single anchored bar, $9(h_d)^2$ (in^2)

A_N = projected area of concrete breakout failure as defined in Figure 3-12 (in^2)

h_d = the embedment depth as defined in Figure 3-10 (in)

c_{min} = the minimum edge distance equivalent to c_1 in Figure 3-10 (in)

f_c' = concrete compressive strength (psi)

3.4.4.2 Deep Embedment Pullout Tests

A total of 123 deep embedment tests were performed by DeVries [38]. Bashandy also performed 25 follow-up tests [22]. Deep embedment tests were distinguished from shallow embedment tests by having a ratio of embedment depth, h_d, to bar clear cover, c_{c1}, greater than 5. The primary variables of DeVries' tests were embedment depth, development length, head orientation, head geometry (including head area, aspect ratio, shape, and thickness), transverse reinforcement, concrete strength, cover, corner versus edge bars, and closely spaced bars. Bashandy's follow-up tests studied the effects of cyclic loading and anchorage of the head behind a crossing bar or against another head. Figure 3-13 shows the basic test set-up.

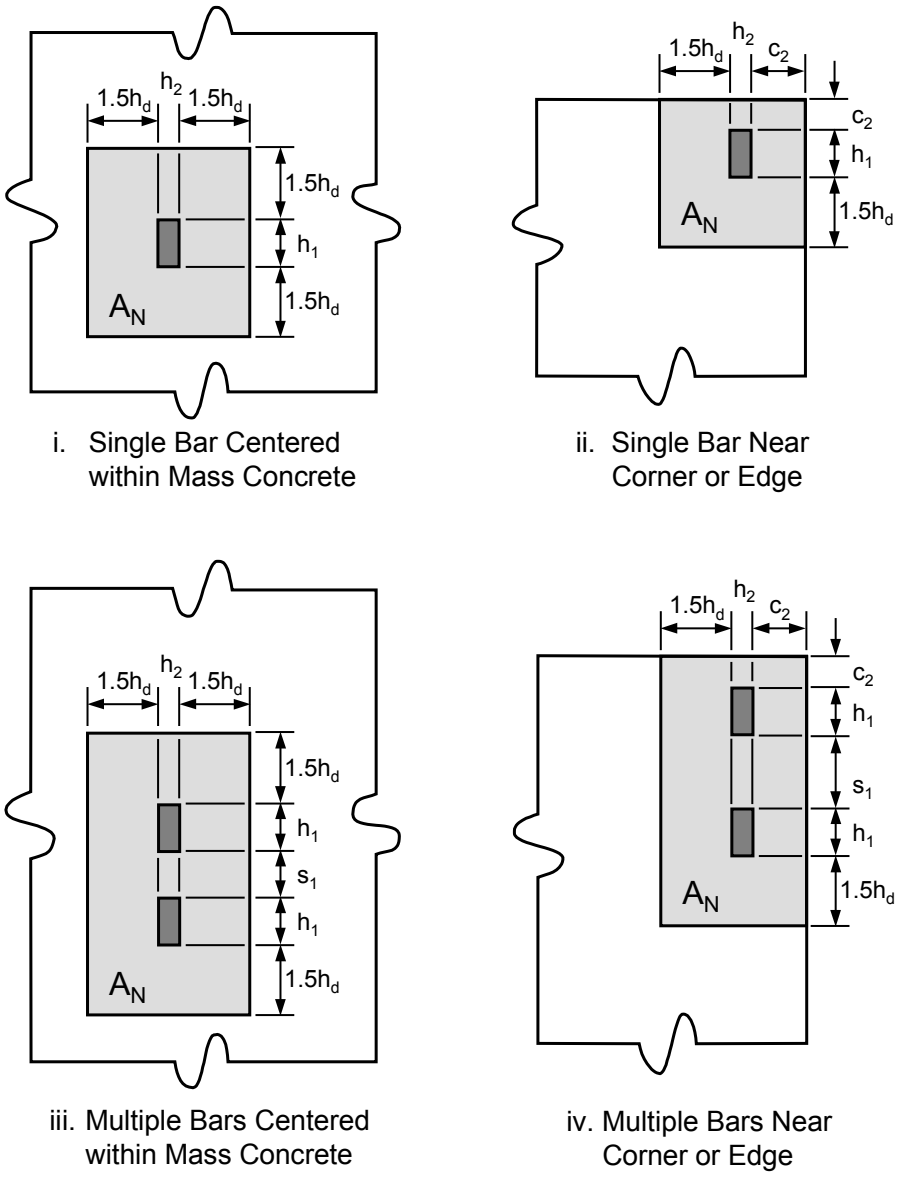

Figure 3-12: Projected concrete breakout areas for different situations

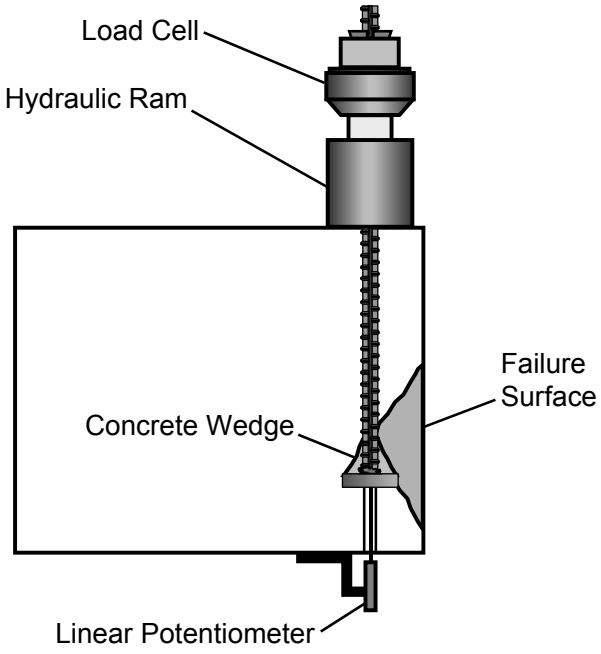

Figure 3-13: Deep embedment pullout specimen used by DeVries and Bashandy

Among the conclusions from the deep embedment studies were:

- The primary mechanism of failure was side blow-out.
- Provided that the embedment depth was sufficient to classify the bar as deeply embedded, further embedment depth did not enhance the ultimate capacity.
- Bonded length did enhance the slip performance of the bar, and provided a small increase in ultimate capacity. The increase in anchorage load due to bond could be reasonably estimated by existing bond equations (here DeVries referred particularly to the Orangun equation used as the basis of the ACI provisions [87]).
- The orientation of rectangular heads had no effect on the ultimate capacity.
- The aspect ratio (width:length) of rectangular heads had no noticeable effect on ultimate capacity.
- The shape of the head (circular versus square) had no visible effect on ultimate capacity.
- Ultimate side blow-out capacity increased with increasing head size and the relationship tended to be linear. DeVries' data were reformulated in terms of bar stress versus relative head area and are shown in Figure 3-14. Many of the bar stresses exceed yield levels because DeVries loaded the bar into the strain hardening range. All the data points presented in Figure 3-14 represent side blow-out failures.
- Ultimate capacity was unaffected by the head thickness even when the head yielded. It should be noted that DeVries' range of head thickness was limited (0.5" – 0.75").

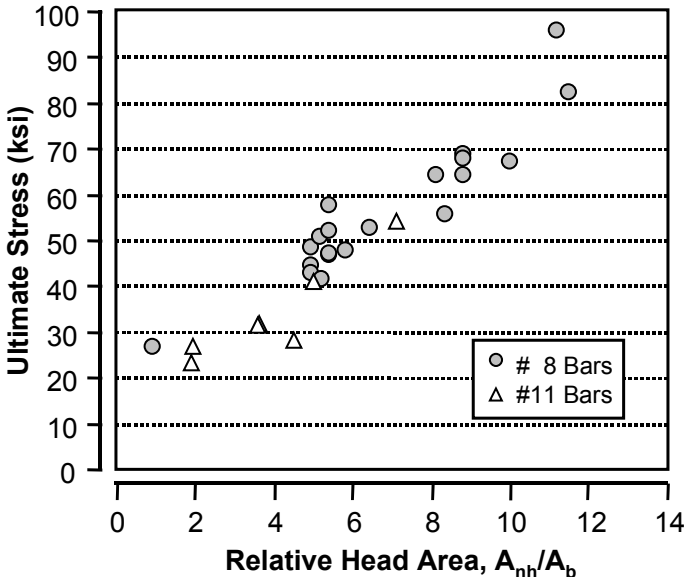

Figure 3-14: DeVries' data on side blow-out capacity versus relative head area

- DeVries studied transverse reinforcement in the form of tie-backs or transverse bars crossing in front of the head. His maximum levels of transverse reinforcement were approximately half the area of the headed bars being anchored. Within those steel limits he found that there was only a small increase in the side blow-out capacity of the headed bar and that the primary benefit of the transverse reinforcement was the residual post-failure capacity provided. Bashandy studied transverse reinforcement in the form of crossing bars and loaded headed bars (ie. a CTT node situation which is discussed further in the next chapter). His transverse levels of steel varied from half to equal amounts of the headed bar area. He found that capacity was improved 10 – 25% by the transverse steel.
- Ultimate capacity improved with increasing concrete compressive strength, and was roughly proportional to $(f_c')^{0.67}$ with much scatter.
- Ultimate capacity improved with increasing edge distance, c_1, and was roughly proportional to $(c_1)^{0.55}$ with much scatter.
- Corner bars had less capacity than bars along only one edge. DeVries recommended that the headed bar should be treated as a corner bar when the maximum edge distance, c_2, was less than 3 times the minimum edge distance, c_1.
- Close bar spacing resulted in a reduction of anchorage capacity similar to edge bars.
- Side blow-out capacity was unaffected by cyclic loading up to a maximum of 15 load cycles.

DeVries determined that the primary variables upon which a design should be based were edge distance, c_1, net head bearing area, A_{nh}, and the concrete compressive strength, f_c'. DeVries compared his data to several models of bearing or side blow-out capacity. He also performed a regression analysis to determine a best-fit equation for capacity. Many existing models of bearing capacity and side blow-out capacity fit the data reasonably well. DeVries' final model of capacity was based on the method recommended in CEB documents [7, 8] for side blow-out of deeply embedded anchor bolts. The CEB formulation is in turn based on research conducted by Furche and Eligehausen at the University of Stuttgart [45]. DeVries recommended the following:

Side Blow-Out Capacity,

$$N_n = \frac{A_{Nsb}}{A_{Nsbo}} \Psi_2 N_{sb} \tag{3-6}$$

$$N_{sb} = 144 c_1 \sqrt{A_{nh} f_c'} \tag{3-7}$$

$$\Psi_2 = 0.7 + 0.3 \frac{c_2}{3c_1} \leq 1 \tag{3-8}$$

N_{sb} = the basic side blow-out capacity (lbs)

Ψ_2 = modification factor for stress disturbance caused corner affects

A_{Nsbo} = basic projected side blow-out area of a single anchored bar, $36(c_1)^2$ (in^2)

A_{Nsb} = projected area of side blow-out failure as defined in Figure 3-15 (in^2)

A_{nh} = the net bearing area of the head (in^2)

c_1, c_2 = the minimum and maximum edge distances (see Figure 3-10) (in)

f_c' = concrete compressive strength (psi)

Additionally, DeVries also recommended that the head be thick enough to prevent yielding of the head steel at ultimate anchorage capacity.

3.4.4.3 Beam-Column Joint Tests

Bashandy tested 32 simulated exterior beam-column joints and one exterior beam- column sub-assemblage [22]. The exterior beam-column joint was designed to be similar to tests performed by Jirsa et al. on hooked bar anchorages in beam-column joints [68, 77]. Figure 3-16 shows the basic configuration. In some tests column ties were included within the joint region to enhance the anchorage confinement of the headed bar or to improve the shear capacity of the joint. Specimens failed by one of two modes: "side blow-out" failure of the headed bar anchorage or shear related failure of the joint region. Bashandy's "side blow-out" failures are placed in quotes because, while they superficially resembled the side blow-out failures in the deep embedment pullout tests, there were some indications of more complex behavior. Similarly, the specimens that failed by a shear related mode could not be easily categorized by either of the distinct modes observed in the shallow and deep embedment pullout studies. Many of the variables studied in the previous headed bar tests were studied here: bar diameter, head geometry (area, aspect ratio, and orientation), embedment depth, side cover, and transverse steel.

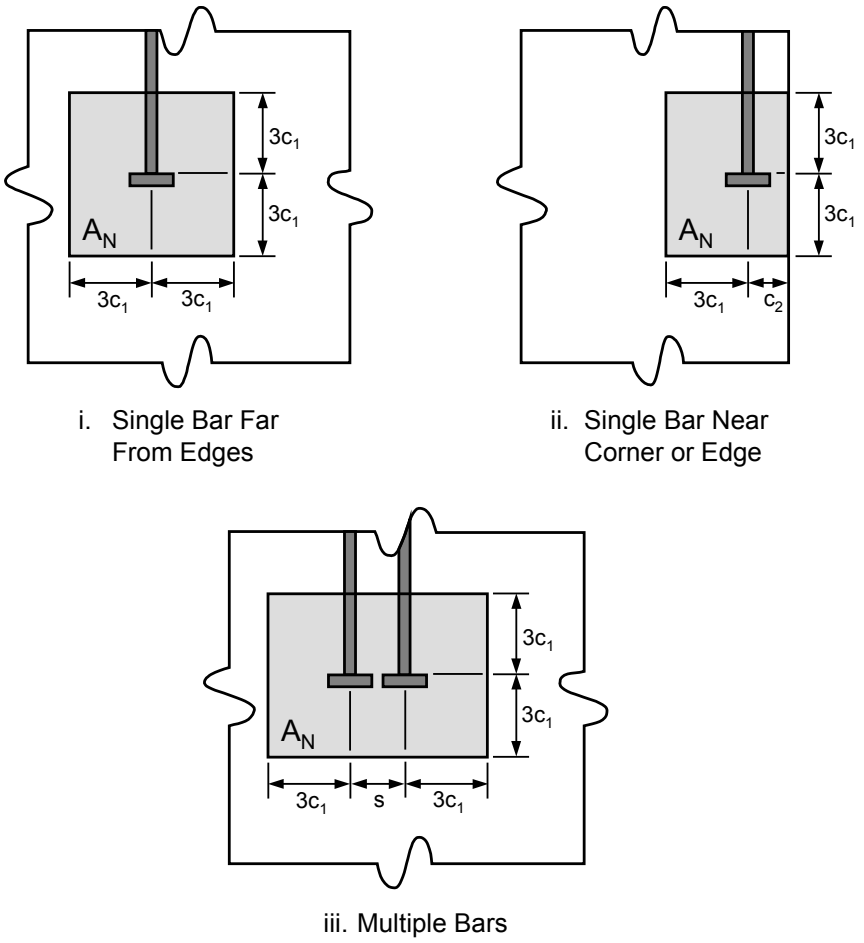

Figure 3-15: Projected concrete side blow-out areas for different situations

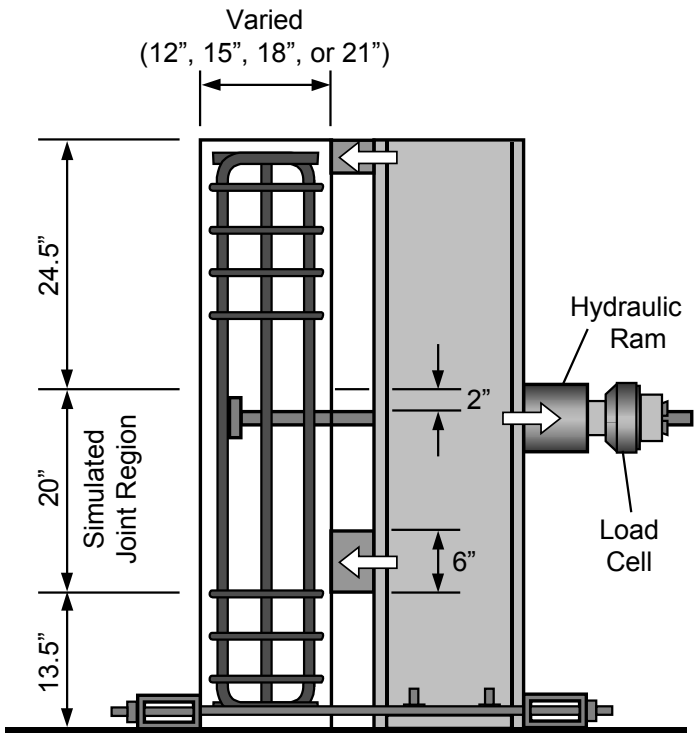

Figure 3-16: Typical exterior beam-column joint studied by Bashandy

Eighteen of the 32 beam-column tests failed by “side blow-out.” The following conclusions were drawn from those tests:

- Among test pairs in which the gross head area and the embedment depth were constant, the bar diameter had no effect on ultimate capacity.
- The results of three companion tests showed that ultimate capacity was improved by increasing the head area of the bar.
- Head aspect ratio and orientation had insignificant effects on ultimate capacity.
- Ultimate capacity increased linearly with embedment depth (measured from the face of the column to the head of the bar). Strain gages indicated that less of the total capacity was carried by the head as embedment depth was increased (Bashandy left the deformed bar unsheathed in these tests). Past a certain embedment length (12”), load in the head did not increase but rather increases in the capacity of the bar were due to bond along the straight lead length.
- Side cover improved the ultimate capacity of the bars.
- Transverse steel confinement was studied in the form of #3 column ties placed parallel to the axis of the headed bars (a typical joint detail). Ultimate capacity was improved with increasing transverse steel which enhanced the anchorage by restraining the side cover from lateral blow-out and by confining the concrete underneath the heads to improve bearing capacity.
- The anchorage performance of headed bars was at least equivalent to and frequently better than analogous hooked bars.

Bashandy compared his test data to data from similar test conditions in DeVries' pullout study. Bashandy found that the capacity of headed bars in joints was 14 – 44% less than analogous bars tested in deep

embedment pullout studies. Bashandy concluded that the capacity of the bars was influenced by the shear in the joint region that affected the failure mode of the bars.

Only one full exterior joint sub-assemblage was tested by Bashandy. Cyclic testing was performed on the sub-assemblage. Bashandy found that the headed bars provided superior performance to hooked bars tested in an equivalent specimen and that capacity degradation and anchorage loss was minimal.

3.4.5 Application Studies

Application studies involving headed bars fall into three categories: tests on joints utilizing headed bars, tests of double-headed bars as shear and confining reinforcement, and studies on the use of headed reinforcement to retrofit and rehabilitate walls and piers for seismic performance.

3.4.5.1 Joint Tests

Five roof corner joint specimens and two exterior beam-column joint specimens were tested at Clarkson University [109]. The research was sponsored by the National Science Foundation with materials supplied by HRC and ERICO. The corner joints utilized HRC friction-welded heads and hooked bars for comparison. The exterior joint specimens used ERICO's Lenton Terminator heads. The tests were intended to test if headed reinforcement could conform to the ACI 352 recommendations for seismic joints in buildings. The researchers found that the headed bars provided greater member stiffness than hooks because there was less slip of the anchorage during cyclic testing. When subjected to cyclic loading eventually all bond was lost and anchorage of the bar was carried solely by the head. At large deformations this caused pushout of the concrete behind the heads when reversed loading placed bottom headed bars in compression. However, this did not occur until unrealistically large deformations had been imposed on the joints.

One bridge column/cap-beam knee joint specimen was tested at the University of California, San Diego [58] with reinforcement provided almost completely by headed reinforcing bars (with the exception of spiral column reinforcement). The research was sponsored by HRC and all of the heads were friction-welded. The specimen was designed to mimic earlier tests using conventional hooked bar anchorage details. The purpose of the test was merely to prove the acceptability of headed bar details for seismic bridge knee joints. The headed bar anchorage was sufficient to carry the anchorage forces and the specimen failed by plastic hinging at the top of the column member. However, the close spacing of the horizontal bars in the cap beam required staggering of the headed anchorages in order to prevent overlapping of head plates. The staggering of the bars within the anchorage zone necessitated a stub extension of the cap beam length beyond the joint region (Figure 3-17).

A follow-up headed bar test at the University of California, San Diego studied the effectiveness of headed reinforcement in a seismic pile/foundation connection [99]. Once again, the research was funded by HRC. They supplied all headed bars used in the specimen. This test was interesting in the fact that Xtender heads were used as anchoring elements for lapped bars. Figure 3-18 shows the basic detail. Short bond bars with large friction-welded heads at one end and Xtender bulb heads at the other were used as bond bars to enhance the anchorage of the pile dowel bars to the foundation slab. This test represents the only known lap splice test of headed bars described in the background literature. Once again, the headed bars were sufficient to provide anchorage and the specimen failed by plastic hinging of the pile element next to the foundation.

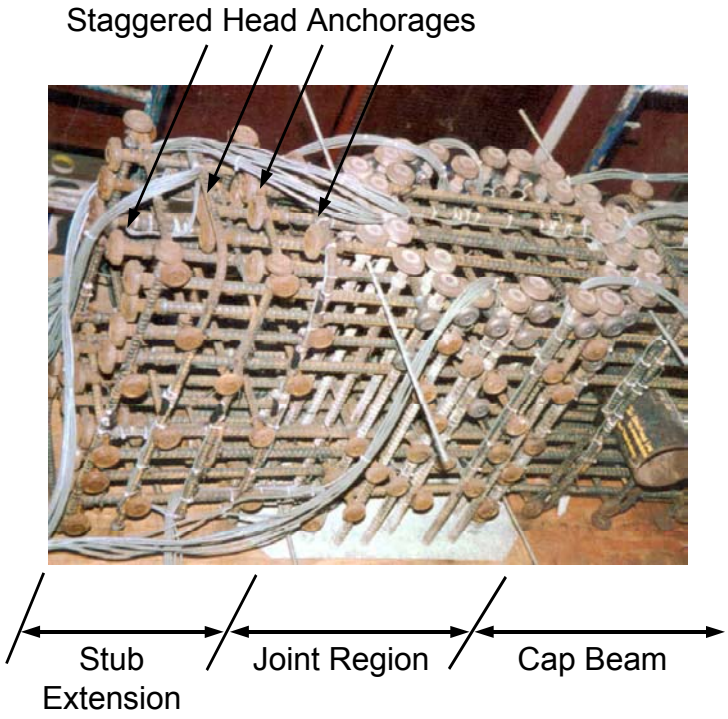

Figure 3-17: Photo of cap-beam/column joint reinforcement from U.C. San Diego study [58]

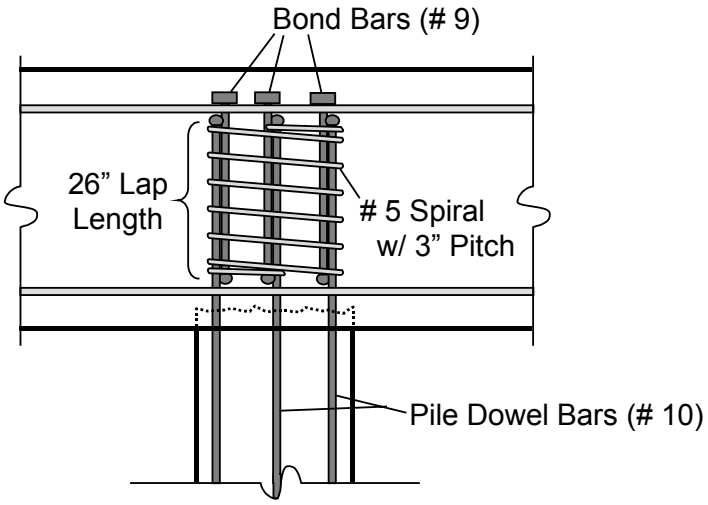

Figure 3-18: Pile/foundation connection studied at University of California, San Diego

Xtender headed bars were studied at the University of Texas at Austin as tie bars for connecting precast bent caps to cast-in-place bridge columns [72]. In the first phase of the study, which was aimed at developing viable pier-cap connection details for precast bent caps, 18 pullout tests were performed on epoxy-coated headed and non-headed bars embedded into grout-filled pockets. The variables of the pullout tests included bar anchorage (Xtender forged heads or non-headed), bar size (#6, #8, and #11), embedment depth ($5 - 18d_b$), grout pockets versus grouted ducts, confining reinforcement around the outside of the grout pocket, and grout parameters including the brand and the inclusion of pea gravel.

Headed bar anchorage underwent four stages: (1) anchorage entirely by bond, (2) formation of splitting cracks in the grout and transfer of bar force from bond to the head, (3) the extension of splitting cracks into the surrounding concrete and the propagation of cracks from the corners of the grout pocket, and (4) failure by yield or concrete breakout. Concrete breakout capacities were compared to the modified CCD equations developed by DeVries [38]. The breakout capacities of the headed bars in the grout pockets were proportional to embedment depth and were about 20% less than the capacities predicted by the modified CCD equations. The reduction in strength was attributed to the influence of cracks propagating from the corners of the grout-filled pockets.

Headed bars were used in several cantilever bridge pier tests at the University of Texas at Austin [20, 112]. The headed bars were tested as anchorage in the CCT and CTT nodes that form at the end of the cantilevered bent and the connection of the bent and the column (Figure 3-19). All of the test specimens were reduced scale, so the headed bars were specially manufactured at the lab. #2 - #5 bar sizes were used with square or rectangular plates fillet-welded to the end of the bar. The relative head areas of the bars varied between 6.5 - 8.8. The researchers found that the headed bars reduced congestion and improved constructabilty of the cages. The anchorage ability of the headed bars was found to be comparable to hooked bars. Comparisons were made on the basis of crack width measurements that showed that the performance of the headed bars was comparable to that of hooked bars.

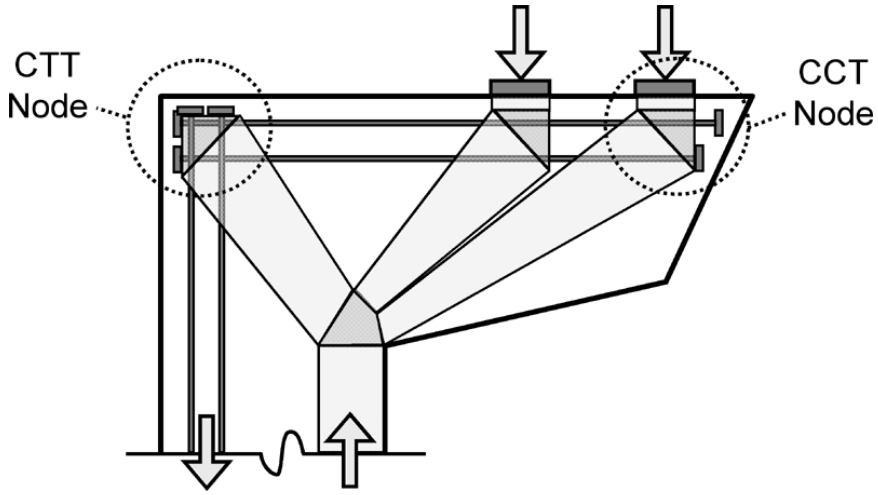

Figure 3-19: Cantilever bridge pier tested at the University of Texas

Following the collapse of the gravity base structure (GBS) of the Sleipner A offshore oil platform on August 23, 1991, a series of full-scale tests were conducted on tri-cell wall joints to verify hypotheses of the collapse causes and to assist in the redesign of the platform. The original and revised plans of the tri-wall cell joint utilized headed bars at a critical juncture and the collapse of the structure was linked to improper anchorage of these headed bars. 10 tri-cell joint specimens were tested by SINTEF in 1992 [34, 59]. Figure 3-20 shows the basic specimen. Failure was attributed to the short anchorage length provided for the double headed bars and the absence of shear reinforcement within the joint zone. Experimental and analytical results indicated that had the headed bar been lengthened 10" on both ends, the failure mode of the tri-wall cell unit would have shifted to the flexure related mode it was designed for rather than the shear-related failure that occurred. This experiment does not indicate that the headed bar did not develop within the provided length. Rather it showed that the as-detailed anchorage point of the headed bar did not correspond to the required location for the tension tie based on strut-and-tie modeling and the flow of forces in the tri-cell wall. The failure crack propagated around the head of the bar. The Sleipner A collapse and corresponding structural tests vividly emphasize that good anchorage should not be confused with good detailing.

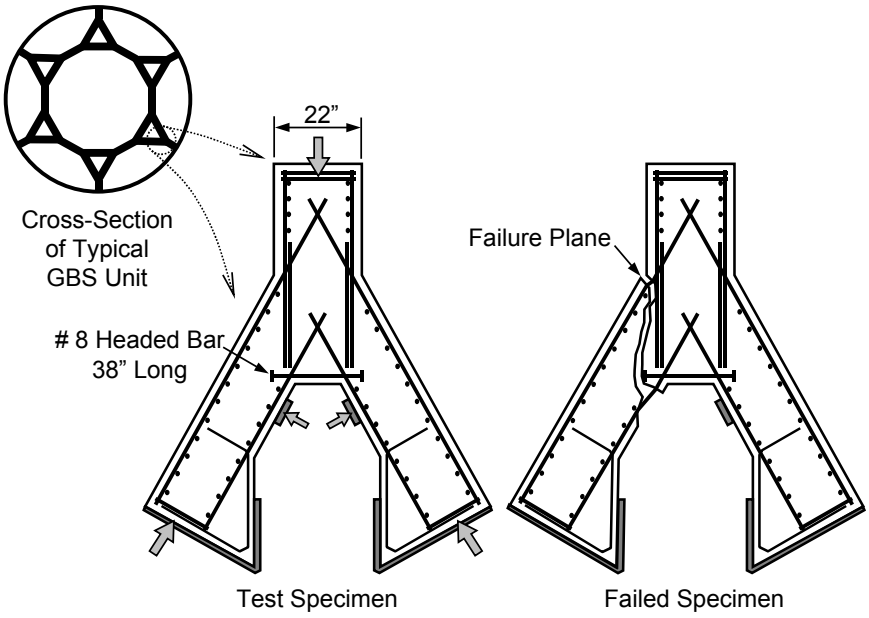

Figure 3-20: Test specimen for Sleipner A collapse investigation

3.4.5.2 Shear and Confining Reinforcement Tests

During the early AOGA (Alaska Oil and Gas) tests on headed bars, a beam test utilizing double-headed stirrups cut from plate steel was tested [25]. The short, deep beam achieved a substantial capacity and sustained that capacity for a ductility factor greater than 40 (due largely to catenary action). A few years later, the consulting firm hired to perform the AOGA tests (Ben C. Gerwick Inc.), was employed by HRC to test three large scale deep beams utilizing HRC manufactured double-headed stirrups [26]. The primary variable was the transverse reinforcing ratio. The beams were supported so that continuous beam conditions were modeled. All three specimens achieved peak ultimate loads that more than doubled the design loads predicted by ACI code equations. After sustained loading, the capacity of the specimens dropped in a ductile manner to the capacity predicted by the ACI code and that capacity was sustained until the tests were halted.

Following their work on studrails for punching shear reinforcement in flat slabs, Dilger and Ghali began to exam usage of double-headed studs as confining reinforcement for wall and shell elements [39]. Five wall specimens were tested at the University of Calgary. One wall contained no transverse confinement and served as a baseline for experimental results. Two walls were confined with conventional bent cross-ties with a 180^{o} bend at one end and a 135^{o} bend at the other. The remaining two walls utilized double-headed ties provided by Decon. The double headed ties utilized heads with the 10 bar area size used in Decon’s Studrail design. Dilger and Ghali found that the double-headed ties provided superior performance to conventional cross-ties. The enhanced performance was due to the fact that the cross-ties did not achieve their full yield capacity before anchorage failure of the bent ends occurred. In contrast, the double-headed ties achieved yield. They also found that the headed ends did not need to engage vertical and horizontal crossing bars in order to achieve yield.

Sixteen large-scale wall elements were tested in the University of Toronto’s Shell Element Tester by Kuchma and Collins [60]. Eight of these wall elements contained double-headed ties as transverse confining reinforcement. The other eight specimens contained no transverse confining reinforcement. Kuchma and Collins found that the capacity and ductility of confined wall elements was superior to that of the analogous unconfined walls. Results of the testing were used to provide transverse confinement

modifiers to analytical formulations for use in non-linear finite element computer programs developed at the University of Toronto for design of offshore oil structures.

3.4.5.3 Rehabilitation and Retrofit Studies

The use of double-headed ties to repair earthquake damaged pier walls was studied at the University of California, Irvine [53]. Walls built to 1971 design standards were tested cyclically to failure then repaired using cross-ties or double-headed ties and re-tested. One out of six wall tests utilized double-headed ties manufactured by HRC. The remaining five tests utilized conventional bent-up cross-ties. The wall repaired with double-headed ties was found to perform better than analogous walls repaired with the cross-ties due to the fact that the cross-ties tended to spall the wall side cover as they acquired load and the bent ends of the ties straightened. The double-headed ties were also found to be far easier to install than the cross-ties. It was determined that the heads did not need to engage buckled longitudinal reinforcement in order to provide confinement.

Four earthquake damaged bridge columns were tested the University of California, Berkeley [63]. Three of the columns had severe damage and different repair schemes utilizing HRC double-headed ties or Xtender mechanical couplers were tried on each column. The first column used the Xtender coupling scheme to replace buckled and fractured longitudinal bars. The remaining two columns used double-headed ties placed longitudinally within an external jacket at the base of the columns. The ties were confined transversely by spiral reinforcement and embedded into the footing member of the bridge column specimens. The three repair schemes were sufficient to rehabilitate the columns to equal or greater capacity than they originally possessed though in some cases the original ductility could not be achieved. The repair schemes were considered successful and the tests proved the potential of the HRC products to be used for seismic rehabilitation of bridge columns.

In addition to the various application studies listed in the proceeding sections, Lenton Terminators were recently used as anchorage for the primary reinforcement in two of four deep beam specimens tested at Purdue University [18]. However, the test specimens were intended to test aspects of structural performance other than anchorage (namely, the performance of diagonal compression struts). Nothing of significance concerning headed bars was noted in the tests other than that the heads provided enough anchorage to sustain yielding of the primary tension steel. Hooked anchorages were used in the remaining two specimens and were also shown to be sufficient.

3.5 RELATED BEHAVIORAL TOPICS

Two phenomena have very similar behavior to the anchorage of headed bars: bearing of rigid plates and anchorage of deeply embedded anchor bolts. These two topics are discussed briefly in this section.

3.5.1 Background on Bearing Capacity

The bearing action of heads very much resembles the bearing action of rigid plates on concrete with the difference that the bond related splitting stresses caused by deformations on the bar disrupt the bearing zone in front of the head (Figure 3-21). Because of the similarities in behavior, it thus seems pertinent to review some of the research on bearing capacity. Only three investigations are summarized herein: the work by Hawkins at the University of Sidney [56, 57], the work by Niyogi at the Indian Institute of Technology [83, 84, 85], and the work by Williams [110]. These studies contain the most extensive research on concrete in bearing and will suffice for an overview of the subject.

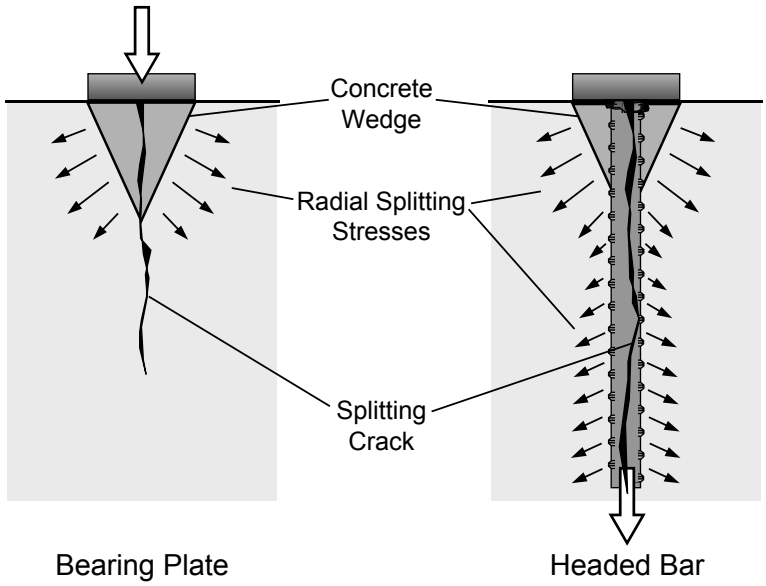

Figure 3-21: Bearing of a rigid plate versus bearing of a headed bar

3.5.1.1 Hawkins

In a two-part study on the bearing strength of concrete, Hawkins performed 300 tests on concrete cube specimens loaded under 113 different test conditions [56, 57]. Hawkins studied such variables as specimen size, specimen shape, plate size, plate shape, plate stiffness, eccentricity of load, edge loading, concrete strength, maximum aggregate size, and aggregate density (lightweight versus normal). He used a theoretical model of failure to develop an equation for the bearing capacity of concrete which he then compared to his test data. Hawkins modeled bearing as a mechanism through which a wedge of concrete forms underneath the bearing plate that subsequently splits the surrounding concrete mass apart as it is pushed downward. Movement of the wedge is resisted by shear friction along the wedge surface and tensile stresses in the surrounding concrete. The resulting model contains components that are added to one another which are proportional to f_c' and $\sqrt{f_c'}$ respectively. The equation that Hawkins derived for concentric loading by a rigid plate is presented below:

$$P_n = f_c' A_1 \left[1 + \frac{K}{\sqrt{f_c'}} \left(\sqrt{\frac{A_2}{A_1}} - 1 \right) \right] \tag{3-9}$$

P_n = the bearing load supported by the plate (lbs)

f_c' = the concrete cylinder strength (psi)

A_1 = the area of the load plate (in^2)

A_2 = the effective unloaded area of concrete (in^2)

K = a constant derived from concrete properties of tensile strength and the angle of internal friction which varied from 50 – 65. Hawkins recommended a value of 50 for design purposes.

Additionally, Hawkins recommended that the effective unloaded area should be concentric with and geometrically similar to the load plate. Furthermore, the area of the effective loading area may be as much as 40 times the area of the load plate before a limit must be imposed. Hawkins also suggested alternative

formulations for strip loading and edge loading of concrete surfaces and proposed a criteria by which a load plate could be considered rigid.

3.5.1.2 Niyogi

Niyogi tested 858 unreinforced concrete specimens under 327 different test conditions [83, 84] and 106 reinforced concrete specimens under 69 different test conditions [85]. He studied variables such as the shape and size of the specimen, the shape and size of the load plate, the position of the load plate, the rigidity of the support conditions for the specimen, the effect of concentrated loading from both ends of the specimen, the concrete strength, and the amount and form of reinforcement under the load plate. Niyogi determined empirical expressions for bearing strength for concentric and eccentric load conditions. His expression for bearing strength under concentric conditions is listed below:

$$P_n = A_1 f_{cc}^{'} \left[0.42 \left(\frac{h_1}{2c_2} + \frac{h_2}{2c_1} + 1 \right) - 0.29 \sqrt{\left(\frac{h_1}{2c_2} - \frac{h_2}{2c_1} \right)^2 + 5.06} \right] \quad (3\text{-}10)$$

P_n = the bearing load supported by the plate (lbs)

f_{cc}' = the concrete cube strength (psi)

A_1 = the area of the load plate (in^2)

h_1 = the width of the load plate (in)

h_2 = the breadth of the load plate (in)

$2c_2$ = the width of the specimen (in)

$2c_1$ = the breadth of the specimen (in)

Niyogi's notation was different than the notation listed above. The notation has been altered to resemble the notation used by DeVries for headed bars (see Figure 3-10). Also note that Niyogi's formula is related to the compression strength of concrete cube tests, not the typical cylindrical compression strength. Cube tests generally provide compressive strength values 15-20% higher than cylinder tests of the same concrete. The conversions $f_c' = {}^5/_6\, f_{cc}'$ or ${}^6/_7\, f_{cc}'$ are typically used.

Niyogi made several observations from his study:

- The bearing capacity of eccentrically loaded blocks was greater than the capacity predicted using a concentric reduced area to calculate load capacity.
- The bearing capacity was affected by the height of the specimens when the breadth and width were greater than the height. Beyond that point, the capacities leveled off. Specimens with smaller ratios of unloaded area to load plate area ($A_2/A_1 < 16$) showed decreasing capacity with increasing specimen height. Specimens with larger ratios ($A_2/A_1 > 16$) showed increasing capacity with increasing specimen height.
- The support medium of the specimen (see Figure 3-22) affected its capacity when the specimen blocks were shallow (height/width < 2). The more compressible the support medium, the less the capacity of the blocks.
- Simultaneous concentrated loading on both ends of the specimen (Figure 3-22, ii.) resulted in reduced bearing capacity. The reduction in bearing capacity was diminished as the specimen height was increased but did not disappear even when the height was increased to twice the width dimension.

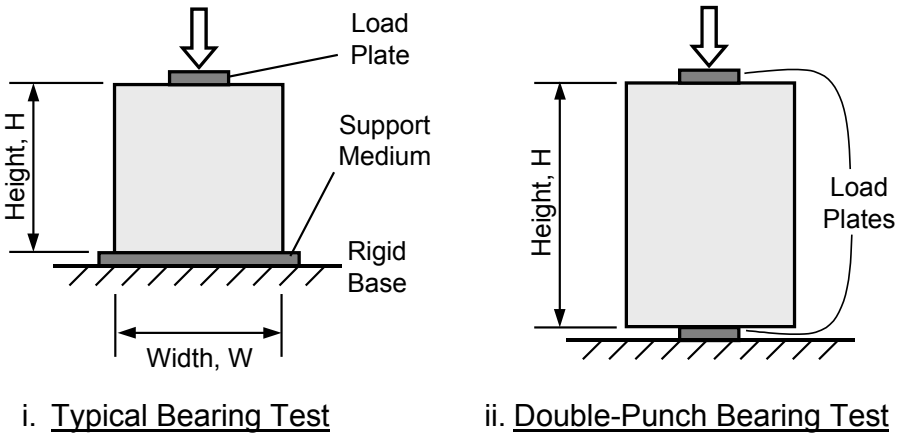

Figure 3-22: Bearing tests on concrete blocks

- At low ratios of unloaded to loaded area ($A_2/A_1 < 4$), the bearing strength was directly proportional the concrete strength, but as the A_2/A_1 ratio was increased, the bearing capacity was proportional to a lesser power of concrete strength.
- A size effect was observed for geometrically proportional specimens of varying sizes. Bearing capacity diminished as the dimensions of the specimen and load plate increased (Figure 3-23).
- Large diameter spirals provided the most effective reinforcement for bearing capacity. The spiral steel closest to the load plate was the most effective portion of the spiral.

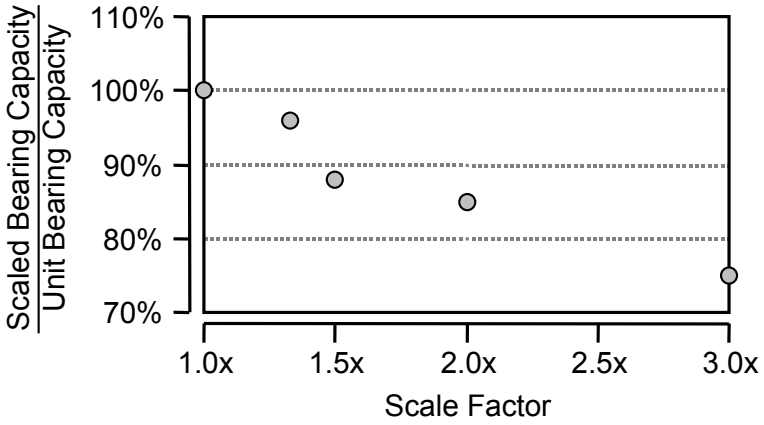

Figure 3-23: Niyogi's size effect data

3.5.1.3 Williams

Williams performed more than 1500 tests under 382 different test conditions [110]. In addition, Williams collected a database of test results from the array of literature on bearing capacity or related behavior such as post-tensioned anchorage plates. His experimental work was aimed at filling in the gaps left in the experimental database. He studied such variables as specimen height, the effect of a softening medium placed between the load plate and the concrete surface, the effect of the concrete surface condition (trowelled or cast flat), eccentric loading, the effect of the secondary width dimension, the effect of support friction, the size effect produced by using a micro-concrete with a very small maximum aggregate

size, and the effect of a lateral shearing component of load on capacity. After performing a regression analysis of the combined database of his work and previous investigations he determined that the following equation best predicted the bearing capacity of concrete:

$$P_n = 6.92 \cdot A_1 f_{ct} \left(\frac{A_2}{A_1} \right)^{0.47} \quad (3\text{-}11)$$

P_n = The bearing load supported by the plate (lbs)

f_{ct} = The concrete tensile strength (determined from split cylinder tests) (psi)

A_1 = The area of the load plate (in^2)

A_2 = The effective unloaded area of concrete (in^2)

For simplicity, Williams recommended that an exponent of 0.5 be used rather than 0.47 for the A_2/A_1 ratio.

In addition, Williams observed the following:

- Specimens with height/width ratios greater than 1.5 were unaffected by the supporting medium on which they reacted.
- Bearing capacity was affected by the placement of a softening medium between the load plate and the concrete surface. In general, the softer the load medium, the lesser the bearing capacity.
- Bearing capacity was affected by the friction and rigidity of the support medium. In general, the softer the support medium and the less friction provided by the support medium, the lesser the bearing capacity.
- Bearing capacity was reduced when the contact surface between the load plate and the concrete surface was not uniform (ie. when the concrete bearing surface was trowelled rather than cast flat).
- The bearing capacity was determined by the resistance of the specimens to splitting, therefore the tensile strength, not the compressive strength, of the concrete is the governing factor for bearing resistance.
- Because capacity was governed by lateral splitting, the affect of lateral tensile loads on capacity can severely reduce the bearing capacity. He did not examine the effect of lateral compression loads.
- For edge loading, increases in the secondary cover dimension (see Figure 3-24) can enhance the bearing capacity. This increase in capacity diminished once the secondary cover dimension exceeds four times the width of the load plate.

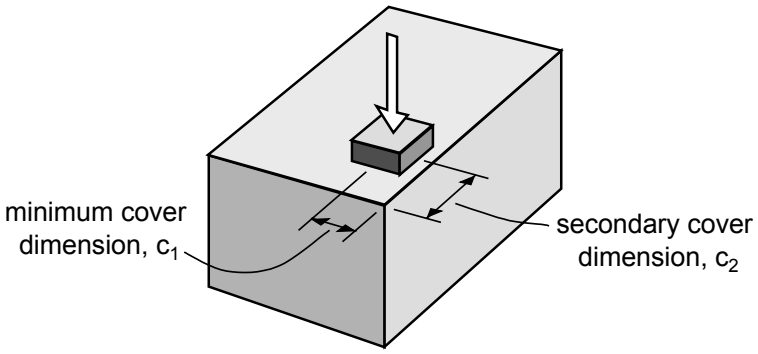

Figure 3-24: Minimum and secondary cover dimensions

3.5.2 Deeply Embedded Headed Anchor Bolts

Deeply embedded headed anchor bolts are frequently used to connect steel columns to concrete support blocks or drilled piers. Deeply embedded headed anchor bolts differ from shallow embedment anchors by the nature of their failure mechanism. Shallow embedment headed anchors fail by the formation of a breakout cone which pulls out of the face of the concrete (see Figure 3-11). Deeply embedded anchors fail by side spalling of the concrete cover near the anchor head which is referred to as side blow-out (see Figure 3-13). DeVries' [38] pullout tests reproduced these two failure modes for headed bars. However, prior to DeVries' research, several studies on the anchorage behavior of deeply embedded headed anchor bolts were performed at The University of Texas in Austin and the University of Stuttgart. The behavior of headed anchor bolts is very similar to the behavior of the headed bars. This section summarizes the research on deeply embedded headed anchor bolts and the similarities and differences in anchorage behavior of headed bars and headed anchor bolts. Emphasis is placed on deep embedment tests because their side blow-out behavior resembles the failure modes which occur in this investigation much more than the concrete breakout failure of shallow embedment tests. Due to the importance of the model for prediction of side blow-out capacity, some in depth background into the development of the model is necessary.

3.5.2.1 Lee and Breen

In the 60's Breen [27] and Lee [62] studied the development length of anchor bolts cast into square footings. Breen performed 36 bolt tests using the test setup shown in Figure 3-25. He studied variables such as bolt diameter ($1^1/_4$" to 3"), embedment depth ($10d_b$ or $15d_b$), and the presence of a nut or a washer and nut at the end anchorage of the bolt. His concrete strengths ranged from 3.2 to 5.3 ksi. Lee performed a follow-up study on 26 anchor bolts using the same type of specimen. In some tests, he modified the load arrangement slightly so that the maximum footing moment occurred at the level of the bolt end anchorages. Lee studied variables such as the clear cover ($1d_b$ to $4d_b$), cyclic loading, the shape of the footing (square or circular), concrete strength (2.5 to 6.0 ksi), and the use of 90^o bend end anchorages. Because many of Breen's bolt specimens yielded before failure of the concrete occurred, Lee used higher strength bolts in his tests.

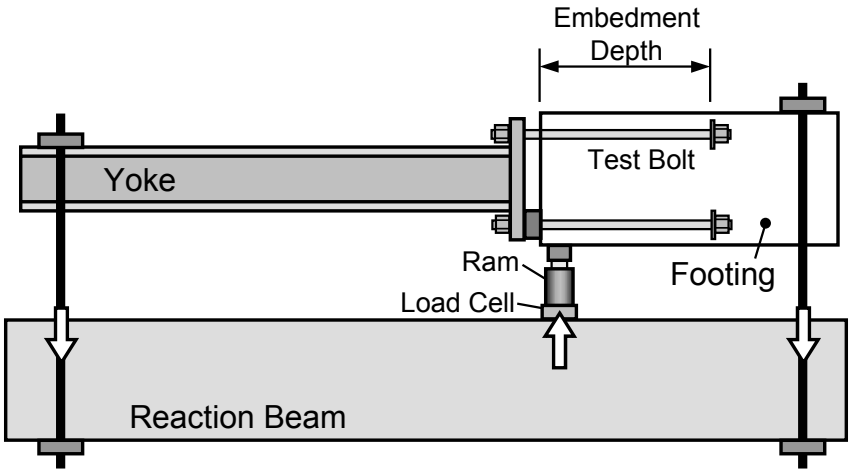

Figure 3-25: Test specimen used by Lee and Breen

Lee and Breen observed the following:

- Bolts failed by one of three mechanisms: longitudinal splitting of the concrete cover similar to the failure of a deformed bar, side blow-out of the cover over the head, or fracture of the bolt steel.
- Initially, adhesion of the bolt shaft to the concrete provided bond anchorage. However, as the bolt load was increased, the bond of the bolt shaft deteriorated until full anchorage was provided by the head only. This behavior was determined by analysis of the loaded end slip.
- The method of loading (varied by Lee) affected the loaded end slip but not the ultimate strength of the bolt.
- The shape of the drilled shaft footing did not affect the slip or ultimate strength behavior of the bolt.
- The primary variables affecting bolt anchorage were cover and concrete strength.

3.5.2.2 Hasselwander and Lo

In the 70's Hasselwander and Lo [54, 55] conducted 35 full-scale and 29 model bolt tests using specimens similar to those used by Lee and Breen. The primary purpose of their study was to develop design equations for the use of deeply embedded high strength anchor bolts. The variables studied in their test program were: bolt diameter ($^1/_2$", 1", or $1^3/_4$"), embedment depth ($10d_b$, $15d_b$, or $20d_b$), clear cover ($1d_b$ to $4.5d_b$), bearing area (A_{nh}/A_b = 1.9 to 19.3), cyclic loading, lateral shear loading of the bolt, bolts in groups of two (center spacing = 5", 10", or 15"), and transverse reinforcement in the form of hairpins (1 or 2 #4 bars placed close to the head).

Hasselwander and Lo observed the following:

- Bolts failed by the three mechanisms previously observed by Lee and Breen. Splitting or spalling of the concrete cover was preceded by the formation of a wedge of concrete at the anchor head that produced lateral splitting forces.
- The primary variables affecting bolt capacity were concrete strength, clear cover, and the bearing area of the head.
- Cyclic loading at or below the service level did not significantly affect the strength or behavior of the anchor bolt.

- Transverse reinforcement significantly increased the strength and ductility of anchor bolts with shallow cover.
- Lateral shear loading significantly reduced the tensile capacity of the bolt.
- The capacity of individual bolts in groups was lower than the capacity of individual bolts in tension. At the spacings studied, the two bolt groups had total capacities approximately equal to the capacity of individual bolts.

Hasselwander performed a regression analysis of the data from bolts that failed by wedge splitting (longitudinal splitting of the cover over the bolt) and developed an equation for the capacity of anchor bolts loaded in tension:

$$T = 140 A_{nh} \sqrt{f_c'} \left[0.7 + \ln\left(\frac{2c'}{d_w - d_b} \right) \right] \tag{3-12}$$

T = ultimate capacity of a single anchor bolt (lbs)

A_{nh} = net bearing area of the anchor head which is limited to $4d_b^2$ (in^2)

d_b = bolt diameter (in)

d_w = washer (head) diameter (in)

c' = clear cover to bolt (in)

Equation 3-10 is limited to anchor bolts with embedment depths greater than $12(d_w - d_b)$.

3.5.2.3 Furche and Eligehausen

In the 80's, Furche and Eligehausen [45] conducted 35 tests of single headed anchors in specimens similar to DeVries'. The variables in their study included embedment depth (h_d = 4" to 20"), cover dimension (c_1 = 1.6" to 3.1"), head area (A_{nh} = 0.41 to 1.71 in^2), and the head angle (θ_{head} = 5^o, 20^o, or 90^o). Figure 3-26 describes the head angle. Their concrete strength was kept constant at 3.8 ksi as was their bolt diameter at 1".

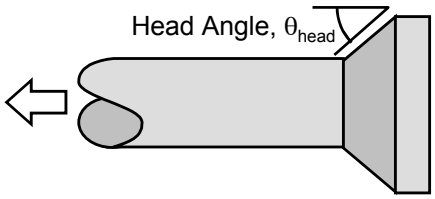

Figure 3-26: Definition of head angle

Furche and Eligehausen's specimens failed by one of two modes: concrete breakout or side blow-out. The transition from concrete breakout failure to side blow-out was dependent on the ratio of cover dimension to embedment depth and the ratio of embedment depth to head bearing area. They determined an equation to define the critical cover/embedment ratio as a function of embedment/bearing area ratio:

$$\frac{c_1}{h_d} = \frac{0.06}{\left(\sqrt{A_{nh}/h_d} - 0.1 \right)} \tag{3-13}$$

c_1 = cover dimension (in)

h_d = embedment depth (in)

A_{nh} = net bearing area (in^2)

Figure 3-27 plots equation 3-11. Cover/embedment values that plot above the transition line fall in the region where concrete breakout failure should occur. Values below the transition line fall in the region of side blow-out failure.

Furche and Eligehausen developed an equation to define the side blow-out capacity of headed anchors:

$$T = 6.4 c_1 \sqrt{A_{nh} f_c'} \tag{3-14}$$

T = ultimate capacity of a single anchor bolt (lbs)

f_c' = concrete cylinder strength (ksi)

The variables c_1 and A_{nh} are as defined for equation 3-11. Equation 3-14 was produced from a regression analysis of Furche and Eligehausen's data as well as the published data of Hasselwander and Lo [54]. Furche and Eligehausen recommended an additional factor of 0.8 to produce a 5% fractile capacity.

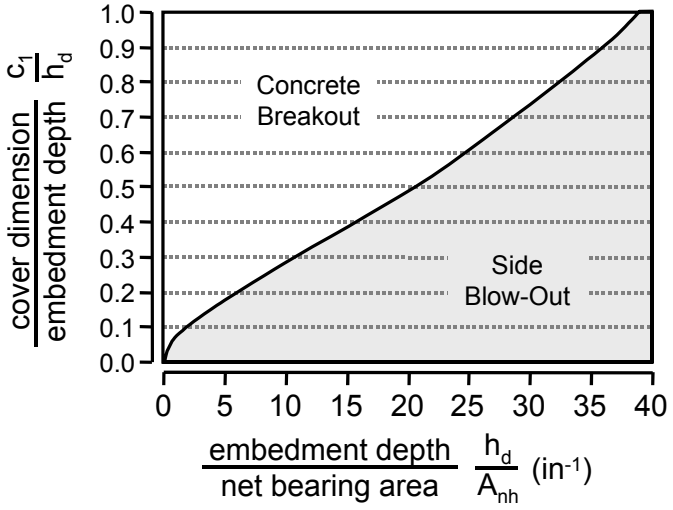

Figure 3-27: Furche and Eligehausen's transition of failure modes for headed anchors

Additionally, Furche and Eligehausen observed the following:

- Of the bolts which failed by side blow-out, the diameter of the blow-out cone was between 6 to 8 times the cover dimension, c_1.
- Measurements of lateral concrete deformations indicated that lateral bulging of the concrete cover did not begin until the peak capacity of the bolt was achieved.
- Shallower head angles resulted in significantly reduced anchorage capacities. For the shallow angles tested by Furche and Eligehausen (5^o and 20^o), the capacity of the bolts was reduced by as much as 50% from the capacity of bolts with head angles of 90^o.

3.6 CODE PROVISIONS

There are no code provisions that provide direct guidance for the detailing of headed reinforcing bars. Both Wright and McCabe [113] and DeVries [38] have proposed anchorage provisions for headed bars which have already been presented. However, neither of the proposed guidelines has been included in the 2002 ACI 318 Building Code. The few guidelines that do exist among the design codes are discussed in

this section. The ACI and AASHTO codes are discussed as well some provisions from the Canadian design and a controversial ASTM specification. Guidelines for bearing plates will also be discussed since they closely resemble the theoretical anchorage behavior of headed bar heads.

3.6.1 U.S. Mechanical Anchorage Provisions

Both the ACI 318 code [2] and the AASHTO Bridge Design Specifications [1] use nearly identical language for their mechanical anchorage provisions. Currently, designers using headed bars would probably take their guidance from the provisions for mechanical anchorage. Section 12.6 of the ACI code and Section 5.11.3 of the AASHTO code provide provisions for mechanical anchorage. Both provisions state the following:

- Any mechanical device capable of developing the strength of a reinforcing bar without damaging the concrete is allowed.
- Such devices may consist of a combination of the mechanical anchorage and bond of the additional embedment length of reinforcement between the point of maximum bar stress and the mechanical anchoring device. The commentary of both provisions specifically states that the yield strength of the bar does not need to be entirely supported by the mechanical anchorage provided that the combination of bond and mechanical anchorage can support the yield strength.
- Documentation of the sufficiency of the mechanical anchoring device shall be provided in contract drawings or presented to the pertinent building official.

Otherwise, no guidelines for design and use of mechanical anchoring devices is provided.

3.6.2 Canadian Shear Provisions

The Canadian Code, CSA A23.3-94 for Design of Concrete Structures [6] allows for the use of headed shear reinforcement in Clause 13.4.8 of the code. Sub-clauses 13.4.8.1-3 of this code requires the following:

- The headed anchorage shall be capable of developing the full yield strength of the bar.
- The head area of the bar shall be at least 10 times the area of the bar unless experimental evidence justifies a smaller size.
- The factored total shear stress resistance (in SI units) shall be no greater than $0.8\lambda\phi_c\sqrt{f_c'}$ which is 1.33 times greater than the total allowed for members with conventional shear reinforcement.
- The factored shear stress contribution from concrete (in SI units) shall be no greater than $0.3\lambda\phi_c\sqrt{f_c'}$ which is 1.5 times greater than that allowed for members with conventional reinforcement.

The second statement undoubtedly derives from the headed stud research performed by Dilger and Ghali [40, 79] at the University of Calgary. The increases in concrete shear capacity result from the enhanced confinement effect that headed bars should presumably provide.

3.6.3 ASTM Specification for Weld Connected Heads

The ASTM A970 Specification for Welded Headed Bars [5] applies to headed bars in which the head is connected to the bar by means of any welded connection. The specification deals primarily with quality control standards for the head-bar weld connection, but also contains requirements for head sizes. Specification 7 deals with the quality control of the weld connection and mandates procedures for several performance tests including static tension and bend tests of the head-bar connection. Additionally,

Appendix X2 includes non-mandatory recommendations for metallurgical and hardness tests of the head and welded zone. The appendixes (in X3.6-7) also recommend extensive record keeping of automated production process parameters specifically citing force, temperature, and revolutions, all of which are parameters associated particularly with friction-welded heads.

Specification 5 "Materials and Manufacture" is the most significant for structural designers. This is the specification that mandates head sizes for welded headed bars. Table 1 lists gross head area requirements that correspond to 10 bar areas for each bar size (or $A_{nh}/A_b = 9$). Note 2 of the table states that such head sizes are to ensure that concrete crushing failure does not occur underneath the head based on a concrete compressive strength of 30 MPa (4.4 ksi) and a bar yield strength of 420 MPa (61 ksi). Note 4 states that the specified head sizes are necessary for anchorage of the bar by the head only. Heads with smaller sizes are permissible provided that the headed bar manufacturer provide documentation that confirm the suitability of the head for the intended application (Specification 5.3).

This ASTM Specification is controversial because of the head size specifications. Some designers and manufactures feel that it is inappropriate for the ASTM document to specify head size and that that decision should rest with the structural engineer. In a correspondence between this author and Steven McCabe of the University of Kansas who was the author of the standard [116], Mr. McCabe stated that the head size recommendations were developed out of a collective work including the SINTEF tests performed for Metalock as well as "hundreds of studies of these [headed bars] in various locations on both sides of the Atlantic." The size recommendations were also influenced by the inclusion within the Canadian CSA Code of a 10 bar area requirement for head size.

The quality control measures specified in the document also bear striking resemblance to those practiced by HRC. The language in parts of the code suggests a bias towards friction-welded headed bars over other potential forms of welded headed bars. Mr. McCabe stated that he worked with representatives from HRC during the formation of the ASTM specifications. Given the fact that HRC is the only manufacturer of friction welded headed bars at the current time and thus have the only documented methods for the quality control of welded headed bars, their standards of production may have overly influenced the writing of the code.

As a result of the head size requirements and the language of the quality control standards, the ASTM specification has been viewed as biased towards HRC's headed bars and biased against their competitor, ERICO's Lenton Terminator. Due to these controversies over the first draft of the ASTM specification, new drafts of the A970 Specification are currently under development. Within the newer drafts, inclusion of quality control standards for other forms of head-bar connections such as the tapered thread used by ERICO may also be included and the minimum head size standards may also be modified or dropped [116].

3.6.4 U.S. Bearing Strength Provisions

Both the ACI and AASHTO code contain similar provisions regarding the bearing strength of concrete. Bearing strength is covered in Section 10.17 of the ACI code and Section 5.7.5 of the AASHTO code. Both codes give the following equation:

$$P_n = 0.85 f_c' A_1 \sqrt{\frac{A_2}{A_1}} \qquad (3\text{-}15)$$

P_n = concrete bearing strength (lbs)

f_c' = concrete compressive stress (psi)

A_1 = loaded area (in^2)

A_2 = notional area defined by a frustum projected beneath the loaded surface, as defined in Figure 3-28 (in^2)

Because there is a limit imposed on the maximum size of A_2 (see Figure 3-28), the maximum bearing strength provided by Equation 3-13 is $1.7f_c'$.

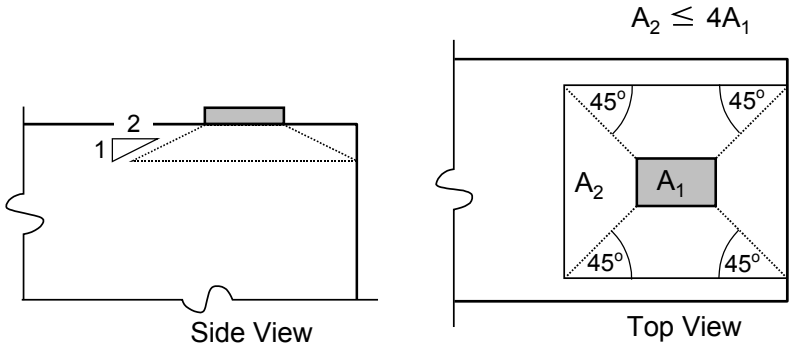

Figure 3-28: Definition of notional area

3.7 FINAL COMMENTS

There are many details from the collection of reviewed literature in this chapter that warrant reflection.

First, among the research that has been performed on headed bars, a disproportionate amount of the work has used only one type of headed bar, HRC's friction welded head. Of the 15 research projects on headed bars that were reviewed, only one project has represented both HRC's and ERICO's head types in the research (the Clarkson study), and even then, the experiments with the friction-welded heads and the threaded heads were not directly comparable to one another. The early Caltrans study was also comprehensive in its representation of a variety of head types, and the pullout tests by DeVries and Bashandy at the University of Texas represented a variety of head sizes. However, despite these exceptions, the predominance of the research has used only one head type: a friction-welded head of a size of about 10 bar areas. This is a major shortcoming of the available research and should be addressed in future studies.

The studies by Caltrans (1974) and the University of Texas (DeVries) have both demonstrated that bond can be a significant component of headed bar anchorage and that the current development length equations can be used to reasonably estimate the contribution of bond stress. Data from Caltrans, the University of Texas, and Clarkson have also indicated that, because of the contribution of bond, head sizes smaller than 10 bar areas can work for certain situations particularly when the embedment length of the bar is large.

The bearing capacity study by Williams has shown that capacity is proportional to the square root of the plate area times the effective unloaded area. If the effective unloaded area is considered to be four times the minimum cover dimension squared, $4c_1^2$ (essentially the largest square which can be inscribed underneath the load plate), then the following results:

$$P_n \propto A_1\sqrt{\frac{A_2}{A_1}} = \sqrt{A_1A_2} = \sqrt{A_1(4c_1)^2} = 2c_1\sqrt{A_1} \qquad (3\text{-}16)$$

The final product shown above is very similar to the basic side blow-out formula which DeVries used to model the behavior of the deeply embedded headed bars and Furche and Eligehausen used for deeply embedded anchor bolts:

$$N_{sb} = 144 c_1 \sqrt{A_{nh} f'_c} \propto c_1 \sqrt{A_{nh}} \tag{3-17}$$

The similarity between the two equations tends to suggest a similarity in behavior. Side blow-out failure and bearing failure both involve the formation of a compressed wedge of concrete at the head or bearing plate. Forward movement of this wedge is resisted by friction parallel to the surface of the wedge and lateral tension stresses in the surrounding concrete. In the case of a bearing plate test, lateral tension results in through splitting of the concrete block specimen (Figure 3-29, part i.). In the case of a headed bar or anchor bolt which is close to an edge, the lateral tension results in splitting and spalling of the concrete surface that provides the least cover (Figure 3-29, part ii). The three types of tests demonstrate similar behavior and their capacities show a dependency on the same variables. Thus, it is reasonable that the collected data from bearing tests, deeply embedded anchor bolt tests, and deeply embedded headed bar tests could be assimilated into one database representing a class of behavior which could be used to calibrate a formula for the bearing capacity in all three types of applications.

Another similarity in behavior between bearing studies, anchor bolt studies, and headed bar studies appears in the term for the modification factor for radial stress disturbances, Ψ_1. While such a term does not appear in any of the bearing capacity formulas, experimental evidence has suggested that such a term might be appropriate. The Ψ_1 term recognizes an improvement in capacity for headed bars in which the secondary cover dimension, c_2, is greater than the minimum cover dimension, c_1 (see Figure 3-30). Williams noted that the capacity of an edge plate was enhanced when additional width was added to the sides of his specimens. Niyogi also noted that capacity calculations based solely on the projection of the load plate in defining the effective unloaded area tended to under-predict the measured capacities of uni-axial eccentric specimens. Williams' and Niyogi's experimental observations suggest that bearing capacity improves as the ratio c_2/c_1 increases and a Ψ_1 type term would be appropriate for bearing capacity formulations.

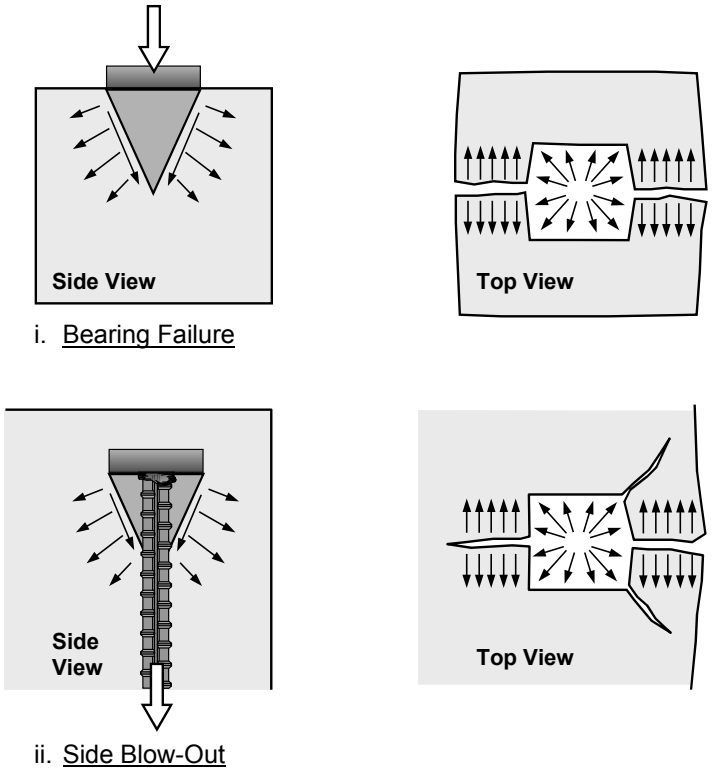

Figure 3-29: Splitting mechanism in bearing and side blow-out failures

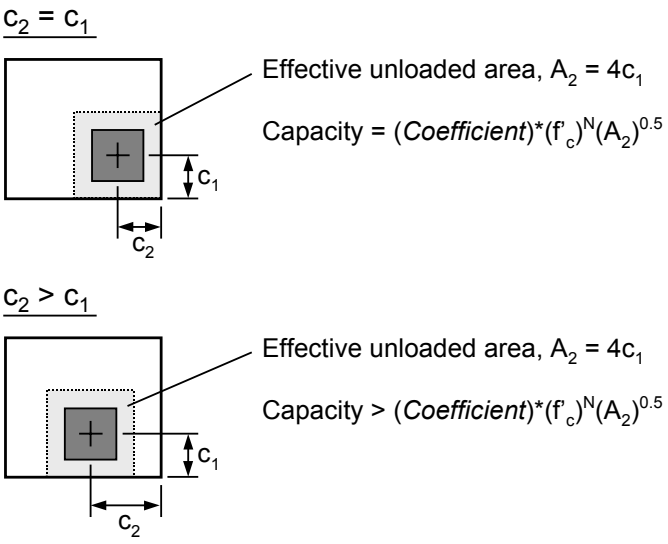

Figure 3-30: Effect of the secondary cover dimension, c_2

CHAPTER 4: BACKGROUND ON STRUT-AND-TIE MODELING

4.1 INTRODUCTION

Strut-and-Tie Modeling (STM) is a detailing and ultimate strength calculation procedure for discontinuity regions within structures. When point loads are introduced onto structural members or abrupt changes in cross-section are introduced, conventional methods of plane section analysis are no longer sufficient. Such locations (termed disturbed regions) are generally detailed using rules of experience or empirical guidelines based on limited research data. Such methods are not based in structural mechanics for ultimate strength determination. Empirical methods are limited to the experience base from which the method derives. It is possible to analyze disturbed regions using complex analysis procedures such as finite elements. However, the computer software necessary for such computation is not readily available to many designers. Furthermore, the cost and time of such analysis, which might constitute a large percentage of the designer's effort, does not always reflect the material and construction cost of the disturbed regions, which may represent only a minor part of the cost of a complete construction project. Strut-and-tie modeling represents an in-between design method for complex structural details that has a basis in mechanics but is simple enough to be readily applied in design.

STM is a method involving the idealization of a complex structural member into a simple collection of struts, ties, and nodes representing, in a general manner, the flow of stress paths within the member. Figure 4-1 shows some typical structural components for which STM could be applied. STM is ideal for deep members, joints, supporting brackets or corbels, dapped beam ends, anchorage zones for post-tensioning, and many other complex structural components.

STM is derived from plasticity theory. STM is a lower bound solution method. According to the theory of plasticity, any statically admissible stress field that is in equilibrium with the applied loads and in which stress levels are on or within the material yield surface constitutes a lower bound solution [82]. Plastic material behavior is a primary assumption of plasticity theory. Strain capacity of the materials is a fundamental requirement to fully satisfy that a lower bound solution occurs. Though plain concrete lacks considerable plastic stress-strain behavior, properly detailed, confined concrete can sustain ductile compressive strains (Figure 4-2). Plasticity theory has been applied to the design of reinforced concrete but only with the proviso that strain limits within the concrete are limited or adequate detailing is provided to enhance the ultimate strain limits of the material.

STM involves the construction of a truss mechanism contained within the boundaries of the member being analyzed. The truss mechanism is composed of struts that model concrete compression fields, ties that model tensile steel reinforcement, and nodes that represent the localized zones in which the tensile steel is anchored into the concrete and strut forces are transferred into the ties. The struts and ties carry only uniaxial stresses. This truss mechanism must be stable and properly balance the applied loads. Failure of the truss mechanism is dictated by yielding of one or more ties or by excessive stresses within the struts or nodes or by an anchorage failure of the reinforcement at one of the nodes. When used properly to detail a structural member, only the first of the aforementioned failure modes should occur. The choice of acceptable concrete stress levels for struts and nodes is an empirical add-on to conventional plastic theory designed to allow for the use of concrete. Allowable stress levels are chosen to prevent local crushing or splitting of struts and nodes and are generally based on the degree of confinement available to the concrete.

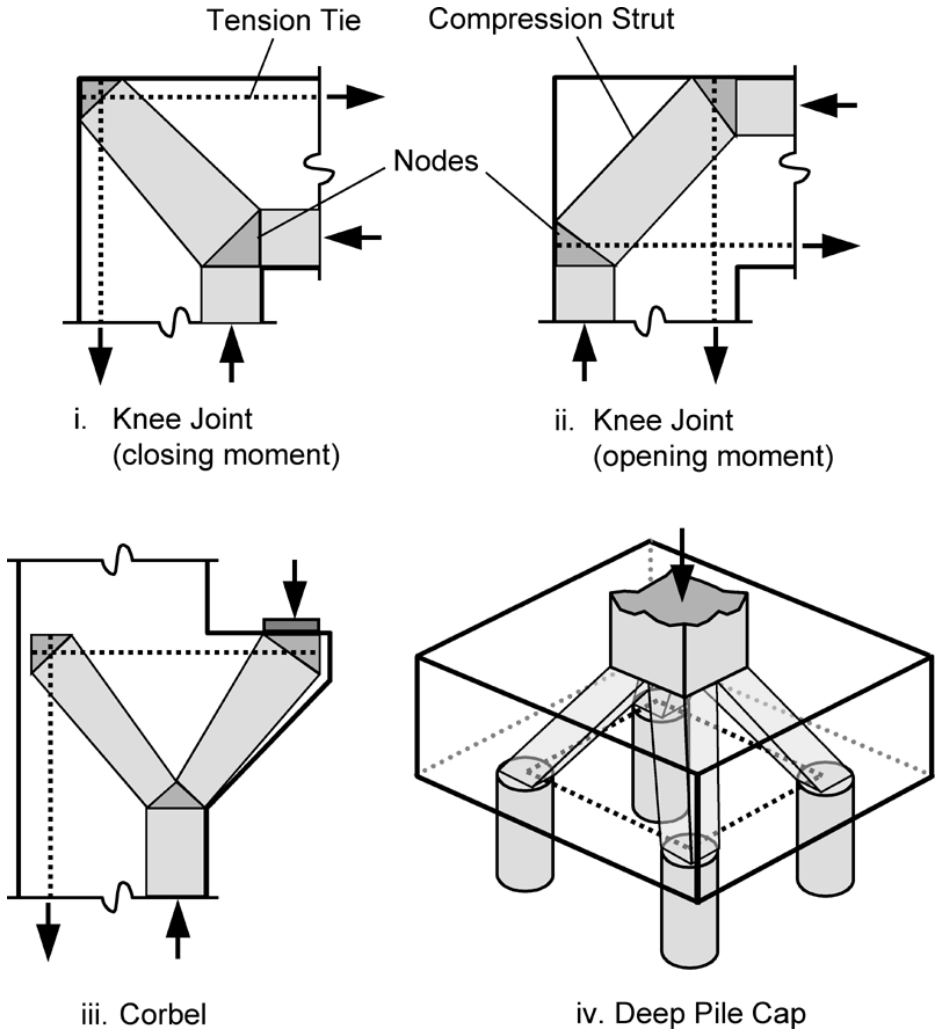

Figure 4-1: Examples of strut-and-tie modeling

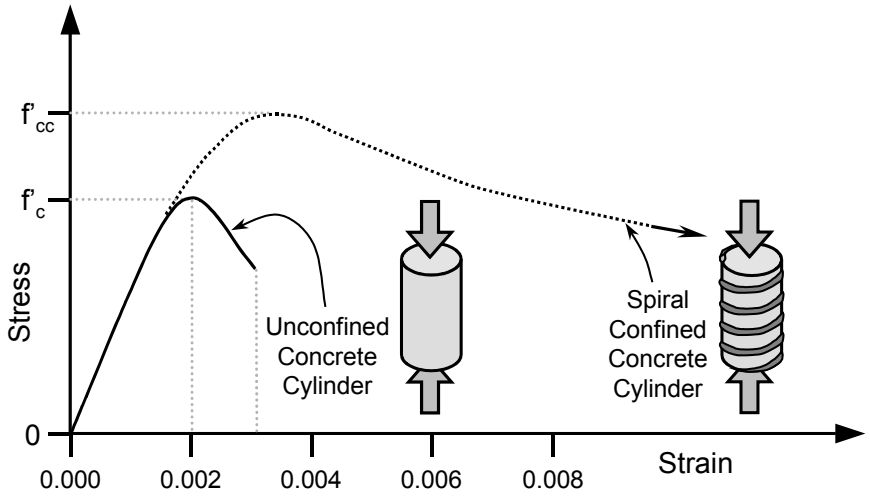

Figure 4-2: Deformation response of plain and confined concrete

In order to apply STM to structural concrete members, it is convenient to delineate disturbed regions from the other parts of the structure that will follow plane section material behavior and which can be analyzed using conventional beam analysis (Figure 4-3). Such regions of the structure are typically termed bending or B-regions. Likewise, the disturbed regions are termed D-regions. The selection of the D-region boundary is based on St. Venant's Theorem and the transition of local stress fields into full section stress fields. Typically, a boundary line is drawn at a distance of 1-1.5 times the depth of the member from the point of applied load or the edge of the abrupt change in section. A static solution is found for the member as a whole to determine all reaction forces, moment diagrams, and the like. Then cracked section analysis (Figure 4-3, ii.) is conducted within the B-regions to determine boundary stresses for the D-regions. Following this step, the D-region can be isolated and treated as a separate entity with all reaction forces and boundary stresses treated as externally applied loads. Consideration must also given to the placement of reinforcement within the B-regions and the continuity of that reinforcement into the D-region. Figure 4-4 shows the separation of a dapped beam into D- and B-regions.

Once the D-region is isolated, a truss mechanism is constructed based on a probable flow path for the internal stresses. As stated before, the truss mechanism consists of struts, ties, and nodes. Figure 4-4 shows some of these components for a dapped beam end. STM allows for several different types of struts and nodes. Figure 4-5 shows some possible strut types. The most likely strut type is the prism strut with a constant cross-sectional shape all along its length. A fan type strut is likely to occur at a deep beam end where the diagonal shear struts converge to a single node. The bottle-shaped strut is likely to occur where large amounts of surrounding concrete allow the compression stresses to bulge outward in the middle of the strut. The spreading within a bottle-shaped strut produces tension stresses that may require transverse reinforcement. A bottle shaped strut may be reduced to an equivalent truss for a better understanding of the flow of forces.

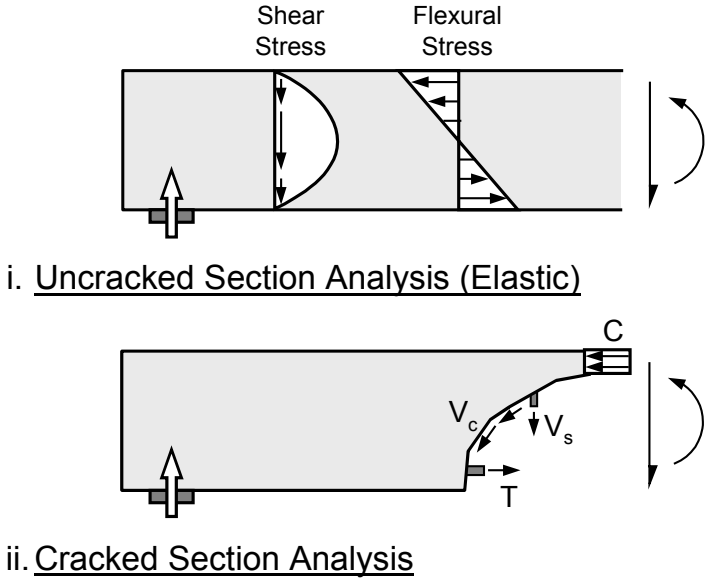

Figure 4-3: Beam analysis methods

Figure 4-6 shows the three basic node types. A Compression-Compression-Compression (CCC) node is the intersection of three compression struts. A Compression-Compression-Tension (CCT) node is the intersection of two struts and a tension tie. A Compression-Tension-Tension (CTT) node represents the intersection of one compression strut with two tension ties. CCT and CTT nodes generally have lower effective strengths than CCC nodes due to the disruption effect created by the splitting associated with bond anchorage of the reinforcing bars. Theoretically Tension-Tension-Tension (TTT) nodes are possible,

but they are not likely in practice. There are, of course, other possible node combinations involving the intersection of four or more struts and ties. In 3-dimensional truss models these are quite possible (see Figure 4-1, iv. Deep Pile Cap).

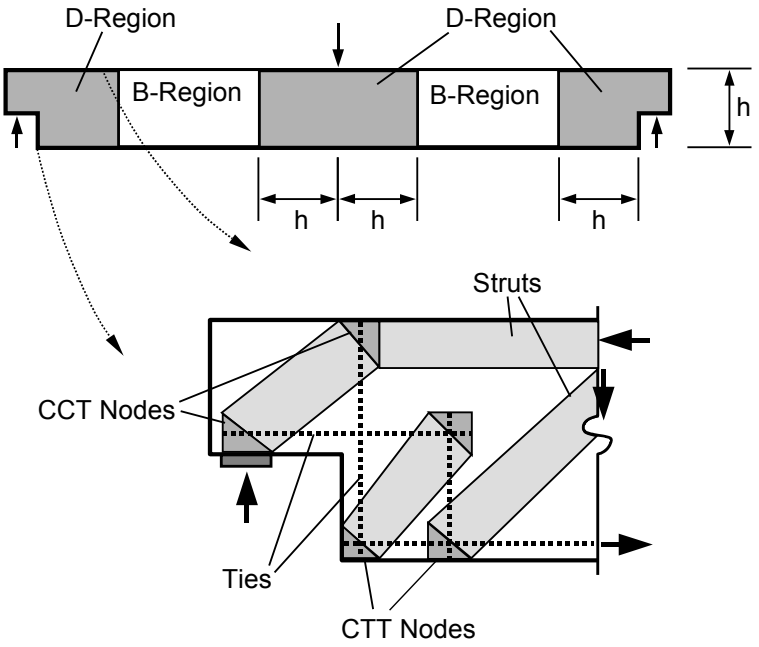

Figure 4-4: Division of dapped beam into B- and D-regions

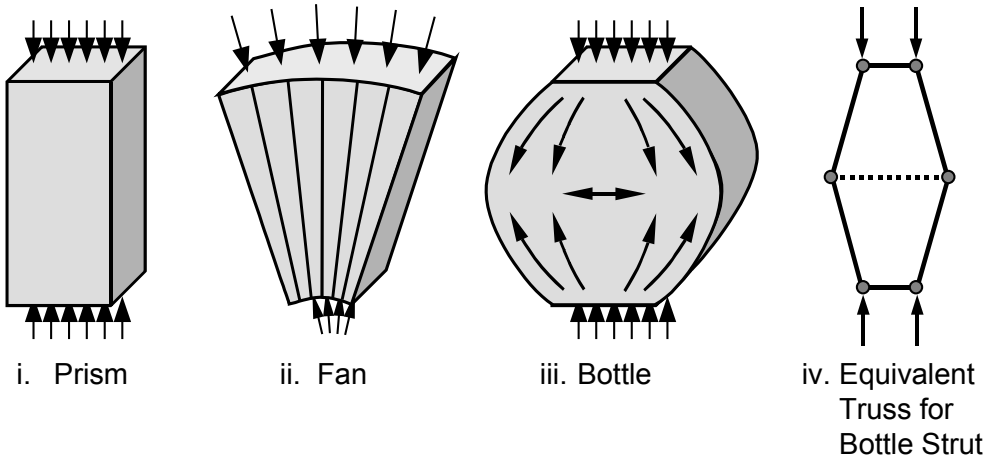

Figure 4-5: Strut types

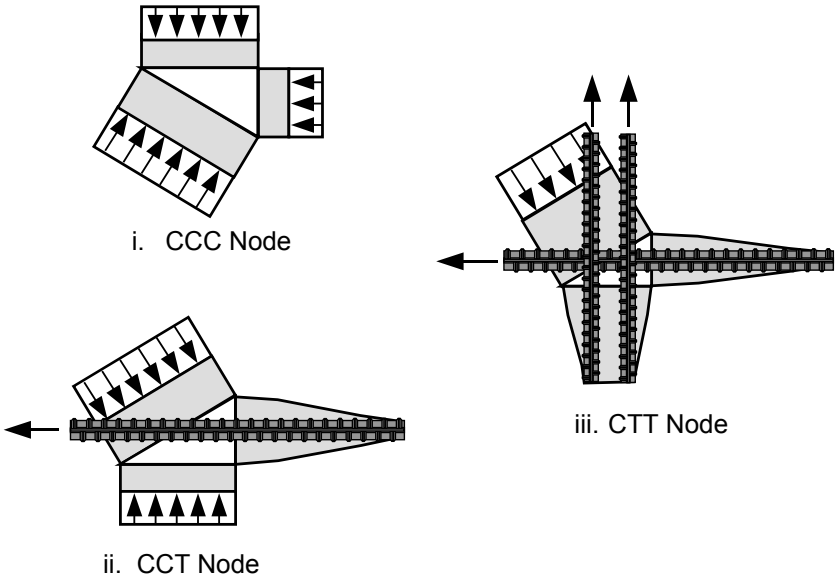

Figure 4-6: Basic node types

4.2 HISTORICAL DEVELOPMENT

The use of truss models to describe behavior of structural concrete members began slightly over 100 years ago when Ritter developed a truss model (Figure 4-7) to analyze the action of shear in reinforced concrete beams [95]. In the following years (from 1900 – 1920's), the shear truss model was refined by Mörsch [80], Withey [111] (who introduced the concept to the United States), and Talbot [101] (who compared truss model analysis to data from experimental beam tests). Experimental testing indicated that the truss models provided very conservative estimates of shear capacity. The truss models simply did not account for shear contributions that came from the tensile capacity of the concrete and other miscellaneous factors. Eventually a more empirical method was developed to calculate shear strength in which the capacity was determined by the summation of a concrete contribution, V_c, and a stirrup contribution, V_s. This practice was first introduced by Richart in 1927 [94], and the truss models for shear soon fell out of fashion. Though truss models were sometimes utilized to explain certain phenomena in simple terms such as the model Mörsch [81] developed for distribution of a concentrated load into a cross-section (Figure 4-8), emphasis on the truss modeling waned in English speaking countries.

The truss model was eventually revisited in the English speaking countries in the late 1960's and early 1970's as a means of calculating the ultimate capacity of beams subjected to combined shear and torsion. Lampert and Thürlimann [61] developed a model for torsion based on the theory of plasticity (Figure 4-9). The torsion model was refined by Lüchinger [65], Mitchell and Collins [78], and Ramirez and Breen [90] so that the space truss could account for all actions of shear, torsion, bending, and axial load in combination.

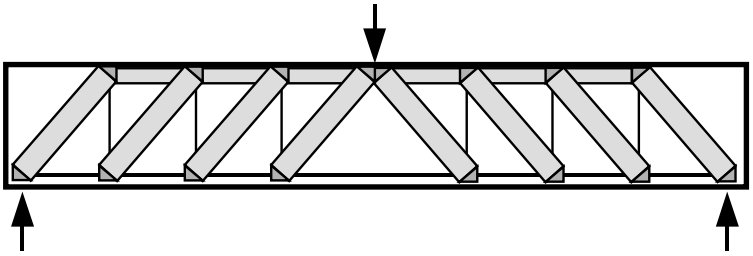

Figure 4-7: The Ritter truss model for shear

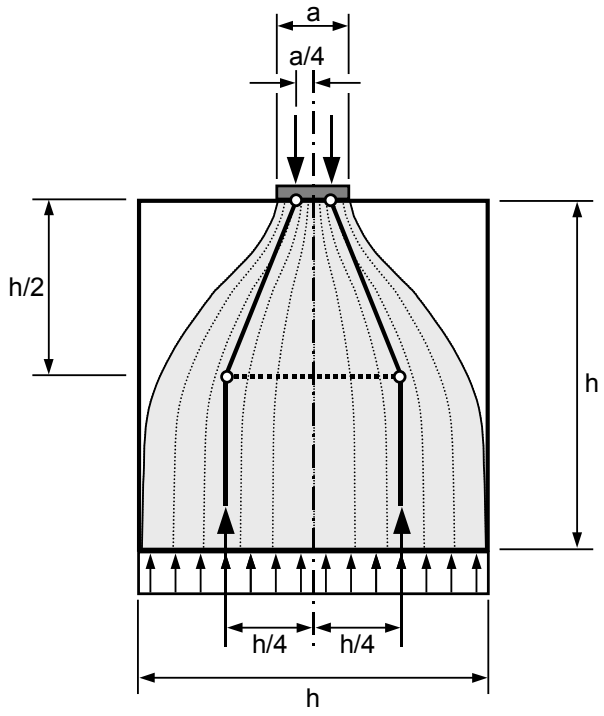

Figure 4-8: Morsch's truss model for concentric, concentrated load

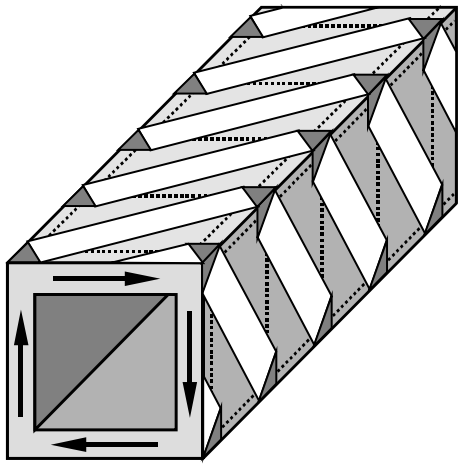

Figure 4-9: Truss model for torsion

Following the resurgence of the truss model in the 1970's for shear, torsion, and bending, a general method of truss modeling began to emerge for all structural situations. The strut-and-tie modeling approach for discontinuity regions was developed and endorsed by Marti [69, 71] and Schlaich [98] in the 1980's. In 1984, the Canadian CSA Standard [6] introduced STM into code draft. STM provisions have been introduced into the AASHTO Bridge Design Specifications [1] and ACI recently included provisions in the ACI 318 Code, 2002 Edition [2].

4.3 STM DESIGN PROVISIONS

4.3.1 Procedure for STM Design

STM is only a small part within the design of a structure, and usually one of the later steps. Figure 4-10 shows the flowchart for structural design and the place of STM within the complete process. STM is a tool that may facilitate detailing disturbed regions. Other methods (empirical or mechanical) may also be available to the designer to guide the detailing of D-Regions. If STM is to be utilized, the primary structural analysis must be performed beforehand. Because compatibility between D- and B-regions must be maintained, STM can only be performed after the primary structural analysis and the determination of the forces at the boundaries of the D-regions and the selection of the primary (B-Region) reinforcing steel that will be continued into and anchored within the D-regions.

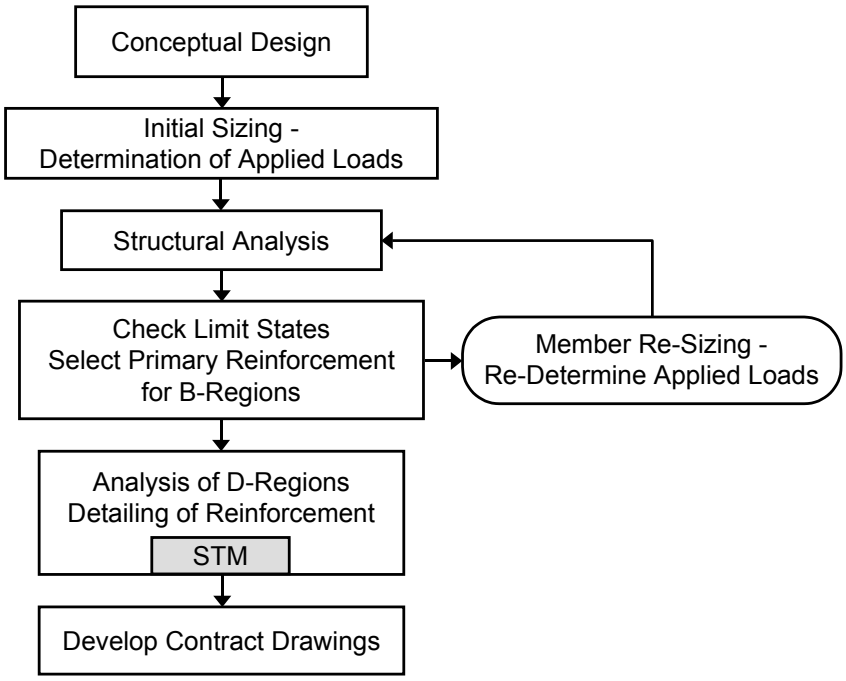

Figure 4-10: Flowchart for structural design

Figure 4-11 outlines the procedure for STM. STM begins with the determination of D-region boundaries and the calculation of boundary forces on the D-region (steps 1 and 2 in the flowchart). Once the geometry of the D-region and the applied loads are known, a truss model can be chosen (step 3). If several load cases exist for the structural member, then different boundary forces may exist for each load case. One truss model may not be sufficient for the different configurations of applied loads and separate truss models may be developed for each load case. Truss models should be determinate if possible. Indeterminate truss models for STM are somewhat questionable since they require elastic properties for the truss members to carry out the analysis of forces. It is difficult to determine reasonable elastic properties for struts and ties because the actual structure will not be a truss, but a complex bulk member with non-uniform stress fields. Since the method is approximate in any case, it makes much more sense to maintain simplicity by keeping the truss determinate and avoiding the additional work required for an indeterminate analysis. An alternative when stress flow paths are complex is to develop multiple truss arrangements and arbitrarily divide the applied loads among the different trusses (This approach has been recommended by Schliach [98] and experimentally confirmed by Maxwell [74] for a wall with an opening). It is important for the designer to keep the approximate nature of STM in mind when performing the process. Exaggerated complexity in the analysis is not likely to enhance the STM design outcome to any significant degree and will only consume time and energy.

Once a basic truss model is chosen, the geometry of the truss must be established. The geometry of the final truss will depend on the depth of nodes, struts, and tie steel. However, these parameters may not be known at the beginning of the STM process and an iterative process must be used. Some geometric parameters may be set because of boundary conditions such as bearing plate dimensions or the centroids of reinforcing steel layers and struts that continue from the B-regions into the D-regions. Such information can be utilized to bring the geometry of the initial truss model close to its final form (step 4). For this reason, it is necessary to have performed an analysis and design of the adjacent B-regions before proceeding with STM. When the geometry of the truss model is determined, then the truss can be analyzed and the forces in the struts, ties, and nodes calculated (step 5).

Following the calculation of the strut and tie forces, the required area of steel for the ties is generally calculated (step 6). Thus bar sizes can be selected and the layout of steel detailed. The layout of the tie steel must be checked to see if it fits within the geometry of the concrete member and must be detailed so that its centroid aligns with the assumed centroid of the tie in the truss model. If the tie steel does not fit, then the designer must redraw the truss model to suit a geometry in which the tie steel will fit and re-calculate the truss forces (step 6a). The designer must then determine if the selected tie steel will still work or if a new bar selection must be made. Once the tie steel has been selected, then the layout of the tie bars can be used to help determine the geometry of the nodes and struts.

The next part of the process (step 7) is the checking of strut and node stresses. The designer must determine some dimensions of depth and width for the nodes and struts, so that the node and struts forces can be converted into stresses and compared to the allowable stress limits imposed by the code provisions. Some designers prefer to work backwards for this step, by using the allowable stress limits to determine what face areas are necessary for the struts and nodes to accommodate the known strut and tie forces. Once the necessary face areas are known, they can be compared against the geometry of the concrete member to see if the truss model would actually fit. If the nodes and struts cannot be made to fit within the concrete dimensions, then the truss model must be redrawn to allow the nodes and struts to fit and the forces in the model must be re-calculated (step 7a). If the forces change significantly, then the struts and nodes must be rechecked and the process repeated as necessary until all of the truss components meet acceptable stress limits and fit within the confines of the overall member dimensions. In complex details, this process can be tedious. One disadvantage of the STM may be the need to iterate solutions until the components of the model meet the restraints of geometry and stress, especially if strut dimensions are critical.

After the locations of the struts, ties, and nodes have been finalized and meet the acceptable stress limits, the last detail to be attended to is anchorage of the primary reinforcement. Development of reinforcement follows the conventional provisions for straight and hooked bars that were discussed in Chapter 2. The critical section where development must occur is generally where the bar intersects the strut(s) that it anchors. Anchorage in strut-and-tie models is a major issue in applying the STM method. Frequently, nodes are not large enough to accommodate the full development length necessary for a straight or hooked bar. In many cases it is necessary to extend the development of the bar past the back face of the node. This may require the extension of the concrete dimensions of the structural member that is being designed. Mechanical anchorage has become an inviting alternative for many anchorage problems in STM because of this.

The design process of the D-regions should flow smoothly from the design of the B-regions and should never require the designer to proceed backward in the process outlined in Figure 4-10. It is possible that some iteration is needed before a final detailing solution for the D-region is achieved, however, struts are less likely to control and tie force and location can be quickly discerned.

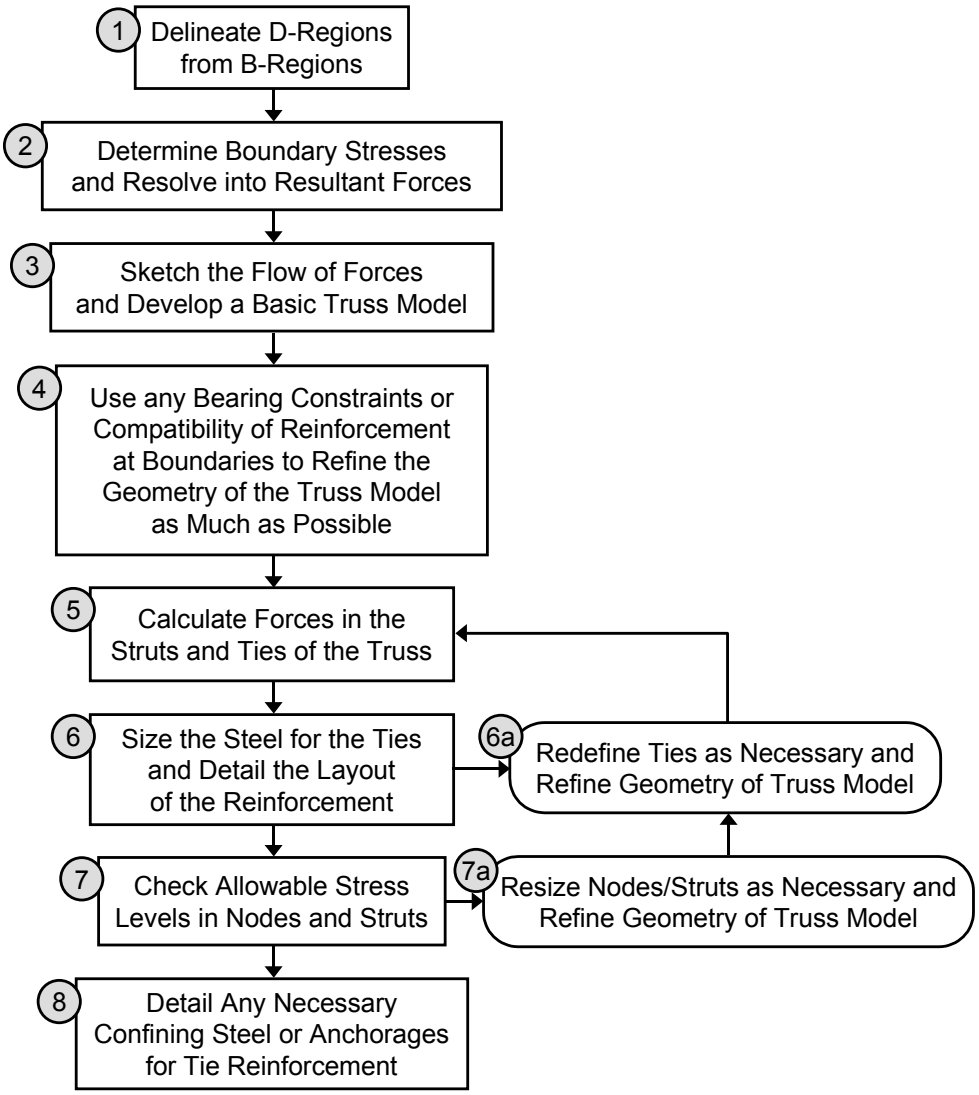

Figure 4-11: Flowchart for the STM process

4.3.2 Dimensioning of Nodes, Struts, and Ties

Dimensioning of nodes, struts, and ties is based on compatibility with boundary conditions when possible. Code guidelines sometimes provide guidance as well. Dimensioning of struts is typically based on the dimensions of the nodes at either end of the strut. Dimensioning of a node is in turn typically based on the detailing of steel tie bars that anchor at the node, bearing plate dimensions that define one or two edges of the node, or compatibility with struts that propagate from the B-regions into the D-regions. Dimensioning of ties is based on compatibility with reinforcing bars that continue from the B-regions into the D-region, detailing requirements such as minimum clear spacing or development length provisions, or recommendations contained with the code literature.

Several factors may govern the selection of tie bars. Limited space available for development length may prompt a designer to choose a large number of smaller bars to provide a tie because smaller bars require less length to develop. Furthermore, most code provisions recommend a wide spacing of tie reinforcement in order to better distribute anchorage stresses at nodes. On the other hand, it is frequently preferable to closely space tie reinforcement and consolidate the tie steel area into larger bars so that the tie force can

be positioned close to the concrete surface. This improves crack control and makes more efficient use of tie steel by increasing the lever arm over which it acts (Figure 4-12). Many times, the layout of tie steel is governed by the continuation of reinforcement from the B-region. However, when continuity is not a concern, the engineer must weigh the conflicting considerations listed above when detailing the layout of tie bars.

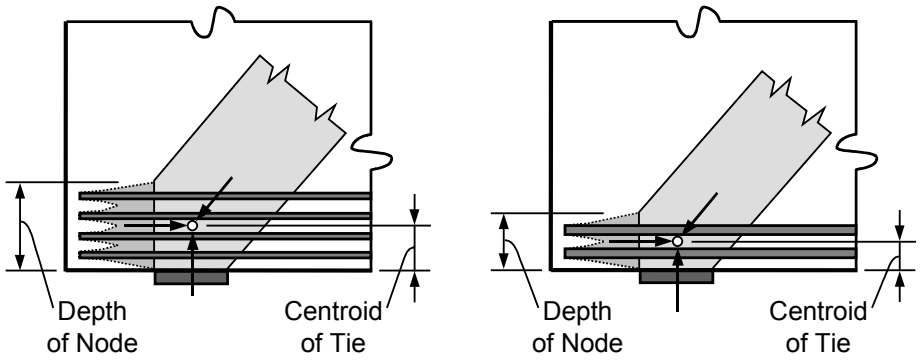

i. Widely Spaced Tie Reinforcement

ii. Closely Spaced Tie Reinforcement

Figure 4-12: Distribution of tie reinforcement

Nodes are generally dimensioned after ties. Most codes specify limits to which nodal boundaries can be assumed to extend beyond the dimensions of the tie reinforcement for CCT and CTT node situations. FIB recommendations [13] allows for the node to extend to the limit of the clear cover or ½ the clear spacing between layers of bars (Figure 4-13). FIB does require that reinforcement be extended at least a distance equal to the clear cover or ½ the clear spacing beyond the face of the node before these limits can be assumed for the node dimensions. The AASHTO Code [1], the Ontario Bridge Code [11], and the CSA Canadian Concrete Building Code [6] all allow the node boundary to be drawn up to six bar diameters ($6d_b$) from the surface of the tie reinforcement (Figure 4-14). Most literature refers to the use of STM within two-dimensional members wherein the model is assumed to act across the full member width. However, if the detailing provides for a very large side cover or if the truss model acts within a three-dimensional body, then the above limits can also be applied to define the transverse limits of the node. The ACI code [2] recommends dimensioning of nodes based on hydrostatic principles.

In addition to the recommended limits, all of the above mentioned codes recommend proportioning of nodes based on "hydrostatic" stress distributions when the face geometry is not governed by the dimensions of tie reinforcement or bearing pads. The term "hydrostatic" implies equal normal stresses along all three axes of the material stress block. In the convention of STM terminology, however, a node is termed "hydrostatic" when the stresses balance along only the two axes defining the plane of the truss. The state of stress along the transverse axis is generally ignored or treated with a separate truss model. When a node is hydrostatic, the dimensions of the faces are in proportion to the forces acting on those faces and the normal stresses are equal on all faces (Figure 4-15). Because the stresses are equal on all three faces, there is presumably no shear stress within the region defined by the node. It is not necessary that a node be hydrostatic. Concrete can bear shear stress to a certain extent and nodes need not be proportioned according to hydrostatic principles. Schlaich [98] recommended that the ratio of the maximum to minimum stress (σ_1/σ_2) in a non-hydrostatic node not exceed a value of two.

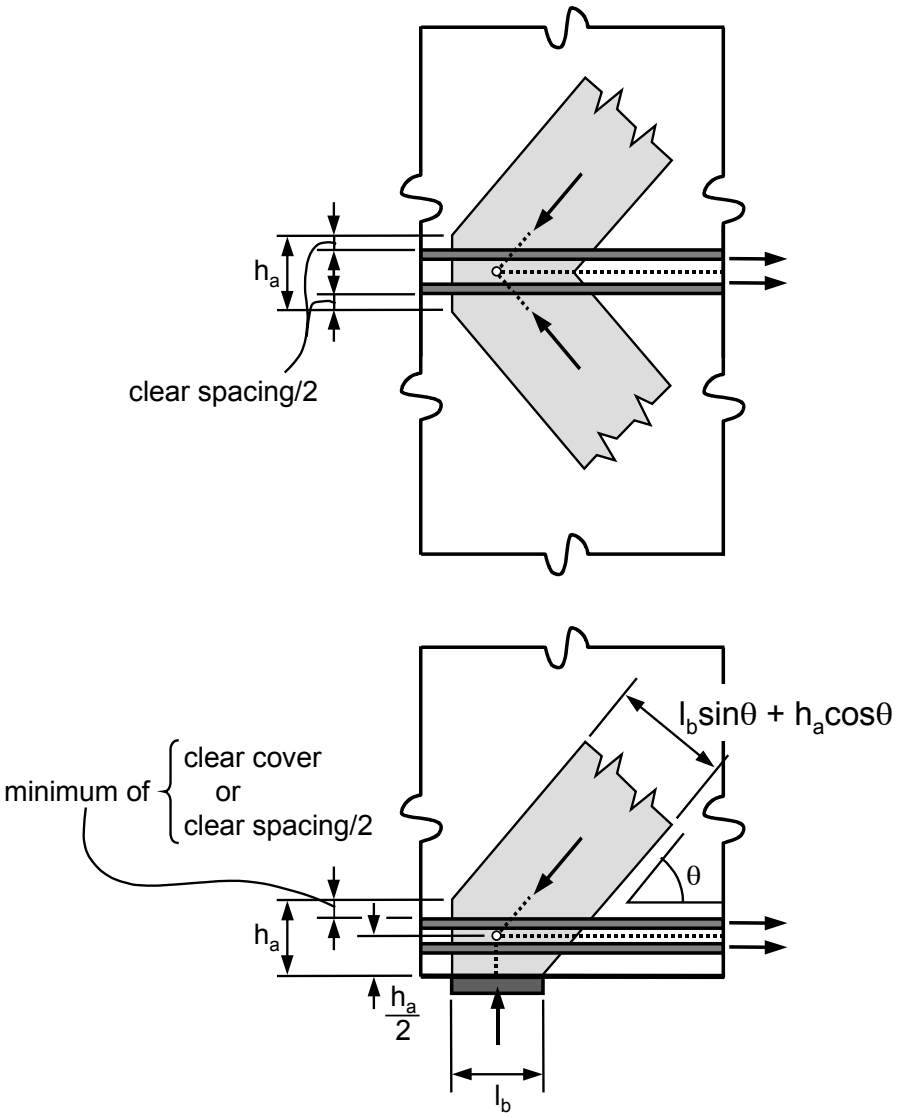

Figure 4-13: FIB recommendations for dimensioning of nodes

Generally nodes are defined by the intersection of three struts and/or ties. However, in some complex truss models, four or more struts or ties may intersect at a single node (termed a "macro-node" for lack of a better term). In such cases, nodes may be subdivided into more basic struts and nodes for easier analysis. Schlaich [98] first provided such an example in which five struts intersected at a single node. Schlaich demonstrated that it was possible to combine some of the struts before they intersected the node, thus cleaning up the node region and simplifying the problem (Figure 4-16, part i.). Sometimes it is preferable to partition a node so that stress at an interior section can be checked (Figure 4-16, part ii.). The geometry of nodes can be subdivided and treated in such manners as long as equilibrium is satisfied and the material stress limits are not violated.

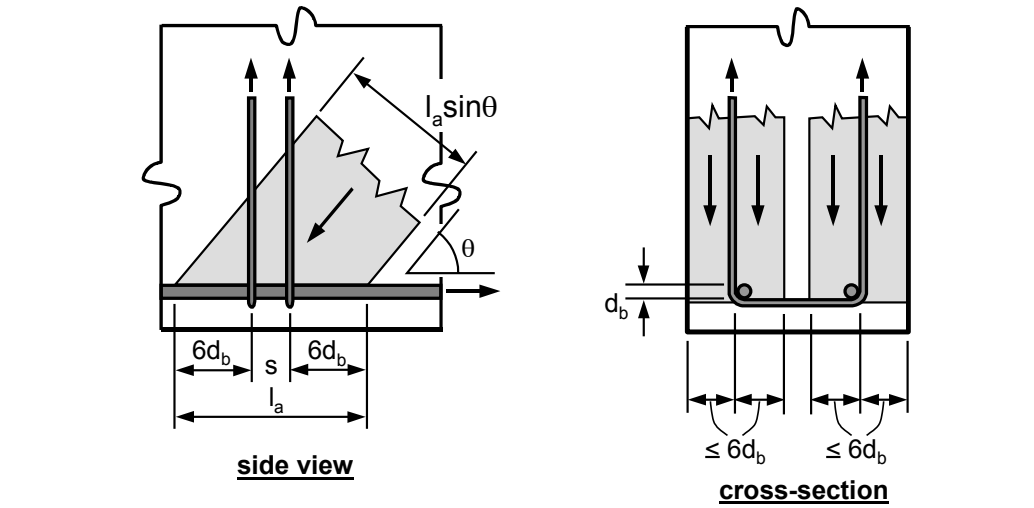

i. Strut anchored by reinforcement (CTT node)

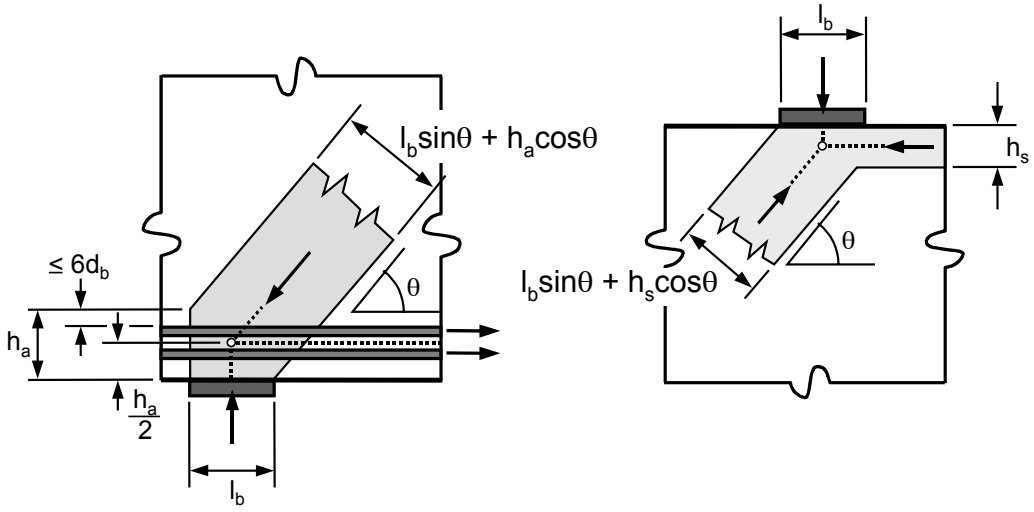

ii. Strut anchored by bearing and reinforcement (CCT node)

iii. Strut anchored by bearing and strut (CCC node)

Figure 4-14: AASHTO recommendations for dimensioning of nodes (after Figure 5.6.3.3.2-1 [1])

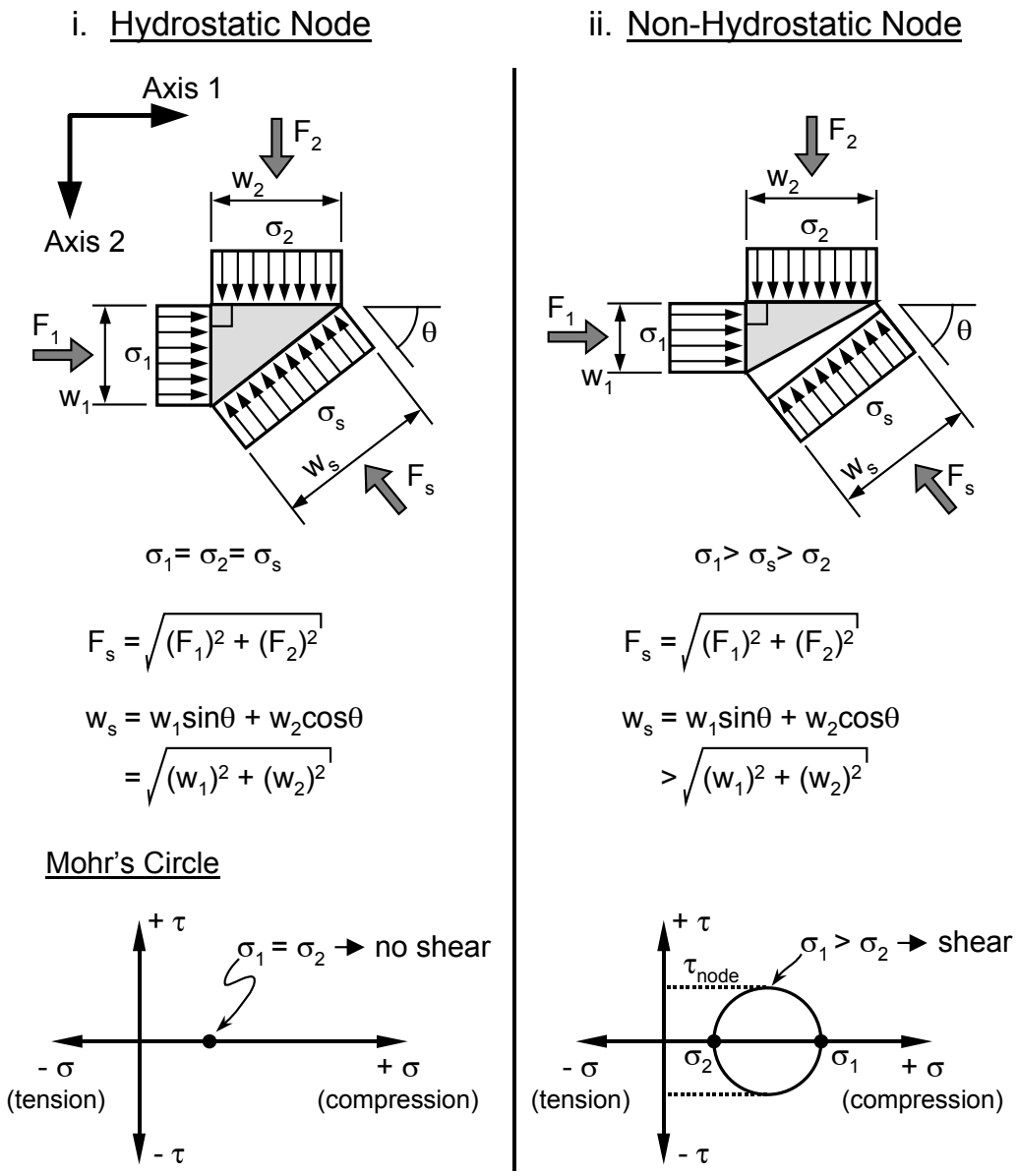

Figure 4-15: Hydrostatic and non-hydrostatic nodes

Once the geometry of the nodes has been set, the struts are drawn. Struts are defined by the face geometry of the nodes that they intersect. Thus, all of the geometric considerations of struts are solved when the nodes are defined. When struts taper from a large node face to a smaller node face, they are generally analyzed at their smaller end where the stress will be greater.

The last consideration in dimensioning is the development length of the tie reinforcement. Most codes allow for the development length of the reinforcement to be measured from the point where the tie steel intersects the struts that they anchor (Figure 4-17). This point is a good approximation of the location of the critical crack in many CCT node situations. When multiple layers of bars are used in the tie, the point where the centroid of the steel intersects the strut is used as the beginning of the development length.

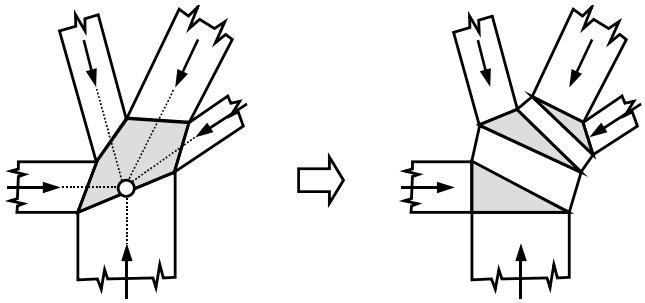

i. Subdivision of Macro-Node into Smaller Units (after Schlaich [98])

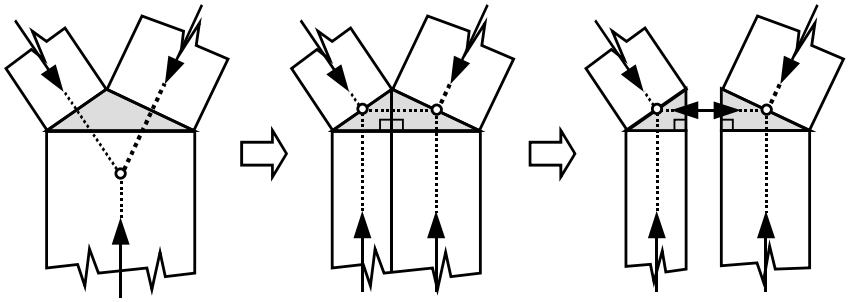

ii. Subdivision of Node at an Interior Section

Figure 4-16: Subdivision and simplification of nodes

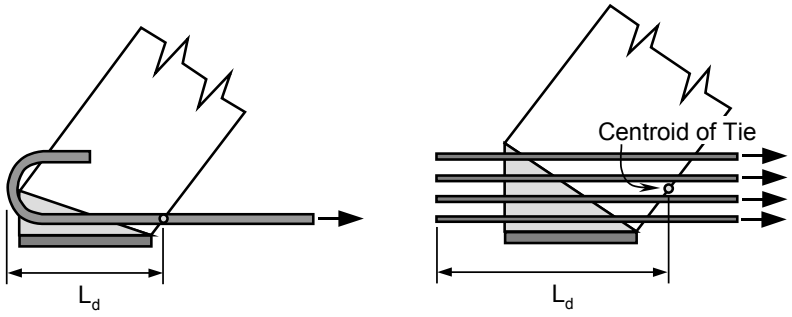

i. Development of a Single Layer of Bars

ii. Development of Multiple Layers of Bars

Figure 4-17: Development of tie reinforcement in nodes

4.3.3 Limitations on Strut-Tie Angle

Various sources (Lampert and Thürlimann [61], Ramirez and Breen [90], and Mitchell and Collins [78]) have proposed limitations on the angle that can be subscribed between a compression strut and a tie that anchors within that strut. Limits on strut angle have been proposed between 15^o to 65^o from various studies. These limits derive from studies of one-way members (beams) in shear and are specifically intended for the application of truss models and compression field theory for shear and torsion. Rational strut angle limits for truss models in less regular conditions have not been studied. Strut angle limits exist as an indirect method of controlling strain in the tie. At low angles, the cracks that develop as the truss mechanism forms become too wide to be acceptable. The AASHTO code [1] bases the capacity of struts

on strut-tie angle (see discussion in Section 4.3.5) and allows less capacity when the angle is low. The ACI code [2] places a lower limit of 25^o on the strut-tie angle in Section A.2.5.

4.3.4 Strength of Nodes

Once the dimensions of the nodes are determined, then the stresses at the faces of the nodes can be checked. The stress limits for nodes are generally some fraction, ν_e, of the concrete compressive strength, f_c', times a reduction factor, ϕ, for safety. The factor ν_e is frequently referred to as an efficiency factor. The efficiency factors for CCC, CCT, and CTT nodes are usually different. CCT and CTT nodes are generally assigned smaller efficiency factors than CCC nodes because the tensile stresses produced by bond of the tie reinforcement are presumed to have a weakening effect on the strength of those nodes. Table 4-1 lists the efficiency (ν_e) and strength reduction (ϕ) factors from various design codes. Note that while many of the codes have different safety reduction factors, they also use different load factors in the design process. Thus the ϕ factors are not always comparable. The Canadian CAN3-A23.3-M94 [6], Ontario Bridge Code [11], and AASHTO LRFD Bridge Design Specifications [1] were all authored by the same person and hence use the same efficiency factors. Notes on the FIB [13] allowable stresses are provided with the table. The units of stress are ksi for all formulations listed in Table 4-1.

Table 4-1: Allowable stresses for nodes

Node Type	Design Code	Limiting Concrete Stress	Strength Reduction Factor, ϕ_c
CCC	ACI 318-02	$1.00\phi f_c'$	0.75
	CAN3-A23.3-M94	$0.85\phi f_c'$	0.60
	Ontario Bridge Code	$0.85\phi f_c'$	0.75
	AASHTO LRFD	$0.85\phi f_c'$	0.70
	FIB*	$0.85(1-f_c/36)\phi f_c'$	0.57
CCT	ACI 318-02	$0.80\phi f_c'$	0.75
	CAN3-A23.3-M94	$0.75\phi f_c'$	0.60
	Ontario Bridge Code	$0.75\phi f_c'$	0.75
	AASHTO LRFD	$0.75\phi f_c'$	0.70
	FIB*	$0.70(1-f_c/36)\phi f_c'$	0.57
CTT	ACI 318-02	$0.60\phi f_c'$	0.75
	CAN3-A23.3-M94	$0.60\phi f_c'$	0.60
	Ontario Bridge Code	$0.60\phi f_c'$	0.75
	AASHTO LRFD	$0.60\phi f_c'$	0.70
	FIB*	$0.60(1-f_c/36)\phi f_c'$	0.57

* The FIB Recommendations use α/γ_c rather than ϕ. At ultimate loads, α, a reduction factor, is equal to 0.85 and γ_c,a partial safety factor, is equal to 1.5. The term $(1-f_c/36)$ is a reduction factor for higher characteristic concrete strengths, f_c, to recognize the more brittle nature of high strength concrete failure.

Most of the codes listed in Table 4-1 require node stress checks only at the faces that abut struts or bearing plates. The faces at which tensile reinforcement is anchored are considered acceptable if the anchorage requirements of the tensile reinforcement are met (ie. if the development length is acceptable). However, the ACI provisions require that allowable stresses not be exceeded on "any face of the nodal

zone or on any section through the nodal zone" (section RA.5.2) [2]. This is a rather stringent and possibly unnecessary requirement.

4.3.5 Strength of Struts

Struts are checked at both node faces that define their ends. The allowable stress in the strut can depend on several factors: the orientation of confining reinforcement across the strut (if any), the extent of cracking along the strut at the ultimate limit state, tensile or compression stresses perpendicular to the axis of the strut, and the slenderness of the beam web if shear compression struts are being modeled. The Canadian Code [6], the Ontario Bridge Code [11], and the AASHTO LRFD Bridge Design Specifications [1] all use a stress limit recommended by Collins [78] that accounts for the orientation of the strut with respect to ties (strut angle) and the principle tensile strain perpendicular to the axis of the strut. The FIB uses a simple stress limit similar to those used for nodes. The ACI code recommends various efficiency factors based on the condition of the concrete through which the strut passes.

The formulation used in the Canadian Code, the Ontario Bridge Code, and the AASHTO Bridge Code is given below:

$$f_{cu} = \frac{f_c'}{0.8 + 170\varepsilon_1} \le 0.85 f_c' \tag{4-1}$$

$$\varepsilon_1 = \varepsilon_s + (\varepsilon_s + 0.002)\cot^2 \theta_s \tag{4-2}$$

f_{cu} = ultimate stress of the strut (ksi)

f_c' = concrete compression strength (ksi)

ε_1 = principal tension strain perpendicular to the axis of the strut (in/in)

ε_s = tension strain in tie steel crossing the axis of the strut (in/in)

θ_s = angle between the axis of the strut and the axis of the tie that it anchors

It is permissible to assume a design value of 0.002 for ε_s in order to simplify the calculation. The strength of the strut is then determined solely by its inclination to the axis of the tie that it anchors. In Figure 4-18 the ultimate strut stress is plotted as a function of the inclination assuming ε_s equal to 0.002. Additionally, safety factors, ϕ, equivalent to the ones shown in Table 4-1 are used.

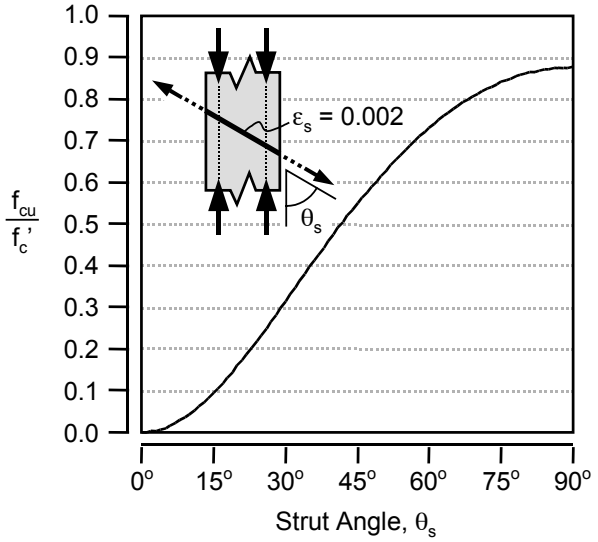

Figure 4-18: Change in strut efficiency factor versus strut angle (AASHTO specifications)

Equation 4-1 was developed based on deep beam and shell element tests. The original definitions of θ_s and ε_s were developed for ties composed of stirrups crossing the paths of shear struts within deep beams at well distributed intervals, not bars that anchor the ends of the struts. The adaptation of equation 4-1 to the general STM case has not been verified by tests, nor has it been demonstrated that the equation is even suitable for such situations as stout, compact elements like corbels or three-dimensional strut-and-tie models such as in pile caps and post-tensioned deviation saddles to name but a few examples.

The ACI specifications use a more basic design assumption. Strut-tie angle is limited to 25^o, which corresponds approximately to a shear span to depth ratio of 2, the limit that defines a deep beam from a slender beam. Strut ultimate stress is determined by:

$$f_{cu} = 0.85\beta_S f_c' \tag{4-3}$$

where β_2 is chosen from the following conditions:

- struts passing through uncracked concrete in a uniaxial fashion (such as in the compression zone of a beam): $\beta_S = 1.00$
- struts passing through concrete in tension: $\beta_S = 0.40$
- bottle shaped struts with appropriate reinforcement: $\beta_S = 0.75$
- bottle shaped struts with no reinforcement: $\beta_S = 0.60$
- all other cases: $\beta_S = 0.60$

Appropriate reinforcement for bottle shaped struts must satisfy the following:

$$\sum \frac{A_{si}}{bs_i} \sin\gamma_i \geq 0.003 \tag{4-4}$$

A_{si} = area of steel in spacing, s_i, that crosses the path of the strut (in^2)

s_i = spacing of reinforcement crossing the path of the strut (in)

b = the width of the strut perpendicular to the axis of the crossing reinforcement (in)

γ_i = the angle between the axis of the strut and the axis of the crossing reinforcement; γ must be greater than 40^o if only one layer of reinforcement crosses the strut

Subscript i refers to the i^{th} layer of reinforcement. Typically there would be two layers of reinforcement: horizontal and vertical. Additionally, the concrete stress is reduced by a strength reduction factor, ϕ, of 0.75.

The FIB uses only one formulation:

$$f_{cu} = 0.6\left[1 - \frac{f_c}{36}\right] f_c' \tag{4-5}$$

f_{cu} = ultimate concrete stress (ksi)

f_c = characteristic concrete stress (a statistical formulation of the concrete strength based on cylinder tests; it is reasonable to substitute $f_c' - 1.1$ ksi) (ksi)

f_c' = concrete compression strength (ksi)

Equation 4-5 provides the same stress limit for struts that is used for CTT nodes and conservatively assumes that the concrete in the struts will probably be cracked at the ultimate limit state. The same reduction factors applied to nodes are applied to struts.

4.4 EXPERIMENTAL STUDIES

Numerous experimental studies have been performed to refine truss models for shear in deep beams and prestressed beams (Ramirez and Breen [90], Rogowsky and MacGregor [92, 93], Vecchio and Collins [107, 108], and Alshegeir and Ramirez [19]). These studies have focused primarily on the shear strength provided by struts in plane stress situations. The results of these studies have formed the basis for the compression field theory and various truss models for shear in one-dimensional members (These theories are subsets of STM that have been specialized for the modeling of shear in beams and shell structures). Few experimental studies have examined the application of STM in complex discontinuity regions using the most general application of the method. Fewer still have attempted to perform tests of isolated struts or nodal zones. Summarized herein is a brief overview of the literature of such tests that has been found.

4.4.1 Cook and Mitchell (Disturbed Regions)

Cook and Mitchell studied the use of STM to predict failure loads for four scaled-down specimens at McGill University [35]. They studied a double-sided corbel, a rectangular dapped beam, an inclined dapped beam, and a beam with a rectangular opening in its web. They also compared the experimental results with non-linear finite element analysis. The purpose of the research was to verify the validity of the strut-and-tie method which Cook and Mitchell found acceptable for design purposes but not as accurate for predicting ultimate strength and failure modes as the non-linear finite element analysis. They recommended that the effective bearing area of struts and nodes should ignore cover concrete because this concrete tends to spall away at the ultimate limit state. STM under-predicted the ultimate capacity of all four experimental specimens as expected for a lower bound method.

4.4.2 Beaupre (Deviation Saddles)

Beaurpre applied STM to the analysis of 10 tests of $^1/_3$ and $^1/_5$ scale deviation saddles for external post-tensioned tendons [23]. A deviation saddle for an external bridge tendon redirects the path of a tendon through a sharp angle break. Due to the abrupt change in tendon angle, a large vertical shear force must be transmitted through the deviation saddle into the bridge cross-section. Figure 4-19 shows the cross-section of a typical saddle tested by Beaupre. Beaupre tested 10 such saddles as part of a large-scale research program sponsored by TxDOT to study the design and behavior of post-tensioned box-girder bridges with external tendons. STM was examined as a potential method for deviation saddle design.

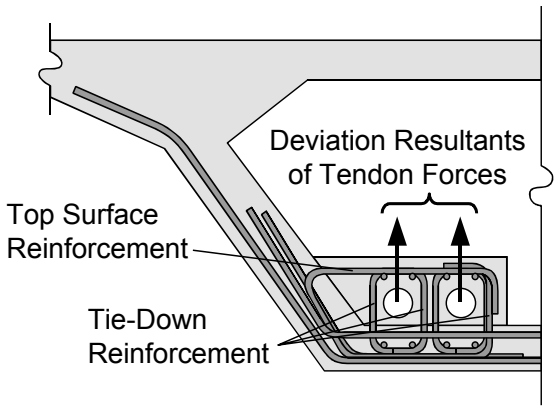

Figure 4-19: Typical deviation saddle tested by Beaurpe

STM for the deviation saddle was conducted in two parts: an analysis of the contribution of the tie-down reinforcement and an analysis of the contribution of the top surface reinforcement. Beaupre's test results averaged 98% of his STM predictions with a standard deviation of 10%. Some test results were only 85%

of his predicted STM values. STM should provide a lower bound solution and a calculated strength not less than the actual capacity of the specimen. Some of Beaupre's over-predictions may have been due to an over-estimation of the contribution from the top surface reinforcement to hold down the tendons. The pullout force of the tendons acts almost perpendicularly to the axis of the top surface reinforcement. In order for the top surface reinforcement to act effectively against the pullout force of the tendons, it must deform substantially out of its plane until it can act at an angle to the applied load. This does not occur until the tie-down reinforcement has yielded substantially. It is very difficult for the two types of reinforcement to act in conjunction with one another and certainly difficult for the top surface reinforcement to contribute significantly to the capacity of the model without substantial distress to the deviation saddle. Omission of the contribution of the top surface reinforcement made Beaupre's STM predictions conservative for six of the ten specimens. The remaining four specimens had potentially significant horizontal deviation forces that were neglected during STM analysis and almost certainly affected the ability of his simple STM model to predict test capacities.

The behavior of the deviation saddles was dominated by tie action of the reinforcing steel. Compressive strength of the struts and nodes and anchorage of the ties was not critical for the capacity of the specimens. Failure of the specimens occurred by violent rupture of the top concrete and fracture of the tie-down steel.

4.4.3 Barton, Anderson, and Bouadi (Dapped Beams and Nodes)

Dapped beams and nodes were studied at the University of Texas as a means of experimentally evaluating the use of STM and providing data for the design of the various components of strut-tie models particularly nodes [21].

The first phase of the research (conducted by Barton) consisted of tests of 4 dapped-end details. Two of the specimens were designed using STM, one using a method suggested by PCI [12], and a third using a method previously used by TxDOT that was suggested by Menon and Furlong [70]. All specimens had the same dimensions and were designed for the same external load. Barton found that all specimens performed adequately. In both cases in which STM was used for design, the capacity of the beam was 27-42% higher than predicted. The Menon and Furlong approach gave the best estimate of strength while requiring the least horizontal and vertical steel reinforcement in the main tension ties (However, a difficult strap reinforcement detail was required.). Failure of specimen ST1 designed with STM occurred through yielding of the primary reinforcement, then crushing of the compression zone within the beam at large deflections. Failure of specimen ST2 designed with STM occurred at a lower load than ST1 by non-ductile crushing of the compression zone within the beam. In both ST specimens, the STM method was applied successfully. Yielding of the primary tension reinforcement was achieved before crushing of the concrete within struts or nodal zones occurred.

Following the tests of the dapped beam ends, isolated node tests were conducted by Anderson and Bouardi as the second phase of the project.

Anderson tested nine isolated CTT nodes modeled after the anchorage point of the primary vertical tensile tie and the longitudinal beam reinforcement within the dapped beam ends from ST1 and ST2 (see Figure 4-20). Anderson tested such parameters as concrete strength (high: 5800 psi or low: 3700 psi), longitudinal bar anchorage (hooked or straight), confining reinforcement, strut width (a full bearing plate, 8", or half width, 4"), and strut angle (45^o versus 30^o). He found that cracking patterns of the isolated nodes were similar to cracking patterns observed in CCT nodes of the dapped beams. Of the nine specimens tested, three achieved the maximum capacity of the test set-up. All three of those specimens were made with high strength concrete and used the same reinforcement details as the ST1 dapped beam design. The following observations were noted for the remaining specimens:

- When the vertical reinforcement detail was altered from looped U-bars to 90^{o} hooks placed parallel to the longitudinal bars, the node failed by spalling of side cover and anchorage failure of the vertical reinforcement.
- When the strut bearing plate was reduced to half its width, the high concrete strength node still achieved the maximum capacity of the test set-up. However, the low concrete strength node failed by crushing under the load plate at a bearing stress of 3800 psi (approximately the compressive strength of the concrete).
- Replacement with straight bar development of the hooked anchorage of the top layer of longitudinal reinforcement resulted in a bar slip failure.
- Alteration of the strut angle from 45^{o} to 30^{0} resulted in higher forces in the longitudinal steel and failure of the straight bar anchorage for the lower layer of bars.
- Cracking within the nodes extended from the bearing plate to the far corner of the node resulting in a severely reduced development length for the lower layer of the longitudinal reinforcement.
- Cracking patterns also indicated that hooked bar anchorages tended to allow deeper struts at the face of the node than when straight bar anchorage was used.

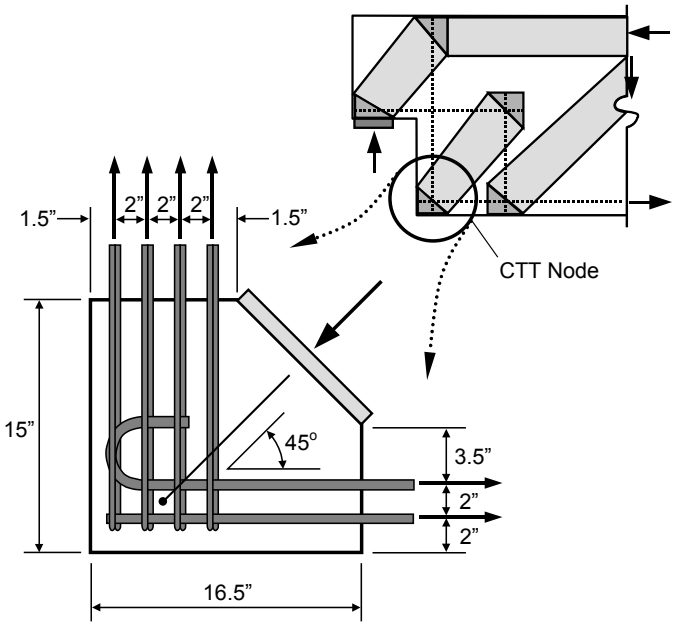

Figure 4-20: Isolated CTT node tested by Anderson

Bouardi tested ten isolated CCT nodes modeled after the intersection of the bearing plate force and the primary horizontal tensile reinforcement (see Figure 4-21). Bouardi tested parameters such as concrete strength (high: 5000 psi or low: 2500 psi), the width of the bottom bearing plate (full, 12”, or half width, 6”), confining reinforcement (none or # 3 hoops at 4”), anchorage of the tie reinforcement (hooked or straight), and bottom concrete cover (small: 1.25” or large: 3.75”). Four out of the ten specimens failed by compression failure. The tie bars began to yield in one specimen, but then an anchorage failure occurred. The remaining five specimens all failed by anchorage failures characterized by spalling of the side cover. Bouardi noted that it was very difficult to perform the isolated CCT node tests. The tests suffered from uneven bearing of the top load plate, horizontal friction at the bottom bearing, and uneven distribution of strain and bending among the tie bars. Despite these problems, Bouardi noted the following:

- Only the low concrete strength specimens failed in compression.

- One low strength concrete specimen failed in anchorage because no confining reinforcement was provided for the tie bars.
- Increased bottom cover increased the capacity of the specimens by 20%.
- Replacing the straight bar anchorage of the bottom layer of tie bars with hooked bars decreased the capacity by a slight amount, 4%.
- Calculation of effective bearing stresses for the four specimens that failed in compression indicated that the efficiency factor of the concrete in bearing was approximately 1.0.

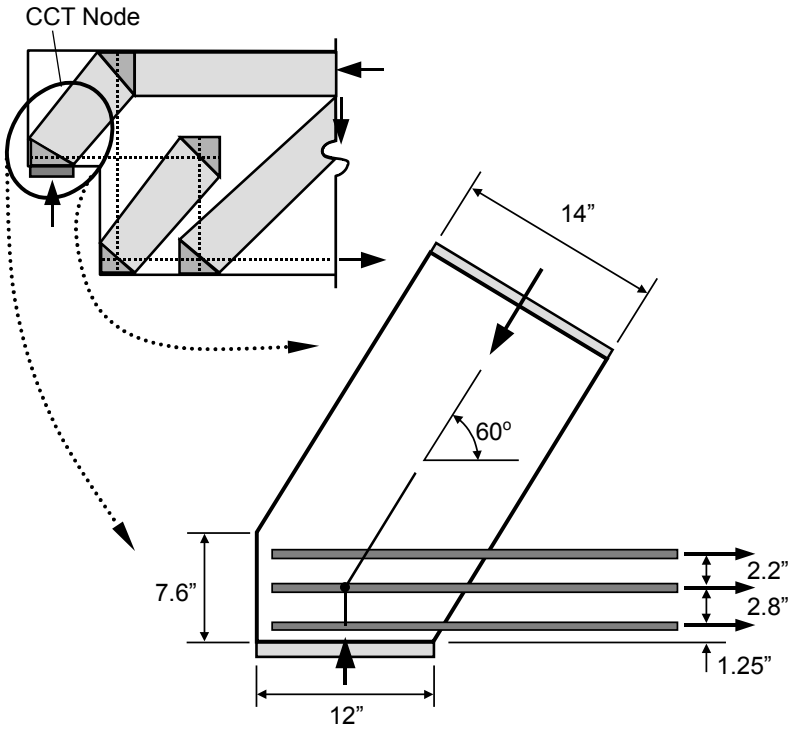

Figure 4-21: Isolated CCT node tested by Bouardi

4.4.4 Roberts, Sanders, Burdet, and Wollmann (Anchorage Zones)

As part of an extensive study sponsored by the National Cooperative Highway Research Program (NCHRP) [28], Roberts performed experimental tests on local anchorage zones and Sanders and Wollmann performed half-scale tests on a number of typical post-tensioned general zone configurations. The local zone essentially constitutes the enlarged CCC node in front of a post-tensioned anchorage plate. The general zone constitutes the remainder of the D-region surrounding the anchorage as shown in Figure 4-22. Note that the distinction between the general and local zone for post-tensioned anchorages has more to do with construction practice and design liability than with structural behavior. The general and local zones represent partitions of design responsibility of the total disturbed region. Roberts studied local zones in order to develop design guidelines for anchor plates and confining steel of the local zone node. Sanders and Wollmann performed experimental tests on general zones for the purpose of verifying the acceptability and accuracy of STM as a method of designing the secondary tie steel required for spreading of the local zone stress into a full cross-section. Burdet performed numerous linear elastic finite element analyses that contributed to the design of test specimens and interpretation of results.

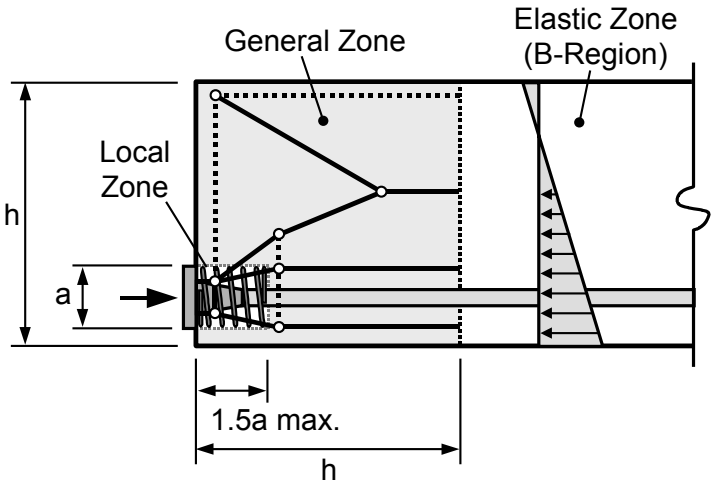

Figure 4-22: Local and general zones of post-tensioned structures

Roberts [91] performed 28 tests of isolated local zones and 3 tests of non-isolated local zones. The purpose of the tests was to rate the quality of the existing acceptance tests for anchorage devices and to develop an improved test method. She studied such parameters as anchor plate type (multi-plane or flat plate), load history (monotonic, cyclic, or sustained loading), cover distance, spiral confinement parameters (pitch and diameter), auxiliary reinforcement in the local zone specimen, and the interaction between the local and general zones. Two interesting results were determined from these tests: the comparison of the local zone capacity to a variety of bearing formulas including a node strength formula developed by Schlaich and Schäfer [97] and the comparison of the results of isolated local zone tests to analogous tests of non-isolated local zones which were a parts of larger general zone elements.

Roberts compared the results of her isolated local zone tests to seven models of bearing capacity. The focus of her analysis was to determine the best model that would account for the impact of the two primary variables of her study: the ratio of the unloaded concrete area to the bearing plate area of the anchorage plate, A_2/A_1 (see the discussion on bearing strength in sections 3.5.1 and 3.6.4 for more discussion on the A_2/A_1 ratio) and the amount of lateral confining steel. Roberts found that the following formula, based on work by Schliach and Schäfer, provided the best fit for her data:

$$f_{bearing} = 0.8f_c'\sqrt{\frac{A_2}{A_1}} + 4.1f_{lat}A_{core}\left(1-\frac{s}{D}\right)^2 \qquad (4\text{-}6)$$

$$0.8f_c'\sqrt{\frac{A_2}{A_1}} \le 3.0f_c' \qquad (4\text{-}7)$$

in which

$f_{bearing}$ = bearing stress of supported by the anchorage device (ksi)

f_c' = concrete cylinder strength (ksi)

A_2 = the unloaded concrete area (refer to Figure 3-28) (in^2)

A_1 = the bearing area of the anchorage device (in^2)

A_{core} = the area of concrete confined by spirals or ties (in^2)

f_{lat} = the lateral confining stress provided by spirals or ties (ksi):

$$\frac{2A_s f_y}{Ds} \quad \text{for spirals}$$

$$\frac{A_s f_y}{Ss} \quad \text{for ties}$$

A_s = the bar area of the spiral or tie confining steel (in^2)

s = the pitch of spiral steel or the spacing of tie steel (in)

D = the diameter of spiral confinement (in)

S = the width tie reinforcement (in)

Robert's recommended formula for the allowable bearing stress of local zones once again shows the reliance of the bearing pressure on the A_2/A_1 ratio which was seen with many other anchorage situations. Furthermore, the formula indicates that even unconfined local zones can sustain a bearing stress as large as $3f_c'$. Since the local zone test was basically a node test, Robert's work implies that the limitations on allowable bearing stresses that were reviewed in section 4.3.4 are very conservative.

Robert's also studied the influence of the general zone configuration on the capacity of the local zone. In a series of five tests, Roberts demonstrated that cracking and ultimate load data from isolated tests of local zones could suffice as lower bound estimates of the behavior of the local zone within a whole disturbed region. This conclusion has significant impact on the determination of node service and ultimate limit states. Robert's work indicates that isolated tests of node zones can be used to conservatively determine limits for the performance of nodes.

Sanders performed 36 tests of end bearing anchorages. He tested such parameters as anchorage eccentricity, multiple anchorages, curved and inclined tendon paths, the distribution of tie reinforcement, the confinement provided by lateral post-tensioning, and concrete strength. Wollmann performed 3 beam tests in which the general zone was influenced by reaction forces, 8 intermediate anchorage tests, and 3 anchorage diaphragm tests. Wollmann's tests represented complex yet commonly occurring instances of post-tensioned anchorages. Sanders' and Wollmann's test results were compared to STM predictions of capacity. Compression struts and nodes were limited by an allowable concrete compressive stress of $0.7f_c'$. The average measured/calculated capacity ratio of all specimens was 1.40 (with a range from 0.95 to 3.33) and the standard deviation was 0.44. The data suggest that STM is an acceptable and often very conservative design method for the post-tensioned anchorage zones.

STM was poor in predicting of the mode of failure of all specimens. Where STM analysis determined that yielding of tie reinforcement would determine failure for most of the specimens, almost all specimens failed by compression in front of the local zone or bursting in the same location. These failure modes occurred because the general zones exceeded their yield capacities. The unanticipated high capacities of the general zones allowed the local (anchorage) zones to reach much higher stress levels than their design values, which resulted in brittle failures.

The goal of much of the research on post-tensioned anchorages was to determine the specific rules that would make STM applicable to design of the anchorages. Thus much of the research interest was in the configuration of truss models and not on the strength of struts and nodes. Among the results of the post-tensioned anchorage zone studies that can be extrapolated to the broad realm of STM application are:

- Serviceability (ie. crack control) within the D-region can best be accounted for if truss models are aligned closely with elastic stress distributions. The centroids of compression struts and tensile ties must match with centroids of compressive and tensile stress field in the elastic solution. An elastic solution must be available to properly implement a strut-and-tie model. For complex geometries in which designer intuition of stress fields will not suffice, elastic FEM analysis is preferred prior to the STM process.

- Compression stresses from the anchor plate spread laterally at a slope of 1:3.
- A simple compression stress limitation of $0.7f_c'$ for struts and nodes provided acceptable predictive results for the experimental tests.
- Roberts' tests imply that a conservative lower bound estimate of local nodal strength can be obtained from isolated tests of the nodal zones.

4.4.5 Zeller (Corbels)

Zeller [43, 114] studied four corbel specimens at the University of Karlsruhe in Germany. He studied the behavior of diagonal spitting in the primary compression strut. The variables were the orientation and amount of splitting reinforcement provided for the corbel struts and the length/depth ration of the corbels. Zeller measured the distribution of strain across the struts in his specimens. He determined that the compression stress was distributed non-uniformly and peaked at the re-entrant corner where the corbel and the support column joined one another (Figure 4-23). The extreme state of stress produced at the re-entrant corner caused all corbel struts to fail in compression at that location, but only after yielding of the tie reinforcement had occurred.

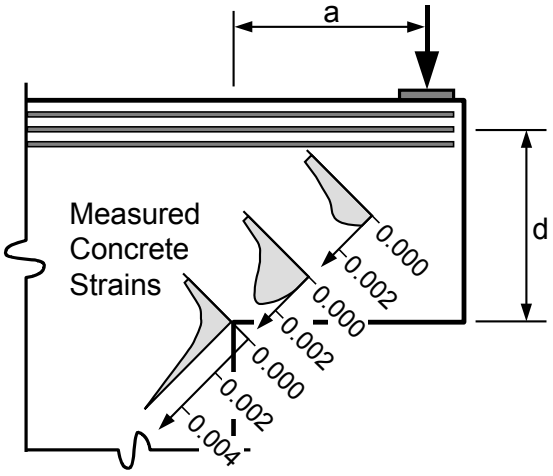

Figure 4-23: Concrete strains in corbels tested by Zeller

4.4.6 Armstrong, Salas, and Wood (Cantilever Bridge Piers)

STM was examined experimentally as an alternative design method for cantilever bridge piers at the University of Texas [20, 112]. Specimens in the study resembled the corbels studied by Zeller [43, 114]. Figure 3-19 of the last chapter presented a schematic of a cantilever bridge pier typical of those studied at University of Texas.

In tests of scaled down pier overhangs [20], researchers found the STM method provided conservative results comparable to conventional design methods. Overhangs designed using the STM method failed in flexure as they were designed to while some specimens designed using ACI provisions for corbels failed in shear when a flexural failure had been designed for. The re-entrant corner of the overhang was found to be the critical design region. Analysis of the CCC node at that region demonstrated that the node had a much higher capacity than predicted using allowable stress criteria recommended by Bergmeister [24]:

Concrete efficiency factor, $$\nu_e = 0.9 - \frac{0.25f_c'}{10{,}000\text{psi}} \quad (4\text{-}8)$$

$$4{,}000 \text{ psi} \le f_c' \le 10{,}000 \text{ psi}$$

Additional tests were later performed to examine design procedures for the CCT node that occurs in the joint at the connection of the overhang to the support column [112]. The researchers found that the STM method was the only suitable method that correctly modeled the actions of the forces in the joint.

4.4.7 Adebar and Zhou (Deep Pile Caps)

Adebar and Zhou have examined the use of STM for design of deep pile caps [15, 16, 17]. They found that the current design practices recommended by ACI for deep pile caps based on punching shear and one-way flexure are unconservative. They proposed a design procedure based on STM (see illustration iv. in Figure 4-1).

As part of their study on deep pile caps, Adebar and Zhou conducted analytical and experimental studies of isolated struts [16]. The isolated strut tests resembled double punch tests of concrete cylinders [30, 70] and they compared their strut results to existing data from double punch studies. Figure 4-24 shows a typical double punch strut specimen. The purpose of the strut studies was to determine the maximum allowable compressive stress before transverse cracking would occur in the strut. In deep pile caps, it is not convenient to place confining reinforcement within the struts, therefore, the compressive stress in the struts must be limited to prevent splitting cracks. Based on the results of 40 experimental tests and their analytical work, Adebar and Zhou derived the following expression for the allowable compressive strength of struts:

$$\text{Allowable Bearing Stress, } f_b \le 0.6 f_c'(1 + 2\alpha\beta) \tag{4-9}$$

$$\alpha = 0.33\left(\sqrt{\frac{A_2}{A_1}} - 1\right) \le 1.0 \tag{4-10}$$

$$\beta = 0.33\left(\frac{h}{b} - 1\right) \le 1.0 \tag{4-11}$$

α = factor for confinement of surrounding concrete

β = factor for aspect ratio of strut

h = length of the strut from node face to node face (in)

b = width of strut, measured at the node faces (in)

A_1 = area of strut at node faces (in^2)

A_2 = area of strut at point of maximum spreading (in^2)

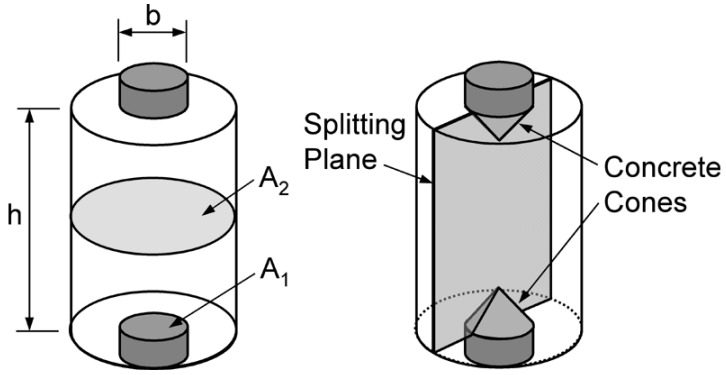

Figure 4-24: Double punch strut test used by Adebar and Zhou

Average values of b and A_1 should be used when the two end node faces of the strut have different geometries. The equation gives an absolute maximum bearing pressure of $1.8f_c'$.

Following their study of struts, Adebar and Zhou used their bearing stress formula in conjunction with strut-and-tie models to predict the strength of 48 experimental tests of fifth-scale to full-scale size pile caps [15, 17]. The experimental data came from a variety of published studies on experimental tests of pile caps. They found that their STM method provided better results than the current ACI and CRSI methods of pile cap design. The range of measured/calculated capacity ratios using STM was 0.99 – 2.88 with a mean of 1.55. The ACI and CRSI methods frequently over-estimated the capacity of the specimens. Despite that success, the ability of STM to predict the failure mode of the pile caps was very poor with only 21 out of 48 failure mode predictions correct. Of the 27 tests in which STM did not predict the correct mode of failure, all specimens were reported to have failed in shear although flexural failure (yielding of the tie steel) was predicted. It is possible that many of the reported shear failures may have actually been of mixed shear and flexural modes and were difficult to properly categorize.

4.4.8 Maxwell (Wall with Opening)

Maxwell [74] studied four small-scale wall specimens modeled after a hypothetical design example provided by Schlaich [98]. The purpose of the experiment was to provide service limit state and ultimate limit state data for a well-known design example using STM. Schliach developed two independent strut-and-tie models for the flow of forces through a discontinuous wall with an opening. Schlaich then used both models in combination by splitting the wall loads 50-50 among the two trusses. His detailing recommendations were based upon the combined analysis.

Maxwell tested four specimens: two specimens based on the two independent truss models developed by Schlaich, a third based upon combining the two trusses in the manner that Schlaich recommended, and a fourth that represented a slight modification of the combined truss analysis of the third specimen. All specimens achieved higher capacities than the design load, thus demonstrating that numerous truss models could be developed for the design of the wall structure and still supply a lower bound estimation of capacity. The combined truss analysis of specimen 3 proved more successful than the independent truss analyses of specimens 1 and 2 providing both a higher capacity and stiffer response to load. Specimen 2 was designed with a truss based most closely on the elastic flow of stresses within the wall. It utilized the least weight of steel for its detailing requirements and achieved a higher capacity per pound of reinforcement than the other three specimens.

4.4.9 Aguilar, Matamoros, and Parra-Montesinos (Deep Beams)

Four deep beams were tested at Purdue University [18]. The study was similar to the Maxwell study in that the main purpose was to examine the effect of various design approaches to the performance of a structural element (in this case a simple deep beam). This type of approach is different from a strictly behavioral study in which only a single parameter is changed from specimen to specimen in order to examine the significance of that parameter without any interfering factors. In a design comparison, the various design approaches may lead to many differences in details from specimen to specimen. It is then much harder to discern the effect of single parameters on the behavior of the specimens. The purpose of the Purdue study was to compare the current ACI design approach for deep beam shear with proposed STM guidelines that are applicable to deep beams. Four deep beams were designed for a given loading and geometry (shown in Figure 4-25). The first beam was designed according to provisions from ACI 319-99, Section 11.8 for deep beam shear members. The remaining three specimens were designed according to various STM approaches all conforming to the new ACI 318 code provisions [2]. The first two specimens used Lenton Terminators for anchorage of the primary reinforcement (The Purdue research was mentioned briefly in Section 3.4.5 of the last chapter because of this). The remaining two specimens used 90^0 hooked anchorages.

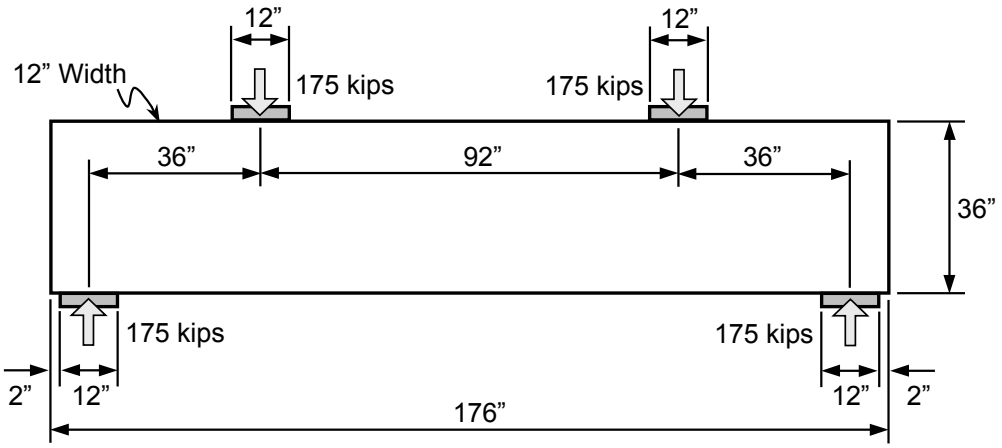

Figure 4-25: Design specimen for the Purdue study

The researchers were primarily interested in the horizontal and vertical splitting steel necessary for confinement of the diagonal shear struts. All specimens exceeded their estimated capacities whether those capacities were calculated using the current ACI shear provisions or the new STM provisions. The STM calculations were shown to be more accurate than the ACI deep beam calculations, though neither gave a close estimate of strength. The STM design approach generally required less splitting steel than the ACI deep beam approach. Two specimens failed in shear and two failed in flexure though both design approaches predicted shear failures for all four specimens. Measured strains indicated that development of primary tension steel occurred over a very short length within the nodal zone located over the reaction bearing pads.

Detailing procedures were different for all four specimens. Only the two specimens that utilized hooked anchorages are directly comparable. Only the amount and placement of splitting steel were different for these two specimens. The lever arm of the primary tension steel was varied in the other two specimens thus precluding a direct comparison of behavior. The behavior of the two comparable specimens showed that there was no significant change in capacity though nearly 80% of the confining vertical and horizontal steel was omitted from the end shear panel regions in one of the specimens. The more heavily reinforced specimen had a somewhat better distribution of cracking in the end regions. Both of these specimens failed by splitting of the diagonal compression struts (shear).

4.5 FINAL COMMENTS

The survey of experimental work and recommended design procedures for STM leads to the following observations and overall trends.

The procedures for strut-and-tie modeling require additional refinement. Particularly, the topics of node stress limits and anchorage at nodes require attention. The code guidelines for dimensioning of nodes are not based on rational models for the flow of forces at the intersections of struts or the anchorages of ties. For example, at the anchorage of a tie bar in a CCT node, it is unlikely that strut stresses would uniformly extend up to 6 bar diameters to either side of the tie (see side views in Figure 4-14). Geometric compatibility requires that the strut stresses must concentrate and flow into the tie bar. Consequently, the stresses in a CCT node must be much greater than would be calculated based on the dimensioning guidelines put forth by the codes and also much greater than the stress limits allowed by the codes. The dimensioning guidelines require experimental study. Realistic dimensioning guidelines for nodes are necessary in order to properly reflect the flow of forces and would allow for larger and more realistic stress limits to be specified in the codes. Experimental studies of the bearing strength of concrete have shown that in many situations bearing stresses can be much larger than the cylinder compressive strength,

f_c'. Similar large bearing strength capacities should also be expected for many node cases. However, the current provisions allow a maximum bearing strength of $1.0\phi f_c$' for the best node case. The stress limits seem to be much too conservative. However, the dimensioning guidelines require unrealistically large node boundaries to be assumed.

The issues with node dimensioning and stress limits are exacerbated by the lack of guidelines for addressing those nodes that do not meet the current requirements. How is a node improved when the stresses acting on it are greater than the code limits? Only two alternatives are available: the D-region must be re-detailed to increase the size of the node and thus reduce the stresses or the concrete strength must be re-specified to meet the stress demands. Neither alternative is appealing. Re-detailing of the D-region requires that tie steel must be redistributed and spread out in order to increase the size of CCT and CTT nodes or that the dimensions of the structure must be enlarged to increase the size of CCC nodes (in many cases CCC can be simply improved by enlarging a bearing plate). Once the D-region is re-detailed, the truss model must be re-drawn and the STM process proceeds through another iteration. This requires additional design time and can lead to detailing compatibility problems at the boundaries between D- and B-regions. The second alternative, increasing the concrete strength, is a radical and expensive solution to accommodate the stress limits of a single node. Currently, though all of the codes allow for improvement of the nodes using confining steel, their procedures do not provide any guidelines for improving the confinement or anchorage details at nodes in order to make them meet stress limits.

Anchorage at nodes also presents similar problems. Space limits at nodes are frequently too small to fully develop straight reinforcing bars and hooked bars may create congestion problems. Designers have previously had few alternatives to address anchorage problems at nodes, but new developments in headed bars offer a promising direction for solving this problem.

These issues regarding design of nodes represent the largest obstacle to the implementation of strut-and-tie modeling in common design practice. Research and re-evaluation of node behavior must be performed and incorporated into STM design procedures. Fortunately, the studies by Anderson (CTT nodes), Bouardi (CCT nodes), and Roberts (local anchorage zones) have confirmed that isolated node tests will provide lower bound results compared to similar nodes in non-isolated situations. Similarly, the research by Adebar and Zhou (pile caps) has confirmed this for isolated tests of struts. This result could be put to good use in determining limits on nodal zone stresses and anchorage requirements. While the application of STM might be limitless, the number and types of node situations that occur may be a much smaller number. Since it seems possible to isolate nodes for experimental testing, it should be reasonable to derive experimentally based design limits for the detailing of nodal zones in STM applications much as Adebar and Zhou were able to do for the analysis of struts.

Finally, in many experimental studies, STM has been shown to be a conservative design approach because it typically provides a lower-bound estimate of capacity. However despite this success it is somewhat discouraging to look back over the extent of the research and recall how often STM fails to properly predict the failure mode of specimens. Sanders and Wollmann noted that tie yielding was predicted for many of their specimens and crushing at the boundary of the local zone actually resulted. Adebar and Zhou also predicted flexural yielding for many of the pile cap tests that they reviewed, but most of the caps failed in shear. Ideally, tie yielding should result in a plastic limit of the specimen capacity and no other failure should occur until material strain limits are exceeded by excessive deformations. However, in tests, post-yielding capacity very often resulted in a brittle failure for specimens as other components of the model reached their limit states. In design practice, it is unlikely that a D-region would be loaded near its design capacity before the capacity of a neighboring B-region was reached, thus limiting the ultimate load that would be placed on the D-region. Therefore, post-yield capacity is probably not an issue. However, it is still a flaw of the STM method that it cannot be relied on to accurately predict the nature of failure for many structural situations.

REFERENCES

1. "AASHTO LRFD Bridge Design Specifications, 2nd ed.," American Association of State Highway and Transportation Officials, Washington, DC, 1998.
2. ACI 318-02, "Building Code Requirements for Structural Concrete and Commentary," American Concrete Institute, Farmington Hills, Michigan, October 2002.
3. ASTM A615/A615M-96a, "Standard Specification for Deformed and Plain Billet-Steel for Concrete Reinforcement," American Society for Testing and Materials, West Conshohocken, Pennsylvania, September 1996.
4. ASTM A944-99, "Standard Test Method for Comparing Bond Strength of Steel Reinforcing Bars to Concrete Using Beam-End Specimens," American Society for Testing and Materials, West Conshohocken, Pennsylvania, September 1999.
5. ASTM A970/A970M-97, "Standard Specification for Welded Headed Bars for Concrete Reinforcement," American Society for Testing and Materials, West Conshohocken, Pennsylvania, September 1997.
6. CSA Standard CAN3-A23.3-94, "Design of Concrete Structures for Buildings with Explanatory Notes," Canadian Standards Association, Rexdale, Ontario, 1994.
7. CEB Bulletin No. 216, "Fastenings to Concrete and Masonry Structures," Lausanne, Switzerland, July 1994.
8. CEB Bulletin No. 226, "Design of Fastenings in Concrete: Draft CEB Guide – Part 1 to 3," Lausanne, Switzerland, August 1995.
9. "Fracture Mechanics of Concrete: Concepts, Models and Determination of Material Properties," Report by ACI 446, Fracture Mechanics (Z. P. Bažant, Chairman), Detroit, Michigan, December 1989.
10. International Conference of Building Officals (ICBO) Evaluation Report ER-5309, Whittier, California, May 1997.
11. "Ontario Highway Bridge Design Code, 3rd Edition," Canadian Ministry of Transportation, Toronto, Ontario, Canada, 1991.
12. PCI Design Handbook 3rd Edition, Prestressed Concrete Institute, Chicago, Illinois, 1985.
13. "Structural Concrete: The Textbook on Behavior, Design, and Performance - Volume 2: Basis of Design," Federation Internationale du Beton (FIB), Lausanna, Switzerland, July 1999.
14. Abrams, D.A., "Tests of Bond Between Concrete and Steel," Engineering Experiment Station, University of Illinios Bulletin No. 71, Urbana, Illinios, December 1913.
15. Adebar, P., Kuchma, D., and Collins, M.P., "Strut-and-Tie Models for the Design of Pile Caps: An Experimental Study," ACI Structural Journal, Proceedings Vol. 87, No. 1, pg. 81-92, Detroit, Michigan, January-February 1990.
16. Adebar, P. and Zhou, Z., "Bearing Strength of Compressive Struts Confined by Plain Concrete," ACI Structural Journal, Proceedings Vol. 90, No. 5, pg. 534-541, Detroit, Michigan, September-October 1993.
17. Adebar, P. and Zhou, Z., "Design of Deep Pile Caps by Strut-and-Tie Models," ACI Structural Journal, Proceedings Vol. 93, No. 4, pg. 437-448, Detroit, Michigan, July-August 1996.
18. Aguilar, G., Matamoros, A., Parra-Montesinos, G., Ramirez, J.A., and Wight, J.K., "Experimental and Analytical Evaluation of Design Procedures for Shear Strength of Deep Reinforced Concrete Beams," Final Report to the Reinforced Concrete Research Council, ACI, Purdue University, Lafayette, Indiana, May 2001.
19. Alshegeir, A.A. and Ramirez, J.A., "Analysis and Design of Disturbed Regions with Strut-Tie Models, Parts I and II," Purdue University, Structural Engineering Report No. CE-STR-93-1, Lafayette, Indiana, 1993.

20. Armstrong, S.D., Salas, R.M., Wood, B.A., Breen, J.E., and Kreger, M.E., "Behavior and Design of Large Structural Concrete Bridge Pier Overhangs," Center for Transportation Research Report CTR-1364-1, Austin, Texas, February 1997.

21. Barton, D.L., Anderson, R.B., Bouardi, A., Jirsa, J.O., and Breen, J.E., "An Investigation of Strut-and-Tie Models for Dapped Beam Details," Center for Transportation Research Report No. CTR 3-5-87/9-1127-1, Austin, Texas, May 1991.

22. Bashandy, T.R., "Application of Headed Bars in Concrete Members," PhD Dissertation, The University of Texas at Austin, Austin, Texas, December 1996.

23. Beaupre, R.J., Powell, L.C., Breen, J.E., and Kreger, M.E., "Deviation Saddle Behavior and Design for Externally Post-Tensioned Bridges," Center for Transportation Research Report No. CTR 3-5-85/8-365-2, Austin, Texas, July, 1988.

24. Bergmeister, K., Breen, J.E., Jirsa, J.O., and Kreger, M.E., "Detailing for Structural Concrete," Center for Transportation Research Report CTR 0-1127-3F, Austin, Texas, May 1993.

25. Berner, D.E., Gerwick, B.C., and Hoff, G.C., "T-Headed Stirrup Bars," Concrete International, Vol. 13, No. 5, Detroit, Michigan, May 1991.

26. Berner, D.E. and Hoff, G.C., "Headed Reinforcement in Disturbed Strain Regions of Concrete Members," Concrete International, Vol. 16, No. 1, Detroit, Michigan, January 1994.

27. Breen, J.E., "Development Length for Anchor Bolts," Center for Transportation Research Report CTR-55-1F, Austin, Texas, April 1964.

28. Breen, J.E., Burdet, O., Roberts, C., Sanders, D., and Wollmann, G., "Anchorage Zone Reinforcement for Post-Tensioned Concrete Girders," National Cooperative Highway Research Program Report No. 356, Washington, DC, 1994.

29. Chamberlin, S.J., "Spacing of Spliced Bars in Tension Pull-Out Specimens," Journal of the American Concrete Institute, Proceedings Vol. 49, No. 4, pg. 261-274, Detroit, Michigan, December 1952.

30. Chen, W.F., "Double Punch Test for Tensile Strength of Concrete," Journal of the American Concrete Institute, Proceedings Vol. 67, No. 12, pg. 993-995, Detroit, Michigan, December 1970.

31. Chinn J., Ferguson, P.M., Thompson, J.N., "Lapped Splices in Reinforced Concrete Beams," Journal of the American Concrete Institute, Proceedings Vol. 52, No. 2, pg. 201-212, Detroit, Michigan, October 1955.

32. Clark, A.P., "Comparative Bond Efficiency of Deformed Concrete Reinforcing Bars," Journal of the American Concrete Institute, Proceedings Vol. 43, No. 4, Detroit, Michigan, December 1946.

33. Clark, A.P., "Bond of Concrete Reinforcing Bars," Journal of the American Concrete Institute, Proceedings Vol. 46, No. 3, November 1949.

34. Collins, M.R., Vecchio, F.J., Selby, R.G., and Gupta, P., "The Failure of an Offshore Platform," Concrete International, Vol. 19, No. 8, pg. 28-35, Detroit, Michigan, August 1997.

35. Cook, W. and Mitchell, D., "Studies of Disturbed Regions Near Discontinuities in Reinforced Concrete Members," ACI Structural Journal, Proceedings Vol. 85, No. 2, pg. 206-216, Detroit, Michigan, March-April 1988.

36. Darwin, D. and Graham, E.K., "Effect of Deformation Height and Spacing on Bond Strength of Reinforcing Bars," ACI Structural Journal, Vol. 90, No. 6, Detroit, Michigan, November-December 1993.

37. Darwin, D., Zou, J., and Tholen, M.L., "Overview of Research to Improve the Development Characteristics of Reinforcing Bars," Proceedings of the International Symposium "Bond and Development of Reinforcement, A Tribute to Dr. Peter Gergely," ACI Interntional, SP-180, pg. 299-318, Farmington Hills, Michigan, 1998.

38. DeVries, R.A., "Anchorage of Headed Reinforcement in Concrete," PhD Dissertation, The University of Texas at Austin, Austin, Texas, December 1996.

39. Dilger, W.H. and Ghali, A., "Double-Headed Studs as Ties in Concrete," Concrete International, Vol. 19, No. 6, pg. 59-66, Detroit, Michigan, June 1997.

40. Dilger, W.H. and Ghali, A., "Shear Reinforcement for Concrete Slabs," ASCE Journal of Structural Engineering, Vol. 107, No. 12, pgs. 2403-2420, New York, New York, December 1981.

41. Drågen, A., "T-Headed Bars SP2: Fatigue Tests," SINTEF Report STF18 F86048, Trondheim, Norway, 1986 *(proprietary report)*.

42. Dyken, T. and Kepp B., "Properties of T-Headed Bars in High Strength Concrete," Nordic Concrete Research, Publication No. 7, pg. 41-51, Oslo, Norway, 1993.

43. Eibl, J. and Zeller, W., "Untersuchungen zur Traglast der Druckdiagonalen in Konsolen," Bericht, Institut für Massivbau und Baustofftechnologie, University of Karlsruhe, Germany, 1991.

44. Fuchs, W., Eligehausen, R., and Breen, J.E., "Concrete Capacity Design (CCD) Approach for Fastening to Concrete," ACI Structural Journal, Proceedings Vol. 92, No. 1, pg. 73-94, Detroit, Michigan, January-February 1995.

45. Furche, J. and Eligehausen, R., "Lateral Blow-Out Failure of Headed Studs Near a Free Edge," Proceedings of International Symposium "Anchors in Concrete – Design and Behavior," ACI Internatinal, SP-130, pg. 235-252, Farmington Hills, Michigan, 1991.

46. Fynboe, C.C. and Thorenfeldt, E., "T-Headed Bars SP1: Static Pullout Tests," SINTEF Report STF65 F86083, Trondheim, Norway, 1986 *(proprietary report)*.

47. Fynboe, C.C. and Thorenfeldt, E., "T-Headed Bars SP3: Fatigue Tests – Bars Embedded in Concrete," SINTEF Report STF65 F86088, Trondheim, Norway, 1986 *(proprietary report)*.

48. Fynboe, C.C. et al, "T-Headed Bars SP4: Shear," SINTEF Report STF65 F86084, Trondheim, Norway, 1986 *(proprietary report)*.

49. Gambarova, P.G., Rosati, G.P., and Schumm, C.E., "Bond and Splitting: A Vexing Question," Proceedings of the International Symposium "Bond and Development of Reinforcement, A Tribute to Dr. Peter Gergely," ACI Interntional, SP-180, pg. 23-44, Farmington Hills, Michigan, 1998.

50. Goto, Yukimasa, "Cracks Formed in Concrete Around Deformed Tension Bars," Journal of the American Concrete Institute, Proceedings Vol. 68, No. 4, pg. 244-251, Detroit, Michigan, April 1971.

51. Hamad, B.S., "Comparative Bond Strength of Coated and Uncoated Bars with Different Rib Geometries," ACI Materials Journal, Vol. 92, No. 6, Detroit, Michigan, November-December 1995.

52. Hamad, B.S. and Mansour, M.Y., "Bond Strength of Noncontact Tension Lap Splices," ACI Structural Journal, Proceedings Vol. 93, No. 3, Detroit, Michigan, May-June 1996.

53. Haroun, H., Pardoen, G., Bhatia, H., Shahi, S., and Kazanjy, R., "Structural Behavior of Repaired Pier Walls," ACI Structural Journal, Proceedings Vol. 97, No. 2, pg. 259-267, Detroit, Michigan, March-April 2000.

54. Hasselwander, G.B., Jirsa, J.O., Breen, J.E., and Lo, K., "Strength and Behavior of Anchor Bolts Embedded Near Edges of Concrete Piers," Center for Transportation Research Report CTR-29-2F, Austin, Texas, May 1977.

55. Hasselwander, G.B., Jirsa, J.O., and Breen, J.E., "Strength and Behavior of Single Cast-in-Place Anchor Bolts Subject to Tension," Proceedings of the International Symposium "Anchorage to Concrete," ACI International, SP-103, pg. 203-231, Farmington Hills, Michigan, 1984.

56. Hawkins, N.M., "The Bearing Strength of Concrete: 1. Loading Through Rigid Plates Covering Part of the Full Supporting Area," The University of Sydney, Research Report No. 54, Sydney, Australia, March 1967.

57. Hawkins, N.M., "The Bearing Strength of Concrete: 2. Loading Through Flexible Plates," The University of Sydney, Research Report No. 84, Sydney, Australia, August 1967.

58. Ingham, J.M, Priestley, M.J., and Seible, F., "Seismic Performance of a Bridge Knee Joint Reinforced with Headed Reinforcement," University of California, San Diego, Structural Systems Research Project, Report No. SSRP-96/06, La Jolla, California, September 1996.

59. Jakobsen, B. and Rosendahl, B., "The Sleipner Platform Accident," IABSE Structural Engineering International, Vol. 4, No. 3, pg. 190-193, Zurich, Switzerland, August 1994.

60. Kuchma, D.A. and Collins, M.P., "The Influence of T-Headed Bars on the Strength and Ductility of Reinforced Concrete Wall Elements," University of Toronto, Paper Presented at the Spring Conference of the American Concrete Institute, Seattle, Washington, April 1997.

61. Lampert, P. and Thürlimann, B., "Ultimate Strength and Design of Reinforced Concrete Beams in Torsion and Bending," IASBE Publications, No. 31-1, pg. 107-131, Zurich, Switzerland, 1971.

62. Lee, D.W. and Breen, J.E., "Factors Affecting Anchor Bolt Development," Center for Transportation Research Report CTR-88-1F, Austin, Texas, August 1966.

63. Lehman, D.E., Gookin, S.E., Nacamuli, A.M., and Moehle, J.P., "Repair of Earthquake-Damaged Bridge Columns," ACI Structural Journal, Proceedings Vol. 98, No. 2, pg. 233-242, Detroit, Michigan, March-April 2001.

64. Lormanometee, Sumete, "Bond Strength of Deformed Reinforcing Bar Under Lateral Pressure," Master's Thesis, The University of Texas at Austin, Austin, Texas, January 1974.

65. Lüchinger, P., "Bruchwiderstand von Kastenträgern aus Stahlbeton unter Torsion, Biegung, und Querkraft (Ultimate Strength of Box-Griders in Reinforced Concrete under Torsion, Bending, and Shear)," Institut für Baustatik und Konstruktion-ETH, Zurich, Switzerland, Bericht Nr. 69, 1977.

66. Lutz, LeRoy A., "The Mechanics of Bond and Slip of Deformed Reinforcing Bars in Concrete," Department of Structural Engineering, Cornell University, Report No. 324, Ithaca, New York, August 1966.

67. Mains, R.M., "Measurement of the Distribution of Tensile and Bond Stresses Along Reinforcing Bars," Journal of the American Concrete Institute, Proceedings Vol. 48, No. 3, pg. 225-252, Detroit, Michigan, November 1951.

68. Marques, J.L.G., and Jirsa, J.O., "A Study of Hooked Bar Anchorages in Beam-Column Joints," Journal of the American Concrete Institute, Proceedings Vol. 72, No. 5, pg. 198-209, Detroit, Michigan, May 1975.

69. Marti, P., "Basic Tools in Reinforced Concrete Beam Design," Journal of the American Concrete Institute, Proceeding Vol. 82, No. 1, pg. 46-56, Detroit, Michigan, January-February 1985.

70. Marti, P., "Size Effect in Double-Punch Tests on Concrete Cylinders," ACI Materials Journal, Proceedings Vol. 86, No. 6, pg. 597-601, Detroit, Michigan, November-December 1989.

71. Marti, P., "Truss Models in Detailing," Concrete International, Vol. 7, No. 12, pg. 66-73, Detroit, Michigan, December 1985.

72. Matsumoto, E.E., Waggoner, M.C., Sumen, G., Kreger, M.E., Wood, S.L., and Breen, J.E., "Development of a Precast Bent Cap System," Center for Transportation Research Report 1748-2, Austin, Texas, January 2001.

73. Mattock, A.H., "Effectiveness of Loop Anchorages for Reinforcement in Precast Concrete Members," PCI Journal, Vol. 39, No. 6, pg. 54-68, Chicago, Illinois, November-December 1994.

74. Maxwell, B.S. and Breen, J.E., "Experimental Evaluation of Strut-and-Tie Model Applied to Deep Beam with Opening," ACI Structural Journal, Proceedings Vol. 97, No. 1, pg. 142-148, Detroit, Michigan, January-February 2000.

75. McMackin, P.J., Slutter, R.G., and Fisher, J.W., "Headed Steel Anchor Under Combined Loading," AISC Engineering Journal, Vol. 10, No. 2, pg. 43-52, New York, New York, 2nd Quarter, 1973.

76. Menon, G. and Furlong, R.W., "Design of Reinforcement for Notched Ends of Prestressed Concrete Girders," Center for Transportation Research Report No. 196-1F, Austin, Texas, 1977.

77. Minor, J., and Jirsa, J.O., "Behavior of Bent Bar Anchorages," Journal of the American Concrete Institute, Proceedings Vol. 72, No. 4, pg. 141-149, Detroit, Michigan, April 1975.

78. Mitchell, D. and Collins, M., "Diagonal Compression Field Theory – A Rational Model for Structural Concrete in Pure Torsion," Journal of the American Concrete Institute, Proceedings Vol. 71, No. 8, pg. 396-408, Detroit, Michigan, August 1974.

79. Mokhtar, A.S., Ghali, A., and Dilger, W.H., "Stud Shear Reinforcement for Flat Concrete Plates," Journal of the American Concrete Institute, Proceedings Vol. 82, No. 5, pgs. 676-683, Detroit, Michigan, September-October 1985.

80. Mörsch, E., "Der Eisenbetonbau, seine Theorie und Anwendung (Reinforced Concrete, Theory and Application)," Stuggart, Germany, 1902.

81. Mörsch, E., "Über die Berechnung der Gelenkquader," Beton-und Eisen, No. 12, pg. 156-161, Stuttgart, Germany, 1924.

82. Nielson, M.P., "Limit Analysis and Concrete Plasticity, 2nd Edition," CRC Press, Boca Raton, Florida, 1998.

83. Niyogi, S.K., "Bearing Strength of Concrete – Geometric Variations," ASCE Journal of Structural Engineering, Vol. 99, No. 7, pgs. 1471-1490, New York, New York, July 1973.

84. Niyogi, S.K., "Concrete Bearing Strength – Support, Mix, Size Effect," ASCE Journal of Structural Engineering, Vol. 100, No. 8, pgs. 1685-1702, New York, New York, August 1974.

85. Niyogi, S.K., "Bearing Strength of Reinforced Concrete Blocks," ASCE Journal of Structural Engineering, Vol. 101, No. 5, pgs. 1125-1137, New York, New York, May 1975.

86. Orangun, C.O., Jirsa, J.O., and Breen, J.E., "The Strength of Anchor Bars: A Reevaluation of Test Data on Development Length and Splices," Center for Highway Research, Report 154-3F, Austin, Texas, January 1975.

87. Orangun, C.O., Jirsa, J.O., and Breen, J.E., "A Reevaluation of Test Data on Development Length and Splices," Journal of the American Concrete Institute, Proceedings Vol. 74, No. 3, pg. 114-122, Detroit, Michigan, March 1977.

88. Ørjasæter, O., "T-Headed Bars: Fatigue Tests of Embedded Bars," SINTEF Report STF18 F87043, Trondheim, Norway, 1987 *(proprietary report)*.

89. Ørjasæter, O., "Fatigue Tests of Friction Welded Bar / Reinforcement Bar," SINTEF Report STF18 F87042, Trondheim, Norway, 1987 *(proprietary report)*.

90. Ramirez, J. and Breen, J.E., "Proposed Design Procedures for Shear and Torsion in Reinforced and Prestressed Concrete," Center for Transportation Research Report No. 248-4F, Austin, Texas, 1983.

91. Roberts, C., "Behavior and Design of the Local Anchorage Zone of Post-Tensioned Concrete Members," Master's Thesis, The University of Texas at Austin, May 1990.

92. Rogowsky, D.M. and MacGregor, J.M., "Shear Strength of Deep Reinforced Concrete Continuous Beams," The University of Alberta, Structural Engineering Report No. 110, Edmonton, Alberta, November 1983.

93. Rogowsky, D.M. and MacGregor, J.M., "Design of Reinforced Concrete Deep Beams," Concrete International, Vol. 6, No. 8, pg. 49-58, August 1986.

94. Richart, F., "An Investigation of Web Stresses in Reinforced Concrete Beams," University of Illinois Engineering Experiment Station, Bulletin No. 166, Urbana, Illinois, 1927.

95. Ritter, W., "Die Bauweise Hennebique (The Hennebique System)," Schweizerische Bauzeitung, Bd. XXXIII, No. 7, Zurich, Switzerland, 1899.

96. Rosati, G.P. and Schumm, C.E., "Modeling of Local Bar-to-Concrete Bond in RC Beams," Proceedings of the International Conference "Bond in Concrete: From Research to Practice," CEB-RTU, Vol. 3, pg. 12.34-12.43, Riga, Latvia, October 1992.

97. Schlaich, J. and Schäfer, K., "Konstruieren im Stahlbeton," Betonkalender, pg 563-715, Berlin, Germany, 1989.

98. Schlaich, J., Schäfer, K., and Jennewein, M., "Towards a Consistent Design of Structural Concrete," PCI Journal, Vol. 32, No. 3, pg. 74-150, Chicago, Illinois, May-June 1987.

99. Sritharan, S. and Priestley, M.J., "Seismic Testing of a Full-Scale Pile-Deck Connection Utilizing Headed Reinforcement," University of California, San Diego, Structural Systems Research Project, Report No. TR-98/14, La Jolla, California, August 1998.

100. Stoker, J.R., Boulware, R.L., Crozier, W.F., and Swirsky, R.A., "Anchorage Devices for Large Diameter Reinforcing Bars," Caltrans Report CA-DOT-TL-6626-1-73-30, California Department of Transportation, Sacramento, California, September 1974.

101. Talbot, A., "Tests of Reinforced Concrete Beams: Resistance to Web Stresses, Series of 1907 and 1908," University of Illinois Engineering Experiment Station, Bulletin No. 29, Urbana, Illinois, 1909.

102. Tepfers, Ralejs, "A Theory of Bond Applied to Overlapped Tensile Reinforcement Splices for Deformed Bars," Chalmers University of Technology, Publication No. 73:2, Göteborg, Sweden, 1973.

103. Thompson, M.K., Young, M.J., Jirsa, J.O., Breen, J.E., and Klingner, R.E., "Anchorage of Headed Reinforcement in CCT Nodes," Center for Transportation Research Report 1855-2, Austin, Texas, May 2002.

104. Thompson, M.K., Ledesma, A. L., Jirsa, J.O., Breen, J.E., and Klingner, R.E., "Anchorage of Headed Reinforcement in Lap Splices," Center for Transportation Research Report 1855-3, Austin, Texas, May 2002.

105. Thrö, Gerfried Schmidt, Stöckl, Siegfried, and Kupfer, Herbert, "Verankerung der Bewehrung am Endauflager bei einachsiger Querpressung" ("Anchorage of Reinforcement at an End Bearing with Uni-Axial Lateral Pressure"), Deutscher Ausschus für Stahlbeton, Heft 389, pg. 11-98, Berlin, Germany, 1988.

106. Untrauer, R.E. and Henry, R.L., "Influence of Normal Pressure on Bond Strength," Journal of the American Concrete Institute, Proceedings Vol. 62, No. 5, Detroit, Michigan, May 1965.

107. Vecchio, F.J. and Collins, M.P., "The Modified Compression Field Theory for Reinforced Concrete Elements Subjected to Shear," Journal of the American Concrete Institute, Proceedings Vol. 83, No. 2, pg. 219-231, Detroit, Michigan, March-April 1986.

108. Vecchio, F.J. and Collins, M.P., "The Response of Reinforced Concrete to In-Plane Shear and Normal Stresses," The University of Toronto, Department of Civil Engineering Publication No. 82-03, Toronto, Canada, 1982.

109. Wallace, J.W., McConnell, S.W., Gupta, P., and Cote, P.A., "Use of Headed Reinforcement in Beam-Column Joints Subjected to Earthquake Loads," ACI Structural Journal, Proceedings Vol. 95, No. 5, pg. 590-606, Detroit, Michigan, September-October 1998.

110. Williams, A., "The Bearing Capacity of Concrete Loaded Over a Limited Area," Cement and Concrete Association, Technical Report 526, Wexham Springs, Slough, The United Kingdom, August 1979.

111. Withey, M., "Tests of Plain and Reinforced Concrete, Series of 1906 and 1907," Bulletin of the University of Wisconsin, Engineering Series, Vol. 4, No. 2, Madison, Wisconsin, 1907-1908.

112. Wood, B.A., Kreger, M.E., and Breen, J.E., "Experimental Investigation of Design Methods for Large Cantilever Bridge Bents," Center for Transportation Research Report CTR-1364-3F, Austin, Texas, August 1997.

113. Wright, J.L. and McCabe, S.L., "The Development Length and Anchorage Behavior of Headed Reinforcing Bars," University of Kansas Center for Research, SM Report No. 44, Lawrence, Kansas, September 1997.

114. Zeller, W., "Conclusions from Tests on Corbels," IABSE Colloquium on Structural Concrete (Stuggart 1991), IABSE Reports Vol. 62, pg. 577-582, Zurich, Switzerland, 1991.

115. Personal e-mail correspondence between Michael Keith Thompson, PhD candidate at the University of Texas at Austin, and Lou Colarusso, Senior Development Engineer, ERICO, Inc., May 30, 2001.

116. Personal e-mail correspondence between Michael Keith Thompson, PhD candidate at the University of Texas at Austin, and Steven L. McCabe, professor of Civil Engineering at the University of Kansas, June 29, 1999.

117. Company History, Metalock, <http://www.metalock.co.uk> *(as posted during July 2001)*.